UNIVERSITY OF ALBERTA

BLOCK SHEAR FAILURE OF COPED STEEL BEAMS

BY

CAMERON R. FRANCHUK

A THESIS SUBMITTED TO THE FACULTY OF GRADUATE STUDIES AND RESEARCH IN PARTIAL FULFILLMENT OF THE REQUIREMENTS FOR THE DEGREE OF MASTER OF SCIENCE

IN

STRUCTURAL ENGINEERING

DEPARTMENT OF CIVIL AND ENVIRONMENTAL ENGINEERING

EDMONTON, ALBERTA

FALL 2002

National Library of Canada
Acquisitions and Bibliographic Services
395 Wellington Street
Ottawa ON K1A 0N4
Canada

Bibliothèque nationale du Canada
Acquisitions et services bibliographiques
395, rue Wellington
Ottawa ON K1A 0N4
Canada

Your file Votre référence

Our file Notre référence

The author has granted a non-exclusive licence allowing the National Library of Canada to reproduce, loan, distribute or sell copies of this thesis in microform, paper or electronic formats.

L'auteur a accordé une licence non exclusive permettant à la Bibliothèque nationale du Canada de reproduire, prêter, distribuer ou vendre des copies de cette thèse sous la forme de microfiche/film, de reproduction sur papier ou sur format électronique.

The author retains ownership of the copyright in this thesis. Neither the thesis nor substantial extracts from it may be printed or otherwise reproduced without the author's permission.

L'auteur conserve la propriété du droit d'auteur qui protège cette thèse. Ni la thèse ni des extraits substantiels de celle-ci ne doivent être imprimés ou autrement reproduits sans son autorisation.

0-612-81394-0

Canada

UNIVERSITY OF ALBERTA

LIBRARY RELEASE FORM

NAME OF AUTHOR:	CAMERON R. FRANCHUK
TITLE OF THESIS:	BLOCK SHEAR FAILURE OF COPED STEEL BEAMS
DEGREE:	MASTER OF SCIENCE
YEAR THIS DEGREE GRANTED:	2002

Permission is hereby granted to the University of Alberta Library to reproduce single copies of this thesis and to lend or sell such copies for private, scholarly or scientific research purposes only.

The author reserves all other publication and other rights in association with the copyright in the thesis, and except as herein before provided, neither the thesis nor any substantial portion thereof may be printed or otherwise reproduced in any material form whatever without the author's prior written permission.

Cam Franchuk

1810 Tomlinson Crescent NW
Edmonton AB T6R 2T4

Date: August 29, 2002

UNIVERSITY OF ALBERTA

FACULTY OF GRADUATE STUDIES AND RESEARCH

The undersigned certify that they have read, and recommend to the Faculty of Graduate Studies and Research for acceptance, a thesis entitled BLOCK SHEAR FAILURE OF COPED STEEL BEAMS submitted by CAMERON R. FRANCHUK in partial fulfillment of the requirements for the degree of Master of Science in Structural Engineering.

Dr. R. G. Driver, Co-Supervisor

Dr. G. Y. Grondin, Co-Supervisor

Dr. Xiaodong Wang

Date: August 28, 2002

There is nothing so captivating as new knowledge.

– Peter Latham

Abstract

Relatively few tests have been conducted to determine the block shear connection capacity and behaviour of coped steel beams. Furthermore, design standards are inconsistent in the way they treat this failure mode and may predict capacities significantly higher than those determined experimentally. To address these issues, 17 full-scale tests were conducted on coped wide flange beams. Parameters considered in the study include beam end rotation, end and edge distances, and bolt layout. Following the laboratory tests, non-linear numerical analyses of five of these connections was completed. A statistical assessment of current design standards and three proposed strength models was then completed to determine the level of safety being provided. It is found that current design standards do not consistently provide an acceptable level of safety and that the strength of two-line connections are often over-predicted by a considerable margin. A new equation is proposed for design that provides both an adequate and consistent level of safety.

Acknowledgments

The author would like to thank, first, his two advisors, Dr. Robert Driver and Dr. Gilbert Grondin, for their guidance and support throughout this project. The significant ground work conducted by Dr. Geoffrey Kulak that formed the foundation for this project is also acknowledged. The discussions with and advice given by Lindsay Mouser, Bino Huns, Anthony Ng, and Kam Deng are also greatly appreciated. Finally, the technical knowledge and support of Jim Hutton and Chris Hutton were invaluable.

Financial assistance for this project was provided by the Steel Structures Education Foundation (SSEF), the Natural Sciences and Engineering Research Council of Canada (NSERC), the Province of Alberta, and the C.W. Carry Chair in Steel Structures. In-kind support, in the form of donation of the test beams and fabrication of the connections, was provided by Supreme Steel Ltd.

Dedication

To my Parents, for instilling in me
a passion for learning.

To my wife, Kimberley, whose strength and
support made this possible and without whom
I could never have accomplished this.

Table of Contents

1. Introduction 1

1.1 Statement of Problem 1

1.2 Objectives and Scope 2

1.3 Organization of Thesis 3

2. Literature Review 5

2.1 Introduction 5

2.2 Laboratory Tests and Numerical Analyses 5

2.3 Capacity Equations 8

2.4 Design Standards 9

2.5 Summary 12

3. Experimental Program 13

3.1 Introduction 13

3.2 Description of Test Specimens 13

3.3 Material Properties 17

3.4 Description of Test Set-up 19

3.5 Instrumentation 20

3.6 Specimen Installation and Test Procedure 21

3.7 Test Results 22

3.8 Summary 24

4. Numerical Program 49

4.1 Introduction 49

4.2 Description of Models 49

4.3 Material Model 52

4.4 Analysis Procedure 54

4.5 Analysis Results 57

4.6 Summary 60

5. Discussion 71

5.1 Introduction 71

5.2 Laboratory Tests 71

5.3 Numerical Analysis 77
5.4 Current Design Standards 80
5.5 Proposed Capacity Equations 84
5.6 Resistance Factor Assessment 87
5.7 Summary 92

6. Summary, Conclusions, and Recommendations 106
6.1 Summary 106
6.2 Conclusions and Recommendations 107

References 110

Appendix A: Single-Angle Connections with Slotted Holes 113
A.1 Introduction 114
A.2 Description of Test Specimens 114
A.3 Description of Test Set-up 116
A.4 Instrumentation 116
A.5 Specimen Installation and Test Procedure 117
A.6 Test Results 117
A.7 Conclusions and Recommendations 120

List of Tables

Table 3-1: As-Built Connection Dimensions 26
Table 3-2: As-Built Beam Dimensions 27
Table 3-3: Test Parameters Summary 27
Table 3-4: Material Properties 28
Table 3-5: Test Results Summary 30
Table 4-1: Analysis–Laboratory Test Associations 62
Table 4-2: Material Properties Summary 62
Table 4-3: Critical Strains Summary 62
Table 4-4: Finite Element Analysis Results Summary 63
Table 5-1: Professional Factors for Existing Design Standards 94
Table 5-2: Professional Factors for Proposed Design Equations 95
Table 5-3: Parameters for Resistance Factor Calculations 95
Table 5-4: Load Factors and Modification Factors 96
Table 5-5: Resistance Factors Required for Safety Index of 4.5 96
Table 5-6: Safety Indices Provided by Design Equations 96
Table A-1: As-Built Connection Dimensions 122
Table A-2: Test Results Summary 123
Table A-3: Predicted Capacity Summary 123

List of Figures

Figure 3-1: Nominal Connection Properties 31
Figure 3-2: Elevation of Test Set-up 33
Figure 3-3: Plan of Test Set-up 34
Figure 3-4: Section of Test Set-up at Loading Frame 35
Figure 3-5: Section of Test Set-up at Reaction Frame 35
Figure 3-6: Instrumentation Layout 36
Figure 3-7: Failed Connections 37
Figure 3-8: Load vs. Block Shear Deformation Curve, Test A1 40
Figure 3-9: Load vs. Block Shear Deformation Curve, Test A2 40
Figure 3-10: Load vs. Block Shear Deformation Curve, Test B1 41
Figure 3-11: Load vs. Block Shear Deformation Curve, Test B2 41
Figure 3-12: Load vs. Block Shear Deformation Curve, Test C1 42
Figure 3-13: Load vs. Block Shear Deformation Curve, Test C2 42
Figure 3-14: Load vs. Block Shear Deformation Curve, Test D1 43
Figure 3-15: Load vs. Connection Deflection Curve, Test D2 43
Figure 3-16: Load vs. Block Shear Deformation Curve, Test E1 44
Figure 3-17: Load vs. Block Shear Deformation Curve, Test E2 44
Figure 3-18: Load vs. Block Shear Deformation Curve, Test F1 45
Figure 3-19: Load vs. Block Shear Deformation Curve, Test G1 45
Figure 3-20: Load vs. Block Shear Deformation Curve, Test G2 46
Figure 3-21: Load vs. Block Shear Deformation Curve, Test H1 46
Figure 3-22: Load vs. Block Shear Deformation Curve, Test H2 47
Figure 3-23: Load vs. Block Shear Deformation Curve, Test J1 47
Figure 3-24: Load vs. Block Shear Deformation Curve, Test J2 48
Figure 4-1: Typical Beam Mesh, Isometric 64
Figure 4-2: Typical Bolt Hole Mesh Detail 64
Figure 4-3: Typical Transition Mesh Detail 65
Figure 4-4: Bolt Modelling Methods 65
Figure 4-5: Material Model Definition, Model M5 66
Figure 4-6: Load vs. Block Shear Deformation Curve, Model M1 66
Figure 4-7: Load vs. Block Shear Deformation Curve, Model M2 67

Figure 4-8: Load vs. Block Shear Deformation Curve, Model M3 67
Figure 4-9: Load vs. Block Shear Deformation Curve, Model M4 68
Figure 4-10: Load vs. Block Shear Deformation Curve, Model M5 68
Figure 4-11: Load vs. Block Shear Deformation Curve, Model M1-B-Max 69
Figure 4-12: Load vs. Block Shear Deformation Curve, Model M1-B-Int 69
Figure 4-13: Load vs. Block Shear Deformation Curve, Model M2-B-Max 70
Figure 4-14: Load vs. Block Shear Deformation Curve, Model M3-I 70
Figure 5-1: Load vs. Deformation Results, End Rotation Series 1 97
Figure 5-2: Load vs. Deformation Results, End Rotation Series 2 97
Figure 5-3: Load vs. Deformation Results, End Rotation Series 3 97
Figure 5-4: Load vs. Deformation Results, Gross Shear Area Series 98
Figure 5-5: Load vs. Deformation Results, Edge / End Distance Series 98
Figure 5-6: Load vs. Deformation Results, Bolt Diameter Series 98
Figure 5-7: Load vs. Deformation Results, Section Depth Series 99
Figure 5-8: Load vs. Deformation Results, Connection Depth Series 99
Figure 5-9: Load vs. Deformation Results, Number of Bolt Rows Series 99
Figure 5-10: Load vs. Deformation Results, Number of Bolt Lines Series 100
Figure 5-11: Load vs. Deformation Results, Double Cope Series 100
Figure 5-12: Load vs. Deformation Results, Repeatability Series 100
Figure 5-13: Tension Face Stress Distributions, One-line Connections 101
Figure 5-14: Tension Face Stress Distributions, Two-line Connections 101
Figure 5-15: Test vs. Predicted Capacities, CAN/CSA–S16.1–94 102
Figure 5-16: Test vs. Predicted Capacities, CSA–S16–01 102
Figure 5-17: Test vs. Predicted Capacities, AISC LRFD 1999 103
Figure 5-18: Test vs. Predicted Capacities, Eurocode 3 ENV 1993-1-1 103
Figure 5-19: Test vs. Predicted Capacities, AIJ 1990 104
Figure 5-20: Test vs. Predicted Capacities, Proposed 1 104
Figure 5-21: Test vs. Predicted Capacities, Proposed 2 105
Figure 5-22: Test vs. Predicted Capacities, Proposed 3 105
Figure A-1: Nominal Connection Properties 124
Figure A-2: Additional Connection Instrumentation 125
Figure A-3: Connections Failed in Pure Shear 126
Figure A-4: Connections Failed by Bolt Bearing and Tilting 127

Figure A-5: Load vs. Deflection Curve, Test I 128
Figure A-6: Load vs. Deflection Curve, Test II 128
Figure A-7: Load vs. Deflection Curve, Test III 129
Figure A-8: Load vs. Deflection Curve, Test IV 129
Figure A-9: Load vs. Deflection Curve, Test V 130
Figure A-10: Twist vs. Deflection Curve, Test I 130
Figure A-11: Twist vs. Deflection Curve, Test II 131
Figure A-12: Twist vs. Deflection Curve, Test III 131
Figure A-13: Twist vs. Deflection Curve, Test IV 132
Figure A-14: Twist vs. Deflection Curve, Test V 132

Nomenclature

Abbreviations

AIJ	Architectural Institute of Japan
AISC	American Institute for Steel Construction
ASCE	American Society of Civil Engineers
ASTM	American Society for Testing and Materials
CSA	Canadian Standards Association
EC3	Eurocode 3
ECS	European Committee for Standardization
FEA	Finite Element Analysis
HSS	Hollow Structural Section
LRFD	Load and Resistance Factor Design
NRCC	National Research Council Canada

Definitions

Bolt Line	A series of bolts parallel to the direction of the applied load
Bolt Row	A series of bolts perpendicular to the direction of the applied load
Cope Depth	The cut-back distance from the top of the top flange to the top of the web
Cope Length	The cut-back distance from the edge of the beam to the edge of the top flange
Edge Distance	The distance perpendicular to the applied load from the centre of the bolt hole in the line of bolts closest to the beam edge to the edge of the beam
End Distance	The distance parallel to the applied load from the centre of the top bolt hole to the top of the beam web at the cope
Professional Factor	The ratio of the test ultimate load to the predicted ultimate load calculated from a capacity equation
Shear Face	The area of the connection block parallel to the applied load which resists load through shear stresses
Tension Face	The area of the connection block perpendicular to the applied load which resists load through tensile stresses

Symbols

A_{final}	= minimum cross-sectional area of a tension coupon at fracture (mm^2)
A_{gt}	= gross tension area (mm^2)
A_{gv}	= gross shear area (mm^2)
A_{init}	= initial cross-sectional area of a tension coupon (mm^2)
A_{nt}	= net tension area (mm^2)
A_{nv}	= net shear area (mm^2)
b	= flange width (mm)
d	= overall section depth (mm)
d_b	= bolt diameter (mm)
d_c	= cope depth (mm)
d_h	= bolt hole diameter (mm)
E	= elastic (Young's) modulus (MPa)
e_g	= edge distance (mm)
e_s	= end distance (mm)
F_y	= yield strength (MPa)
F_u	= tensile strength (MPa)
g	= transverse spacing (gauge) between bolt lines (mm)
k	= distance from outer face of flange to web-toe of fillet (mm), tension area coefficient for Eurocode 3 ENV1993–1–1
l_c	= cope length (mm)
L_{gt}	= gross tension length (mm)
M_y	= yield moment (kN·m)
P	= ultimate connection capacity (kN)
P_r	= factored ultimate connection capacity (kN)
R_t	= tension face stress reduction factor
s	= longitudinal spacing (pitch) between bolt rows (mm)
S_x	= beam section modulus about strong axis (mm^3)
t	= flange thickness (mm)
w	= web thickness (mm)
V_G	= coefficient of variation of ρ_G
V_M	= coefficient of variation of ρ_M

V_P = coefficient of variation of ρ_P

V_R = coefficient of variation of ρ_R

Y_{M0} = partial safety factor

α_R = separation variable for resistance

β = safety index

γ_D = load factor for dead loads

γ_E = load factor for uncertainties in analysis

γ_L = load factor for live loads

γ_{max} = maximum shear strain

γ_{max}^{crit} = critical maximum shear strain

$\varepsilon_{pr,max}$ = maximum principal strain

$\varepsilon_{pr,min}$ = minimum principal strain

ε_{nom}^{crit} = nominal (engineering) failure strain, nominal strain of a tension coupon at fracture

$\varepsilon_{true}^{crit}$ = maximum principal true failure strain, true strain of a tension coupon at fracture

ε_{true}^{p} = true plastic strain

ρ_G = ratio of mean measured to nominal connection geometric properties

ρ_M = ratio of mean measured to nominal material strength

ρ_P = mean professional factor

ρ_R = ratio of mean to nominal connection capacity

σ_{nom} = nominal (engineering) stress (MPa)

σ_{true} = true stress (MPa)

ϕ = resistance factor

Φ_β = modification factor for ϕ

1. Introduction

1.1 Statement of Problem

Block shear is a connection failure mechanism, most commonly associated with bolted connections, in which a block of material is torn out in a combination of tensile and shear failures. It can be the governing failure mode for gusset plates, angles, and coped beams. A beam is coped when a short length of one or both of the flanges has been removed near the connection to facilitate construction or for compatibility with adjoining structural members. In coped beams with bolted double-angle header connections, the removal of the top flange increases the susceptibility of the web to block shear failure, often making it the governing connection failure mode.

Historically, block shear failure of coped beams has not been well understood. Due to the relatively small number of full-scale tests completed on coped beams, capacity equations are largely based on tests of block shear failure of gusset plates, upon which a significant number of tests have been completed. Although the two failure mechanisms are similar, there are marked differences. The effects of beam end rotation and the asymmetric stress distribution on the block that are not present in typical gusset plates may be influential in the load carrying capacity of coped beams. Examination of current design standards by Kulak and Grondin (2000, 2001) showed that none of the strength models currently in use accurately and consistently predicts block shear failure.

Within the limited number of tests completed on coped beam connections, few connection parameters have been systematically investigated. These include the effects of end and edge distances, number of bolt rows and lines, and double coped specimens. Many other connection parameters exist whose effects need to be quantified to predict accurately block shear failure, including the effects of bolt spacing, connection depth, section depth, and bolt diameter. Most importantly, the effect of beam end rotation needs to be studied as this may adversely affect connection capacity, a parameter that has not been investigated in previous research. Furthermore, only linear elastic finite element analyses have been completed on the topic, even though extensive non-linear material behaviour is expected by the time the

connection reaches its capacity. Therefore, a rigorous research program consisting of both laboratory tests and numerical analyses was required to understand better the block shear failure mode in coped beams.

1.2 Objectives and Scope

The objective of this work was to examine the behaviour of connections on coped wide-flange beams and the effect of many connection parameters on that behaviour. Within this context, existing design equations were to be evaluated to assess the level of safety currently being provided. This was completed through laboratory tests, numerical analyses, and statistical examinations of the resistance of tested connections predicted by existing design standards. Ultimately, a recommendation of an appropriate design model was made. Each of these items is briefly discussed below.

Prior to the research described herein, only 19 full-scale coped beam tests had been completed. Furthermore, as discussed above, few connection parameters had been examined systematically. Existing design equations are inconsistent in their ability to predict the capacities of the 19 tests and, in particular, the strength of two-line connections is often over-predicted. To provide the foundation for a comprehensive evaluation of the existing design equations, the research program commenced with 17 laboratory tests. The effects of many connection parameters were examined including end and edge distances, bolt layout, bolt diameter, and a double cope (a connection with both the top and bottom flanges removed). The effect of connection end rotation was also investigated, a parameter that had not been studied previously. A change in stress distribution may be associated with the rotation of the connection and this may, in turn, affect the connection capacity and ductility. This effect needed to be fully examined to define accurately the failure mechanism. The load vs. deformation response for each connection was recorded.

Following the experimental program, models of five of the connections tested in the laboratory were analyzed using a general purpose non-linear finite element program. The connections modelled were chosen to encompass a wide range of

connection parameters. Attempts were made to predict accurately the load vs. deformation behaviour of these connections as well as the connection load capacity. Various modelling methods were implemented including different bolt models and web tearing procedures. The effect of the initial bolt bearing condition, *i.e.*, the location of the bolts in the holes at the beginning of the test, on initial connection stiffness was also investigated.

The laboratory tests from this research program were combined with those of others to examine critically the existing design standards for conservativeness and consistency in capacity prediction. Additionally, the level of safety being provided by each standard was evaluated. Three new design equations are presented and compared with existing strength models. For each design method, the level of safety being provided was evaluated through the determination of the associated safety index. The resistance factor needed to provide the target level of safety commonly used for connections in the development of steel design standards was also evaluated. Based on the accumulated experimental, numerical, and statistical work, a design equation is recommended for predicting the block shear capacity of coped beams.

An additional series of tests was completed to examine the behaviour of single-angle connections with slotted holes and without plate washers. Using the same test apparatus as that used in the block shear tests, five connections were tested to failure to investigate the pull-out failure model, wherein the bolt head or nut pulls through the deformed bolt holes without fracturing either of the connection elements. No research has been completed to ensure that this failure mode does, in fact, occur, when the restraining effect of plate washers is not present.

1.3 Organization of Thesis

The thesis is separated into six chapters. Chapter 2 reviews research previously completed on block shear failure of coped steel beams, summarizing and discussing the major findings from each of the research programs. Capacity equations proposed by others for the general case of block shear are presented, as are the equations prescribed by current design standards from North America, Europe, and Japan. The

laboratory research program is discussed in Chapter 3. Details of the test specimens, material properties, test apparatus, instrumentation, and test procedure are presented. Test results are shown in the form of connection load vs. deformation curves and briefly discussed. Chapter 4 outlines the models examined in the non-linear finite element analyses. The material model used for each analysis is described and the analysis procedure is summarized. Load vs. deformation curves are presented for each analysis and compared to the associated laboratory test results. The results of the laboratory tests and numerical analyses are discussed in Chapter 5. The effects of the connection parameters studied are quantified and the numerical results are interpreted. A critical analysis of the design standards listed in Chapter 2 is presented and three new design models are introduced. Finally, a summary of the work completed is given in Chapter 6 and conclusions about the behaviour of coped beam connections are drawn. Recommendations for future research are made and a new design equation is recommended. The test procedure and results of the single-angle, slotted hole connection tests are presented in Appendix A.

2. Literature Review

2.1 Introduction

Historically, block shear failure of coped beams has not been well understood. Testing and analysis of these connections is limited and, as such, capacity equations have been largely based on the results of research on block shear failure of gusset plates. Although the two failure mechanisms are similar, there are marked differences including the effect of beam end rotation and the asymmetric stress distribution on the block. These factors are not present in gusset plates and may be influential in the load carrying capacity of coped beams. Prior to the experimental program reported herein, only 19 laboratory tests and nine numerical analyses had been completed. A review of this work and of the block shear capacity equations currently being used in the design of coped beams follows.

2.2 Laboratory Tests and Numerical Analyses

Birkemoe and Gilmor (1978) first identified block shear failure in coped beams. The authors tested one coped beam and one uncoped beam as part of a study on double-angle beam-to-column connections. These tests were prompted largely by a significant increase in allowable bolt bearing stresses in the standards of the day (*e.g.*, CAN/CSA–S16–74), making certain connections more susceptible to failure by block shear. The three-bolt, single-line connections were identical but for a 150 mm long cope and fabricated on the same CAN/CSA–G40.21 grade 300W W460x67 beam. Each connection was loaded to its ultimate capacity in a nearly pure shear condition resulting in little beam end rotation. Inspection of the coped specimen after the tests revealed that the tension face had necked and cracked and the web had locally buckled at the cope. The ultimate capacity of the coped connection was 24% lower than that of the uncoped connection, and it was recognized that new design equations were required to account for this reduction. The authors suggested that the block shear strength be the sum of the shear resistance acting over the shear area and the tensile resistance acting over the tension area, but gave no definitive equation.

Yura *et al.* (1982) carried out research on wide-flange beams supported by double-angle connections, some of which incorporated slotted holes. Of the nine tests

completed, three were coped beams that failed in block shear. As with the work of Birkemoe and Gilmor, the connections were tested predominantly in shear, with little beam end rotation. The tests were all single-line connections on ASTM grade A36 W460x89 beams and the variables were end distance and slot length. An increase in end distance from 25 mm to 50 mm resulted in a 16% increase in capacity, and a connection with 48 mm x 21 mm slots showed a 16% reduction in capacity over one with 21 mm round holes. No recommendations on capacity prediction were reported.

Shortly thereafter, Ricles and Yura (1983) completed eight additional double-angle connection tests. Of these, seven were coped beams and all had two lines of bolts on ASTM grade A36 W460x89 beams. The major variables were end and edge distance, slot length, and number of holes. All connections failed in block shear and the web buckled at the cope in four of the specimens. The results indicated that increasing the end distance from 25 mm to 50 mm increased capacity by 10%, while the same increase in edge distance increased capacity by 18% to 37% leading to the conclusion that edge distance has a greater effect on capacity than does end distance. A connection with 49 mm x 21 mm slotted holes had a 9% lower capacity than one with 21 mm round holes. Tests of two-line connections showed that capacity is not affected by the number of bolt holes on the shear face, indicating that the shear component of the resistance is likely developed over the gross section rather than the net section. The authors suggested that more three- and four-bolt pattern connections be tested to fully understand this effect.

Following the full-scale tests, Ricles and Yura (1983) analyzed nine two-dimensional linear elastic finite element models. The authors modelled eight two-line specimens, similar to those from their laboratory program, as well as one single-line configuration. The models consisted of the entire beam as well as the double-angle connections and were loaded to 445 kN. Elastic stress distributions along the shear and tension faces of the connections were plotted and analyzed. In general, for two-line connections, the shear stress distribution was found to be nearly constant. Along the tension face, the normal stress distribution was found to be nearly linear for connections with minimum edge distance, varying from a maximum at the beam edge

to a value close to zero at the furthest bolt line. For connections with a larger edge distance, the stress distribution can be approximated as bi-linear, with the maximum stress occurring near the first line of holes. The authors proposed the following capacity equation based on the calculated stress distributions and test observations:

$$P = 0.5A_{nt}F_u + 0.6A_{gv}F_y \qquad [2\text{-}1]$$

where:

P is the ultimate connection capacity (kN),
A_{nt} is the net tension area (mm^2),
F_u is the tensile strength (MPa),
A_{gv} is the gross shear area (mm^2), and
F_y is the yield strength (MPa).

Equation 2-1 implies that the connection capacity is the sum of a triangular normal stress block on the net area of the tension face and shear yielding on the gross shear area. The authors suggest that this is appropriate for connections with minimum edge distance and conservative for larger edge distances. The equation produces reasonable predictions when compared to the full-scale tests completed by Ricles and Yura.

Aalberg and Larsen (2000) tested eight coped beam specimens—four each with single and double copes. Welded I-shaped beams were fabricated using normal and high strength steel plates (Grades S355 and Weldox 700, respectively) for the webs with three connection configurations. The tests utilized a double shear tab connection in which two plates were welded to the reaction column and bolted to the beam. A short shear span was used, minimizing beam end rotation, and the specimens were loaded until both the tension and shear faces had ruptured. The data showed that the onset of failure occurred at a similar displacement in all cases, irrespective of the steel strength (vertical displacement of the top flange at the cope was measured). The authors compared the results to Canadian, American, and European standards and

showed that, in general, the design standards are inconsistent in their predictions of connection capacity. No comment on the adequacy of these equations is made.

2.3 Capacity Equations

Several authors have critically examined block shear capacity prediction equations. Hardash and Bjorhovde (1985) completed the first such analysis and, although their work was specific to gusset plates, the results can be applied to block shear in general. It was found that if the stress on the tension face at the connection capacity is assumed to be the material tensile strength and to act over the net area, then the shear stress can be assumed to act on the gross area with an average magnitude, F_{eff}, that lies between the yield and tensile strengths. The authors found that F_{eff} varies linearly with connection length. A regression curve was fit to the laboratory data to quantify this relationship and an equation was proposed. The authors suggest that the connection capacity be the sum of the ultimate strength acting over the net tension area and the effective shear strength acting over the gross shear area. Although this work is not derived based on coped beam tests, a similar method could be applied to coped beams to derive a capacity equation.

Cunningham *et al.* (1995) examined the effects of block aspect ratio and in-plane eccentricity by studying experimental data from the literature. It was found that neither of these factors affects the tension component of the resistance, but both have a significant effect on the shear component. However, for connections with a high aspect ratio (*i.e.*, $A_{nv}/A_{nt} > 5.0$, where A_{nv} is the net shear area (mm^2)), these may have no effect on the ultimate strength. Most single-line coped beam connections with minimum edge distance have a block aspect ratio greater than five, while two-line connections tend to have smaller aspect ratios. The authors, therefore, note the need for more tests of connections with high block aspect ratios. They also conclude that the shear rupture constant of 0.6 may not accurately predict the shear contribution of the connection capacity. This supports the similar conclusion made by Hardash and Bjorhovde (1985).

Kulak and Grondin (2000, 2001) examined capacity equations from Canadian, American, European, and Japanese design standards. It was found that, in general, the equations predicted ultimate loads for gusset plates relatively accurately but were inconsistent in the predictions for coped beams. The authors suggest that the single shear plane present in coped beams creates a rotation of the block and results in a non-uniform stress distribution, an effect that may reduce the connection capacity. On this basis, the authors suggest a reduction factor of 0.5 for the tension contribution, as proposed previously by Ricles and Yura (Equation 2-1), to account for this.

2.4 Design Standards

The block shear capacity equation for coped beams in the previous edition of the Canadian standard, CAN/CSA–S16.1–94 (CSA, 1994), assumes that the ultimate tensile strength of the net tension area and the ultimate shear strength of the net shear area can be reached simultaneously:

$$P_r = 0.85\phi(A_{nt}F_u + 0.6A_{nv}F_u) \qquad [2\text{-}2]$$

where:

P_r is the factored ultimate connection capacity (kN), and
ϕ is the resistance factor.

The equation combines a resistance factor, ϕ, equal to 0.90 with a further reduction of 0.85. This additional factor reduces the probability of failure to an acceptable level for connections. However, it was shown by Kulak and Grondin (2001) that this equation can overestimate capacity by as much as 50%.

Based on the recommendations of Kulak and Grondin (2001), the most recently published edition of the Canadian standard, CSA–S16–01 (CSA, 2001), provides two equations wherein the contribution of the tension area to the connection capacity is reduced by one-half:

$$P_r = \phi(0.5A_{nt}F_u + 0.6A_{gv}F_y) \quad [2\text{-}3]$$

$$P_r = \phi(0.5A_{nt}F_u + 0.6A_{nv}F_u) \quad [2\text{-}4]$$

The standard states that the lesser of the two equations should be used as the connection capacity. This first equation assumes that when the connection reaches its capacity, the net tension area has a non-uniform stress distribution with a mean stress of $0.5\,F_u$ and the gross shear area is at the shear yield stress, while the second equation limits the shear contribution to rupture of the net shear area. The resistance factor, ϕ, remains as 0.90, but the reduction factor of 0.85, present in the 1994 standard, is not present in this edition. This equation results in more conservative and consistent predictions of capacity than provided by Equation 2-2.

The American standard, AISC LRFD 1999 (AISC, 1999), utilizes two equations, the use of which is dependent on the relative ultimate strengths of the tension and shear net areas of the connection:

for $A_{nt}F_u \geq 0.6A_{nv}F_u$:

$$P_r = \phi(A_{nt}F_u + 0.6A_{gv}F_y) \leq \phi(A_{nt}F_u + 0.6A_{nv}F_u) \quad [2\text{-}5]$$

for $A_{nt}F_u < 0.6A_{nv}F_u$:

$$P_r = \phi(A_{gt}F_y + 0.6A_{nv}F_u) \leq \phi(A_{nt}F_u + 0.6A_{nv}F_u) \quad [2\text{-}6]$$

where:

A_{gt} is the gross tension area (mm^2).

The combination of ultimate stress on the net tension area and yielding on the gross shear area is logical (Equation 2-5), but the qualifying statement effectively precludes it from being used; in coped beams, the ultimate strength of the tension area is often much smaller than that of the shear area. Equation 2-6 combines yielding on the gross tension area and rupture of the net shear area, which seems unlikely and is not supported by laboratory test observations. In both equations, the capacity is limited by rupture of both the tension and shear net areas. The standard employs a resistance

factor of 0.75, which is comparable to the combined factor used in CAN/CSA–S16.1–94.

Eurocode 3 ENV 1993–1–1 (ECS, 1992) utilizes a series of equations for the capacity prediction of block shear in coped beams. When the equations are combined, a single equation can be derived:

$$P_r = \frac{1}{Y_{M0}}\left(\frac{1}{\sqrt{3}} w(L_{gt} - kd_h)F_u + \frac{1}{\sqrt{3}} A_{gv}F_y\right) \qquad [2\text{-}7]$$

where:

Y_{M0} is the partial safety factor,
w is the web thickness (mm),
L_{gt} is the gross tension length (mm),
k is the tension area coefficient, and
d_h is the bolt hole diameter (mm).

The equation combines shear yielding acting over the gross shear area with a reduced normal stress acting over the tension area. The factor k is assigned the value of 0.5 for one-line connections and 2.5 for two-line connections. This results in using the net tension area for one-line connections but is a smaller area for two-line connections. The justification for this and for the reduction of the normal stress by $1/\sqrt{3}$ is unknown. The partial safety factor, Y_{M0}, is given as 1.1, resulting in a resistance factor similar to that used in CSA–S16–01.

The Architectural Institute of Japan's Standard for Limit States Design of Structures (Draft) (AIJ, 1990) provides a procedure that is, theoretically, more conservative than any of the others presented. It combines tensile and shear stresses acting over net areas in two equations for unfactored resistance presented below:

$$P = A_{nt}F_u + \frac{1}{\sqrt{3}} A_{nv}F_y \qquad [2\text{-}8]$$

$$P = A_{nt} F_y + \frac{1}{\sqrt{3}} A_{nv} F_u \qquad [2\text{-}9]$$

The lesser of the two equations is to be taken as the block shear capacity. Although there is little support in the literature for the combination of yield stresses acting over net areas, the equations provide a theoretically conservative estimate of capacity.

2.5 Summary

It has been shown (Kulak and Grondin, 2000, 2001) that existing design standards overestimate the capacity of many of the tests described above. The relatively small number of laboratory tests and numerical analyses makes it difficult to define a method that closely reflects the true behaviour of these connections. Many important connection variables have been considered in the experiments completed prior to the research presented herein, but some important factors have not yet been investigated. For example, the effect of beam end rotation on coped beam connection capacity was not studied in previous research. Given the limited data available, it is clear that more laboratory tests and a finite element study that includes non-linear effects are required. Analysis of current design equations for block shear of coped beams shows that in many cases an adequate level of safety is not being provided. Furthermore, the level of safety is not consistent among the various connection configurations studied. With further testing and an improved understanding of the connection behaviour, an appropriate level of safety can be provided.

3. Experimental Program

3.1 Introduction

In order to expand the available experimental database for block shear failure of coped steel beams, tests were completed on 17 full-scale connections. The test program includes parameters that have not been investigated prior to this research including the effect of beam end rotation arising from flexural deformations, bolt diameter, and section depth. Other parameters that have been investigated previously, such as end and edge distance and number of lines of bolts, were also examined. A summary of the connection properties, the test set-up, including instrumentation, and the test procedure follows. Load vs. deformation plots are also presented for each test. The experimental results were used to validate a non-linear finite element model for predicting block shear behaviour, as well as to assess the adequacy of current capacity equations. A discussion of the test results, the numerical analyses, and existing design equations is presented in Chapter 5.

3.2 Description of Test Specimens

Nine wide-flange beams of two sizes—eight W410x46 and one W310x60—were provided for the experimental program by Supreme Steel Ltd. of Edmonton, Alberta. Each beam was 3.6 m long with test connections fabricated at both ends. A two-character alphanumeric identifier was assigned to each connection as follows: the beams were each designated by a letter (A through J, excluding I) and each connection was designated by a number (1 or 2). As such, two W310x60 connections and 15 W410x46 connections (only one end of beam F was used) were tested. Beams A through G were sandblasted to remove surface rust, while beams H and J were not cleaned. Nominal dimensions for the 17 connections are shown in Figure 3-1. The top flange cope dimensions were fixed for all connections, with the cope length extending 50 mm past the line of bolts furthest from the beam end and the cope depth extending to 25 mm below the bottom of the top flange. Only beam D2 had the bottom flange coped as well. All bolt holes were punched and of standard size. As-built connection and beam dimensions are listed in Tables 3-1 and 3-2, respectively. Table 3-1 also depicts how "end" and "edge" distance, as well as

"rows" and "lines" of bolts, have been defined herein. To facilitate the interpretation of the test results, a list of tests in which only one parameter was varied is shown in Table 3-3. Nominal values of each parameter under examination are specified in the table.

Three series of tests were completed to investigate the effect of connection end rotation on block shear capacity and behaviour. The first series was completed on three identical single-line, four-bolt connections, each with a different applied end rotation: 0°, 2°, and 3.5°. This connection configuration represents a typical single-line connection in which the connection depth is a significant portion of the section depth remaining after coping—in this case, approximately 75%. The no rotation case was carried out as a baseline test to be compared with research previously completed. The intermediate rotation, 2°, was chosen to represent a rotation that might be expected in a real structure. The final case, a large rotation of 3.5°, was chosen to represent an extreme magnitude of rotation. This was determined to be near the upper limit of reasonable deformations and could occur in a long beam that is heavily loaded. The second series of tests in which only end rotation was varied used the same three rotation magnitudes. In this case, the connections had a single-line, three-bolt configuration, and the connection depth was only 50% of the section depth at the cope. The final end rotation series was completed on two-line, six-bolt connections and only two rotations were examined: 0° and 2°. This series investigated the effect of end rotation on a typical heavy, two-line connection. The largest rotation magnitude was excluded because such connections usually occur on shorter, heavily loaded beams for which flexural deformations are relatively small. Early results (*i.e.*, end rotation series one) indicated that end rotation likely did not affect these connections significantly and, therefore, all tests in which end rotation was not a parameter were completed with no applied end rotation. In these cases, the beam reaction support was not lowered during the test.

A series of tests was completed to determine over which area the shear stresses develop on the block: gross shear area or net shear area. This was completed by comparing tests B2 and C1, which had identical net tension areas and net shear areas,

but different gross shear areas. The three-bolt connection, C1, had slightly larger bolt row spacing than the four-bolt connection, B2, in order that the two connections had identical net shear areas. This resulted in a larger gross shear area for Connection B2 (1750 mm^2) than for Connection C1 (1603 mm^2). Comparing the response of these two connections would indicate the governing shear area.

All connections used minimum end and edge distances, namely 25 mm for 19.1 mm (3/4") bolts and 32 mm for 25.4 mm (1") bolts, except for the two tests specifically investigating these parameters. Connection E1 had an edge distance of 50 mm, a typical value used by local fabricators for increased edge distance for 19.1 mm bolts. The connection configuration was identical to Connection B2 apart from the increased edge distance. The end distance was increased on Connection E2 to 50 mm. Again, the connection was identical to Connection B2 apart from the increased end distance. The effect of both end distance and edge distance has been examined previously by Yura *et al.* (1982) and Ricles and Yura (1983). The parameters were included in this study to increase the data pool of available tests and to assess consistency in results between research projects. As well, increases in end and edge distance constitute the simplest and most widely used method to increase the capacity of these connections and it is, therefore, important to gain a full understanding of these effects.

Standard 19.1 mm (3/4") bolts were used for all connections except Connection D1 in which 25.4 mm (1") bolts were used. Connections C1 and D1 were both three-bolt, single-line connections and the bolt row spacing was varied slightly such that the net shear areas were identical. Both connections used minimum end and edge distances—25 mm for C1 and 32 mm for D1. Bolt diameter had not been investigated as a parameter in previous research with all prior tests being completed with either 19.1 mm or 20 mm bolts.

Two section depths were used in this research—W410x46 and W310x60—with similar web thicknesses—7.0 mm and 7.5 mm, respectively. Identical three-bolt, single-line connections were fabricated on the two sections to investigate the effect of

section depth on block shear behaviour. A small variability in the ultimate capacities was expected, due to the difference in the web thicknesses, but any significant variation would indicate that section depth plays a role in block shear capacity. Different section depths have been tested in previous research, but the effect on block shear behaviour has not been explicitly investigated.

Two three-bolt, single-line connections with different bolt row spacing were tested, resulting in connections with varying connection depths. A difference in ultimate capacity was expected given that Connection C1 had a significantly larger shear area than Connection F1. However, any variation in capacity or behaviour that could not be attributed to this would indicate a change in the load carrying system due to the change in connection depth. It is possible that the stress distributions on the tension and shear faces of the block would be affected by this change in geometry.

The number of bolt rows was varied between Connections B2 (four rows) and F1 (three rows) with all other parameters constant, including bolt row spacing. As with the connection depth tests, this series was intended to investigate the effect of geometry on connection capacity, and a difference in ultimate capacity was expected due to the larger shear area of Connection B2.

A similar set of tests was completed investigating the effect of the number of bolt lines. Connections C1 and C2 both had three rows of bolts, but with one and two lines of bolts, respectively. Although many two-line connections have been tested previously, this was the first series of tests to directly examine the effect.

The shear behaviour of these connections was investigated through the test of a double coped specimen, *i.e.,* a connection with both the top and bottom flanges coped. Connection D2 was identical to Connection E1, but for the bottom cope. A bottom end distance of 25 mm was chosen to ensure that this connection would fail by pure shear, rather than block shear. By removing the tension component of the resistance, the shear component could be identified and examined. One limitation of this method is that the restraint provided by the bottom flange and the web that are present in the single coped specimen are not present in the double coped specimen, which may lead

to a different distribution of stress along the shear face. However, double coped connections occur in real structures and few such tests have been completed.

To assess repeatability of the test results, two identical connections were tested on the opposite ends of the same W310x60 beam. Since the connection geometry was nominally identical and the material properties were unlikely to vary significantly between the beam ends, this provided an opportunity to examine the testing procedure for consistency.

Two additional tests were completed that are not listed in Table 3-3. Test A1 was intended to be an additional test of repeatability to be compared with Connection B2. However, problems with the loading frame during the test did not allow the test to be completed and total block shear failure did not occur due to localized distortion at the cope. Connection J2, on the other hand, was included in the research program simply to expand the data pool of applicable tests. The two-line, four-bolt connection represents a compact two-line connection, a configuration that had not been previously examined.

Bolted double-angle header connections were used with L127x127x9.5 angles for connections with a single line of bolts and 10 mm thick bent plates for the two-line connections. The bent plate was used since an angle with sufficient leg size could not be provided. As with the bolt holes in the beam webs, holes were punched and of standard size.

3.3 Material Properties

Tension coupons were fabricated from the web of each beam to determine the material properties. After the connection tests were completed, material samples were cut from the midspan of the beam, a location that remained elastic throughout the tests. The coupons were oriented transverse to the axis of the beam in all cases except for beam G where the reduced section depth necessitated cutting the coupons in a longitudinal orientation. A second sample was taken from beam B in the longitudinal direction to assess variability of the material properties in the two orthogonal directions. The designation B(2) was given to these specimens.

Three sheet-type coupons were fabricated and tested from each material sample according to ASTM standard A370 (ASTM, 1997). Stress was calculated as the specimen load divided by the initial area of the coupon, while strain was measured using an extensometer with a 50 mm gauge length. Static readings were taken on the yield plateau, along the hardening curve, and at the tensile strength.

A summary of the test results is shown in Table 3-4. For beams F, G, and H, only two of the three coupons are shown because a combination of technical and human errors resulted in the loss of data for the third. The results of the two remaining material tests for each beam were, in themselves, consistent and it was therefore determined that additional coupons did not need to be fabricated and tested. The elastic modulus was calculated by applying a linear regression analysis to the elastic portion of the test data. Two to four static points were taken along the yield plateau to define the static yield stress, and mean of these values is given in the table. The Static Ultimate Stress is the stress from the static reading taken near the ultimate load. The stress in the coupon determined from the final load reading taken just prior to fracture is shown as the Failure Stress. The strain at the end of the linear portion of the stress vs. strain curve is shown as the Yield Strain and the Hardening Strain is the strain at the end of the yield plateau. The strain at the peak stress during the test is listed under the Ultimate Strain column, while the strain at fracture is shown as the Failure Strain. The Reduction of Area is calculated from the initial and final cross-sectional dimensions as per ASTM standard A370 (ASTM, 1997). Mean values of all these parameters for each beam are also listed in the table.

Material properties meet the requirements of CAN/CSA–G40.21–98 350W steel (CSA, 1998) for all beams except beam H, which had a tensile strength below the prescribed minimum. The yield point for this beam, however, was above the minimum set in the standard. No significant differences in strength were noted between the longitudinally and transversely oriented coupons of beam B, although the longitudinally oriented specimens exhibited slightly more ductility.

3.4 Description of Test Set-up

The test set-up was designed to ensure a block shear mode of failure and to simulate a typical beam-to-column connection. The inclusion of end rotation as a parameter in this study necessitated a method to control it accurately. As such, a hydraulic jack was used as the opposite reaction instead of the fixed support condition used in previous research that prevented vertical displacement. Lowering the jack as the load was applied simulated the rotation of the connection due to beam action. The test set-up is shown in Figures 3-2 through 3-5.

The beam was connected to the reaction column through a conventional double-angle connection. New 19.1 mm (3/4") or 25.4 mm (1") A325 bolts were used in each test to connect the beam to the angles and in all cases the threads were not in either shear plane. A 12.7 mm (1/2") cover plate was attached to each of the angles on the column-side leg to reduce the angle deformation. These plates supplied additional strength to resist the bending of the angles away from the column. The connection was in bearing prior to the application of load to the beam and the bolts were tightened to the snug-tight condition as described in CSA–S16–01 (CSA, 2001). A minimum factor of safety of 1.8 against angle failure was used to ensure that, during the test, failure would occur in the beam.

A vertical load was applied to the beam approximately 350 mm from the connection with an 890 kN hydraulic jack. A roller and knife edge assembly was installed between the jack and the beam to prevent longitudinal and rotational restraint. An identical 890 kN hydraulic jack was placed at the far end of the beam as the reaction point. A roller and knife edge assembly was also installed at that support. Electronic load cells were used in both the loading and support assemblies to measure forces at these locations. The loading jack was controlled with an air-driven hydraulic pump, while the reaction support was controlled with a hand pump.

Lateral supports were provided at two locations—at the reaction end (opposite end to the test connection) and at the load point. The reaction end lateral supports were provided by steel wheel assemblies clamped to the top flange of the beam and

bearing against adjacent support columns. The load point supports were provided by a steel wheel assembly attached to the adjacent column and bearing against an HSS 51x25x3.2 clamped vertically to the edges of the beam flanges. In both locations, supports were provided on both sides of the beam. For tests with two lines of bolts and for the double coped specimen, an additional lateral support was provided at the cope using an assembly similar to that used at the load point. Details of the lateral supports can be seen in Figures 3-4 and 3-5. The lateral support assemblies were designed with wheels to provide lateral restraint, while minimizing friction. Nevertheless, the supports were tapped with a rubber mallet at regular intervals during the test to release any small frictional forces that might have developed.

Stiffeners were provided at the load point for Tests C2 and J1. The large capacity of these connections required 300x60x16 mm stiffeners welded on both sides of the beam to prevent localized deformations from occurring. For the remaining tests, two full-depth HSS 76x51x4.8 were clamped to the web on either side to prevent local web crippling.

3.5 Instrumentation

Electronic measurements of load, deflection, rotation, and strain were taken during the test. In addition, lateral displacements were monitored manually. Forces in the loading and reaction jacks were measured using 890 kN load cells. Deflection measurements were taken at four locations using cable transducers with the connection deformation assessed through two measurements of vertical deflection. One cable transducer was mounted to the bottom flange directly below the line of bolts nearest the beam end and a second was mounted to the top of the web directly above the same line of bolts. The difference in these two displacements was taken as the deformation of the web alone. This includes only deformation of the block and does not include connection slip, bolt bearing distortions, or angle deformations. An additional measurement of vertical displacement was taken directly below the load point. At the reaction jack, another cable transducer measured the jack stroke, which was used to ensure that, in the tests without end rotation, the reaction jack did not significantly deflect under the load. A clinometer was secured to the beam web at

mid-height near the connection to measure the end rotation. Strain gauges were mounted at the beam midspan primarily to provide a redundancy of measurements for confirming that the frictional forces in the system could be neglected. Two gauges were applied to the top flange, two to the bottom flange, and two on the beam web. A dial gauge was secured to the top flange of the beam at the cope to assess lateral displacements. A graphical representation of these locations is shown in Figure 3-6. Electronic data was gathered through an electronic data acquisition system and a personal computer, while the dial gauge readings were recorded manually.

3.6 Specimen Installation and Test Procedure

Initially, the double-angle connections with cover plates were attached loosely to the support column using 25.4 mm (1") A325 bolts. The beam was then moved into place, attached through one bolt to the double angles, then levelled and centred in the apparatus. The remaining bolts were installed and all were tightened to a snug-tight condition with an open-ended wrench.

The hydraulic pressure in the loading jack was increased slowly to raise the load in approximately 10 kN increments until non-linear behaviour commenced. The specimen was loaded under stroke control. Electronic readings of load, displacement, rotation, and strain were taken at each load increment, and at regular intervals—approximately 50 kN—loading was stopped and the system allowed to reach its static equilibrium. Manual readings of lateral displacement were taken at each static point and the lateral supports were tapped to remove any build-up of frictional forces. Once non-linear behaviour commenced, the displacement at the bottom flange at the test connection was increased in approximately 0.25 mm increments, with static readings being taken approximately every 3 mm. The test was continued either until the specimen fractured completely or until the load decreased significantly.

The stroke of the reaction jack was also monitored and increased or decreased as the test dictated. For tests with an applied end rotation, the jack was lowered at each load increment in a linear relationship with the connection load. The predicted ultimate load and desired ultimate rotation were used to calculate a desired rotation

per unit load. The displacement was controlled to achieve a rotation within ±0.02° of the desired rotation as measured by the clinometer. For tests without end rotation, the jack stroke was increased slightly during the test as the increased load caused compression of the jack. The beam elevation was kept within ±0.25 mm of its original elevation throughout the test.

3.7 Test Results

All test connections failed by block shear except for the double coped specimen, which failed in pure shear. Photographs of each connection in its failed state are shown in Figure 3-7. Most tests exhibited a classical tear-out in which the entire block was removed from the web. In three cases, Tests C2, H1, and H2, a partial tear-out occurred, in which the block remained attached to the beam web through a portion of the shear face of the block. The block from Connection A1 did not exhibit complete rupture due to the development of local distortions near the cope, although necking and cracking along the tension face were observed after the test. Examination of the specimen deformation indicated that load was being resisted in a combination of tensile and shear stresses, suggesting that a block shear failure was occurring.

A summary of the test results is given in Table 3-5. The ultimate vertical reaction in the connection is listed for each test, as well as connection moment and deformations that occurred simultaneously. The load and moment were calculated from statics using the measured forces in the two load cells and the measured distances between the connection, the load point, and the reaction point. The friction in the lateral supports at the reaction point was evaluated using the data gathered from the six strain gauges at the beam midspan. The moment at that location was calculated based on measured beam dimensions and measured material properties, and through statics, the frictional force developed at the reaction point during the test was evaluated. It was found that, in general, the frictional force did not exceed 1% of the connection load. This is sufficiently small to be neglected in the calculation of connection load and moment. The lateral supports provided at the reaction point consisted of a small diameter wheel (38.1 mm) on a lubricated axle, while at the load

point a larger wheel (76.2 mm) complete with lubricated roller bearings was used. Although it was not possible to evaluate the frictional forces in the lateral supports at the load point, it is concluded that this superior wheel mechanism produced frictional forces less than those developed at the reaction point. Therefore, all frictional losses have been neglected in the calculation of connection load and moment.

The connection moment is, in all cases, small compared to the yield moment, M_y, of the beam. For the W410 section, the nominal yield moment is approximately 270 kN·m and it is 297 kN·m for the W310 section. The connection moment at ultimate is approximately 0.5% to 5% of M_y. The sign convention used in Table 3-5 is a moment is less than zero when the top flange is in tension. It is expected that the moments generated at a connection of this type are always negative. However, it is noted that, in some cases, the connection moment is greater than zero, implying that the bottom flange is in tension. This is likely a product of the assumption that the frictional forces can be neglected. The small vertical forces developed in the lateral supports, especially at the reaction end of the beam, have long moment arms and could result in moments with a magnitude sufficient to reverse the sign. However, since the moments generated are small and, therefore, the moment likely does not affect connection behaviour, this sign reversal is of little consequence.

The displacements of the bottom and top of the connection, as described in section 3.5, and the Block Shear Deformation, *i.e.*, the difference between the two measured displacements, are also shown in Table 3-5. The end rotation at the ultimate load, as measured by the clinometer at the connection, is shown for each test. For the tests with no applied end rotation, the measured values are small, usually less than 0.5%. However, no rotation was applied to these connections and the rotation that is measured is attributed to a combination of elastic beam bending over the 3.6 m span and localized deformations at the connection. Elastic rotations for this beam configuration should be less than 0.5° at peak load and, for the most part, the rotations are less than this. In the cases where the rotation has exceeded this level, the increase can be attributed to localized deformations of the web near the connection near ultimate load. In the cases where an end rotation was applied and controlled, the final

rotation is not always equal to the nominal rotation. This is attributed to a combination of localized deformations, as described above, and to a difference in the predicted ultimate load and the actual ultimate load. Since the rotation per unit load was applied until non-linear behaviour occurred, the rotation, in some cases, was higher than expected. In one case, Connection F1, the end rotation was measured as less than zero. This does not indicate that the connection rotated in the opposite direction, but is indicative of localized distortions.

Load vs. deformation plots for each test are presented in Figures 3-8 through 3-24. For all single coped connections, the deformation presented is the algebraic difference between the measured vertical displacements of the bottom of the connection and the top of the connection, the Block Shear Deformation. For the double coped connection, Test D2, the displacement at the bottom of the connection is used as the deformation indicator since little block shear deformation occurred (the connection exhibited little difference in top and bottom displacements).

In two of the tests, the connection was unloaded and reloaded prior to the ultimate load being reached. In Test A1, a gradual movement of one column of the test frame was detected as load was applied to the connection. In order to remedy this, the test specimen was unloaded and the column anchor bolts pretensioned. Re-loading of the connection caused a buckle in the web near the cope and the test was therefore stopped prior to the development of a block shear failure. To address the web buckling issue, two HSS members were clamped to the web below the load point for the remaining tests. In Test J1, the web again buckled near the cope prior to the ultimate load being reached. In this case, a 16 mm stiffener was already present under the load point. Additional, full-depth stiffeners, cut to fit the slightly buckled shape of the web, were added on each side at the cope to strengthen the beam. The connection was then re-loaded until block shear failure occurred.

3.8 Summary

To address issues of current over-prediction of block shear capacity in coped beams and the fact that relatively few laboratory research programs have been

completed on the topic, 17 full-scale tests were carried out. Connection configurations were chosen to encompass a wide range of connection parameters including end rotation, end and edge distances, bolt diameter, bolt layout, and double cope. The effect of connection end rotation had not been investigated previously, with all previous research completed holding the beam horizontal throughout the test. Here, a rigid body rotation was applied to the beam to simulate the effect of beam action on the connection. Connection geometry and beam dimensions were measured and material properties of each beam web were determined through standard tension coupon tests. The test set-up was constructed to represent a conventional double-angle beam-to-column connection, and lateral support was provided to the top flange at two locations for one-line tests and three locations for two-line tests. Deflections of the bottom flange at three locations and of the top of the web at the cope were measured, as were connection rotation, top flange lateral displacement at the cope, and longitudinal strains in the beam at mid-span. Complete load vs. deformation behaviour for each connection was collected and is presented both numerically and graphically. The results of these tests were used to validate the non-linear finite element model and to evaluate existing and proposed capacity equations.

Table 3-1: As-Built Connection Dimensions

Connection Designation	e_s (mm)	s_1 (mm)	s_2 (mm)	s_3 (mm)	e_g (mm)	g (mm)	d_h† (mm)
A1	36.3	75.1	75.3	75.1	24.8	—	20.6
A2	25.2	63.1	75.1	74.9	25.3	—	20.6
B1	26.5	75.3	75.3	75.6	24.1	—	20.9
B2	25.1	74.9	75.1	75.0	26.0	—	20.7
C1	25.6	101.6	101.9	—	26.2	—	20.7
C2	25.1	101.9	102.4	—	24.9	76.1	20.7
D1	32.0	103.3	103.1	—	31.6	—	27.0
D2	25.3††	75.4	75.3	74.8	50.2	—	20.7
E1	24.3	74.7	75.1	75.1	50.4	—	20.6
E2	49.4	75.3	75.4	75.0	24.2	—	20.6
F1	25.2	75.0	75.4	—	25.8	—	20.7
G1	25.8	75.3	75.0	—	25.1	—	20.7
G2	26.1	75.3	75.0	—	23.6	—	20.7
H1	26.5	74.8	75.0	—	25.1	—	20.7
H2	26.5	74.8	75.0	—	25.4	—	20.7
J1	26.7	101.9	101.8	—	24.1	76.4	20.7
J2	27.5	75.3	—	—	24.7	75.0	20.7

Connection Designation	l_c (mm)	d_c (mm)
A1	73.7	36.3
A2	74.9	36.4
B1	73.3	34.9
B2	73.8	36.6
C1	74.4	36.2
C2	149.5	35.5
D1	79.7	36.3
D2	98.4††	35.1††
E1	99.4	37.8
E2	74.8	35.9
F1	74.4	36.3
G1	74.4	37.3
G2	74.5	37.3
H1	76.3	35.4
H2	77.5	35.6
J1	150.3	34.7
J2	152.1	32.9

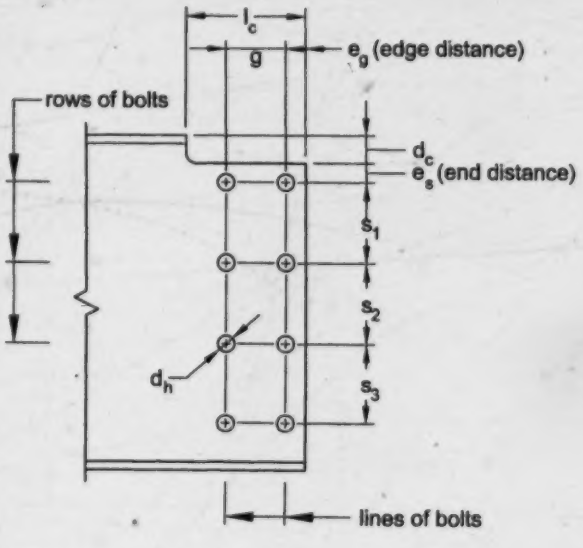

† Mean diameter for all bolt holes in connection

†† Bottom End Distance 26.80 mm
Bottom Cope Length 98.1 mm
Bottom Cope Depth 90.3 mm

Table 3-2: As-Built Beam Dimensions

Beam Designation	d (mm)	b (mm)	t (mm)	w (mm)	k† (mm)	S_x (mm^3)
A	401.5	138.5	10.56	7.03	19.2	717 300
B	401.5	138.4	10.70	7.00	20.3	723 100
C	401.5	138.6	10.46	6.95	19.6	711 000
D	402.4	140.8	10.47	6.87	18.9	720 400
E	401.6	138.5	10.37	7.01	19.4	708 500
F	401.6	138.6	10.45	6.94	19.4	710 600
G	303.8	201.9	12.58	7.95	22.9	803 900
H	403.8	144.0	10.78	6.93	21.9	753 700
J	403.5	137.9	11.13	7.16	19.6	749 600

† Mean distance for four fillets

Table 3-3: Test Parameters Summary

Parameter	Connection Designations	Nominal Values of Parameter
End Rotation	B2, B1, A2	0°, 2°, 3.5°
End Rotation	F1, H1, H2	0°, 2°, 3.5°
End Rotation	C2, J1	0°, 2°
Gross Shear Area	B2, C1	1750 mm^2, 1603 mm^2
Edge Distance	B2, E1	25 mm, 50 mm
End Distance	B2, E2	25 mm, 50 mm
Bolt Diameter	C1, D1	19.1 mm, 25.4 mm
Section Depth	F1, G1, G2	W410, W310, W310
Connection Depth	C1, F1	229 mm, 175 mm
Number of Bolt Rows	B2, F1	4, 3
Number of Bolt Lines	C1, C2	1, 2
Double Cope	E1, D2	Single, Double
Repeatability	G1, G2	—

Table 3-4: Material Properties

Coupon Mark	Elastic Modulus, E (MPa)	Upper Yield (MPa)	Lower Yield (MPa)	Mean Static Yield, F_y (MPa)	Static Ultimate, F_u (MPa)	Rupture Stress (MPa)	Yield Strain (%)	Hardening Strain (%)	Ultimate Strain (%)	Rupture Strain (%)	Reduction of Area (%)
Beam A											
i	201 500	398	368	349	523	481	0.20	1.9	14.8	18.0	44.2
ii	206 400	391	378	368	518	505	0.20	1.7	15.4	17.4	42.3
iii	191 800	390	380	365	516	478	0.21	1.8	15.7	18.0	43.0
Mean	199 900	393	375	361	519	488	0.20	1.8	15.3	17.8	43.2
Beam B											
i	202 000	398	377	371	512	475	0.18	1.9	14.5	20.8	43.3
ii	206 600	406	380	367	513	408	0.20	2.1	15.4	20.3	43.1
iii	201 800	402	378	364	515	451	0.20	1.8	15.4	20.3	41.5
Mean	203 500	402	378	367	513	445	0.19	1.9	15.1	20.3	42.6
Beam B(2)†											
i	195 600	407	389	362	513	431	0.20	2.0	17.1	32.3	54.1
ii	196 500	408	385	363	513	419	0.21	1.9	18.2	32.5	55.4
iii	210 200	393	383	365	516	412	0.19	1.9	18.0	33.0	55.3
Mean	200 800	403	385	363	514	421	0.20	1.9	17.8	32.6	54.9
Beam C											
i	205 200	400	382	370	518	469	0.21	2.0	15.1	20.9	41.0
ii	205 600	396	377	363	513	506	0.20	2.0	14.9	20.0	41.0
iii	221 000	389	382	367	517	493	0.22	1.9	14.9	20.5	38.0
Mean	210 600	394	380	366	516	489	0.21	2.0	15.0	20.5	40.0
Beam D											
i	206 900	411	389	378	523	437	0.20	2.0	14.5	20.8	30.2
ii	207 500	415	400	378	524	491	0.21	2.0	16.5	26.3	43.1
iii	192 900	402	394	373	523	483	0.21	1.8	16.3	23.8	45.8
Mean	202 400	410	394	377	523	470	0.21	1.9	15.8	23.6	39.7

† Coupons oriented in the longitudinal direction

Table 3-4: Material Properties (cont.)

Coupon Mark	Elastic Modulus, E (MPa)	Upper Yield (MPa)	Lower Yield (MPa)	Mean Static Yield, F_y (MPa)	Static Ultimate, F_u (MPa)	Rupture Stress (MPa)	Yield Strain (%)	Hardening Strain (%)	Ultimate Strain (%)	Rupture Strain (%)	Reduction of Area (%)
Beam E											
i	206 800	393	381	370	520	482	0.20	1.8	15.7	22.6	41.1
ii	210 600	395	381	368	520	469	0.22	1.9	16.2	21.5	45.2
iii	186 100	385	379	371	525	504	0.26	1.7	15.5	19.1	41.9
Mean	201 200	391	380	370	522	485	0.23	1.8	15.8	20.9	42.7
Beam F											
i	208 700	390	379	364	513	477	0.22	1.8	15.7	20.1	40.2
ii	206 300	398	384	371	520	513	0.21	1.9	16.4	20.0	35.4
Mean	207 500	394	382	368	517	495	0.22	1.9	16.1	20.1	37.8
Beam G†											
i	203 200	413	378	367	478	353	0.21	2.8	20.0	37.0	64.6
ii	194 400	393	384	369	480	345	0.24	2.2	18.7	35.0	64.2
Mean	198 800	403	381	368	479	349	0.23	2.5	19.4	36.0	64.4
Beam H											
i	202 100	398	350	353	427	354	0.20	4.0	19.8	34.5	58.1
ii	215 800	392	379	356	431	360	0.19	3.8	20.9	33.5	58.0
Mean	209 000	395	365	355	429	357	0.20	3.9	20.4	34.0	58.1
Beam J											
i	203 000	429	393	376	513	413	0.21	2.6	18.8	33.1	55.4
ii	203 800	411	398	379	514	415	0.24	2.6	18.4	34.4	59.7
iii	209 400	421	398	378	516	412	0.20	2.7	18.4	32.8	58.0
Mean	205 400	420	396	378	515	413	0.22	2.6	18.5	33.4	57.7

† Coupons oriented in the longitudinal direction

Table 3-5: Test Results Summary

Connection Designation	Ultimate Connection Vertical Reaction (kN)	Connection Moment† at Ultimate (kN·m)	Displacement of Bottom of Connection at Ultimate (mm)	Displacement of Top of Connection at Ultimate (mm)	Block Shear Deformation†† at Ultimate (mm)	End Rotation at Ultimate (°)
A1	439	-5.2	9.1	5.0	4.1	0.2
A2	496	-7.6	15.7	8.2	7.5	3.3
B1	514	-12.1	14.9	5.4	9.5	2.0
B2	475	-4.3	13.2	5.8	7.4	0.1
C1	402	6.4	9.3	3.2	6.1	0.2
C2	537	-14.2	7.7	3.7	4.0	0.7
D1	448	-3.5	12.6	3.4	9.2	0.2
D2	529	1.7	6.2	4.5	1.7	1.9
E1	568	-4.8	9.5	4.9	4.6	1.1
E2	517	-0.7	10.3	4.9	5.4	0.5
F1	324	-2.9	11.2	3.5	7.7	-0.1
G1	379	-7.8	12.5	2.8	9.7	0.1
G2	387	-4.3	14.7	3.4	11.3	0.1
H1	324	-2.7	20.4	5.5	14.9	1.6
H2	341	2.7	15.0	6.3	8.7	3.3
J1	667	8.6	9.7	6.5	3.2	3.8
J2	338	5.3	11.2	6.1	5.1	0.0

† Negative moment indicates top flange in tension

†† Block Shear Deformation is difference between Bottom of Connection Displacement and Top of Connection Displacement

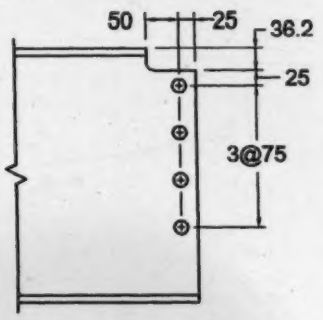

A1 - W410x46
A2 - W410x46
B1 - W410x46
B2 - W410x46

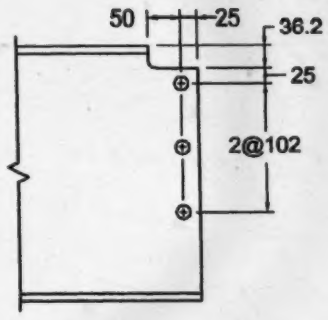

C1 - W410x46

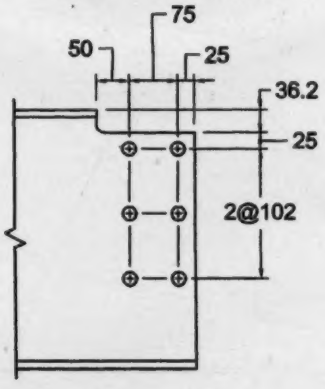

C2 - W410x46
J1 - W410x46

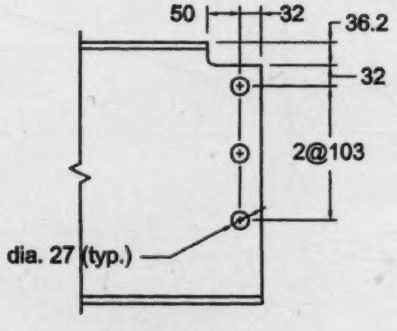

D1 - W410x46

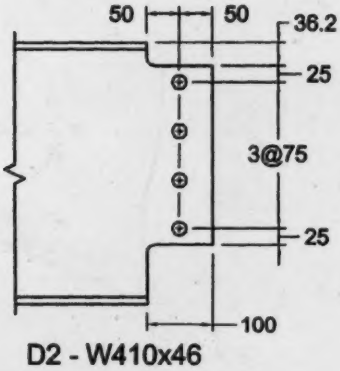

D2 - W410x46

Note: All dimensions in millimeters. All hole diameters 21 mm unless noted otherwise. All cope radii 12.5 mm.

Figure 3-1: Nominal Connection Properties

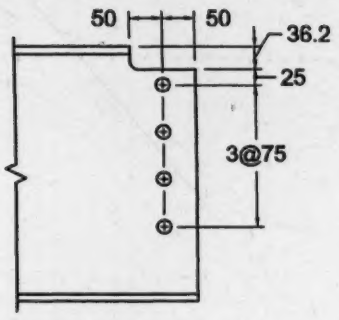

E1 - W410x46

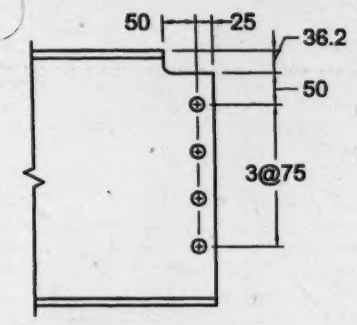

E2 - W410x46

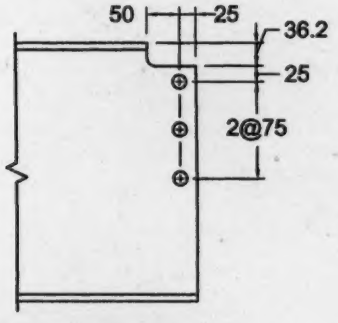

F1 - W410x46
H1 - W410x46
H2 - W410x46

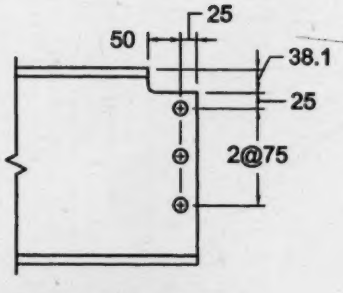

G1 - W310x60
G2 - W310x60

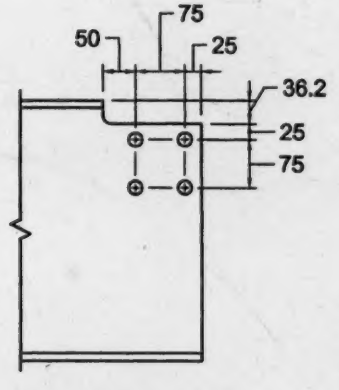

J2 - W410x46

Note: All dimensions in millimeters. All hole diameters 21 mm unless noted otherwise. All cope radii 12.5 mm.

Figure 3-1: Nominal Connection Properties (cont.)

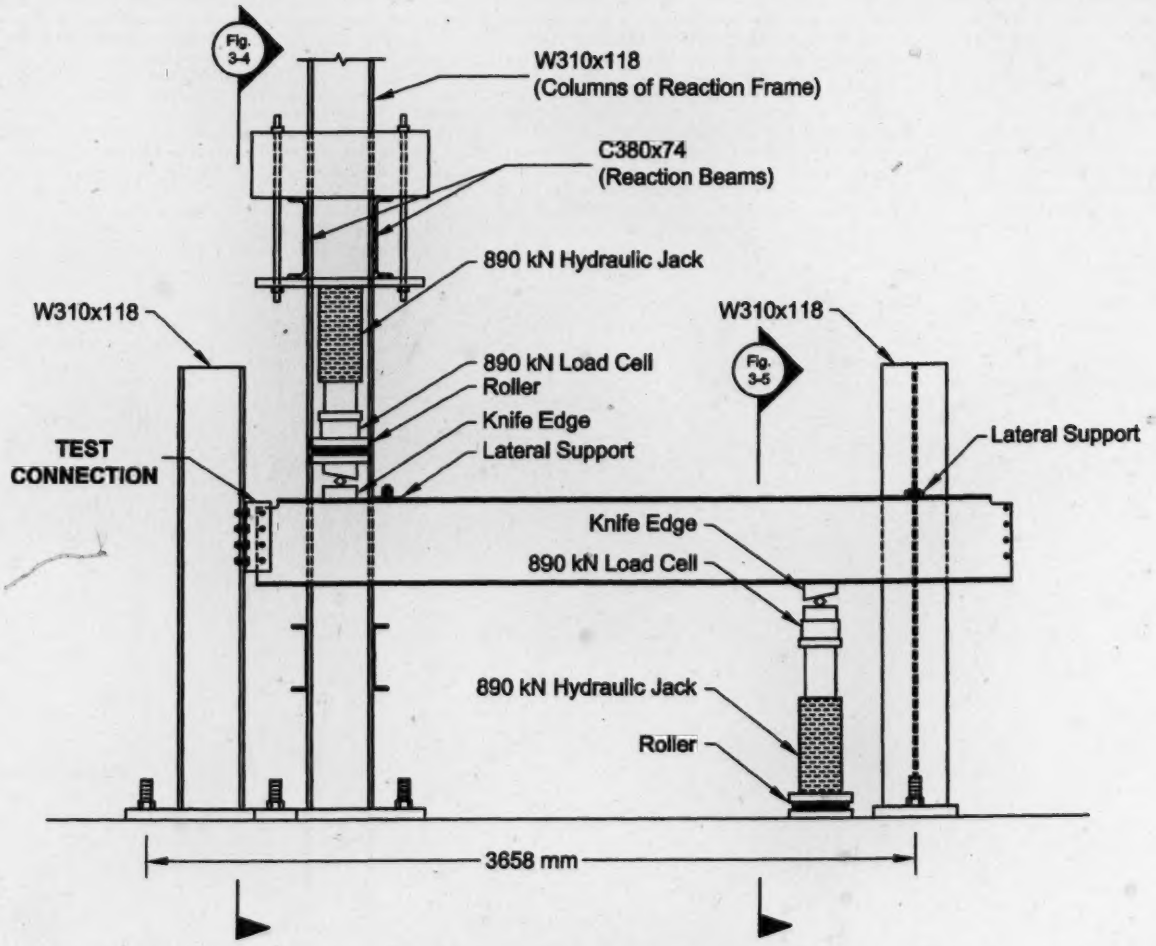

Figure 3-2: Elevation of Test Set-up

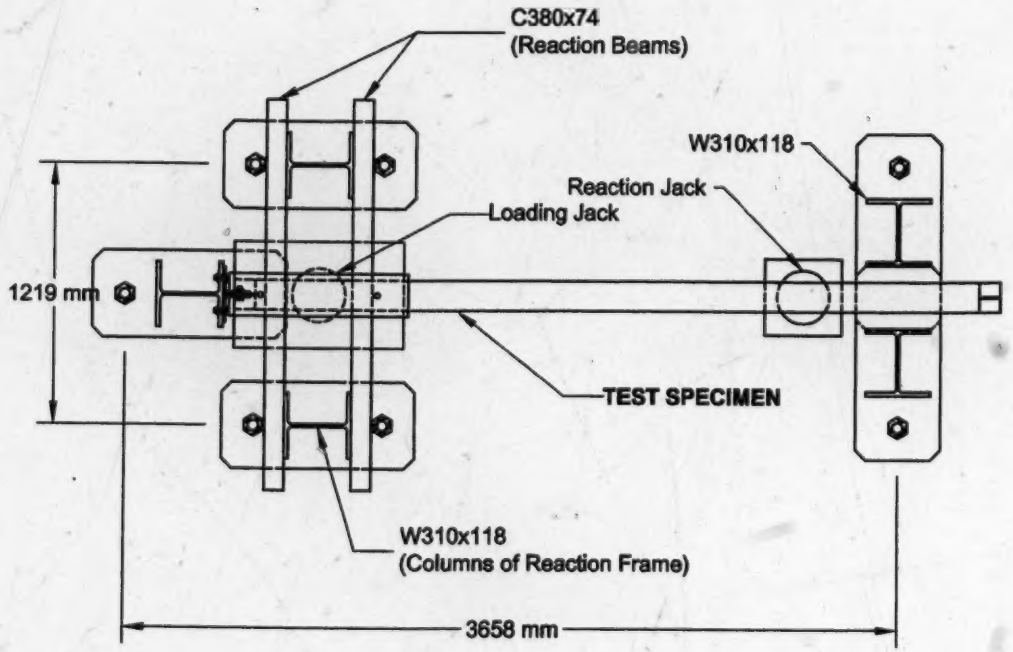

Figure 3-3: Plan of Test Set-up

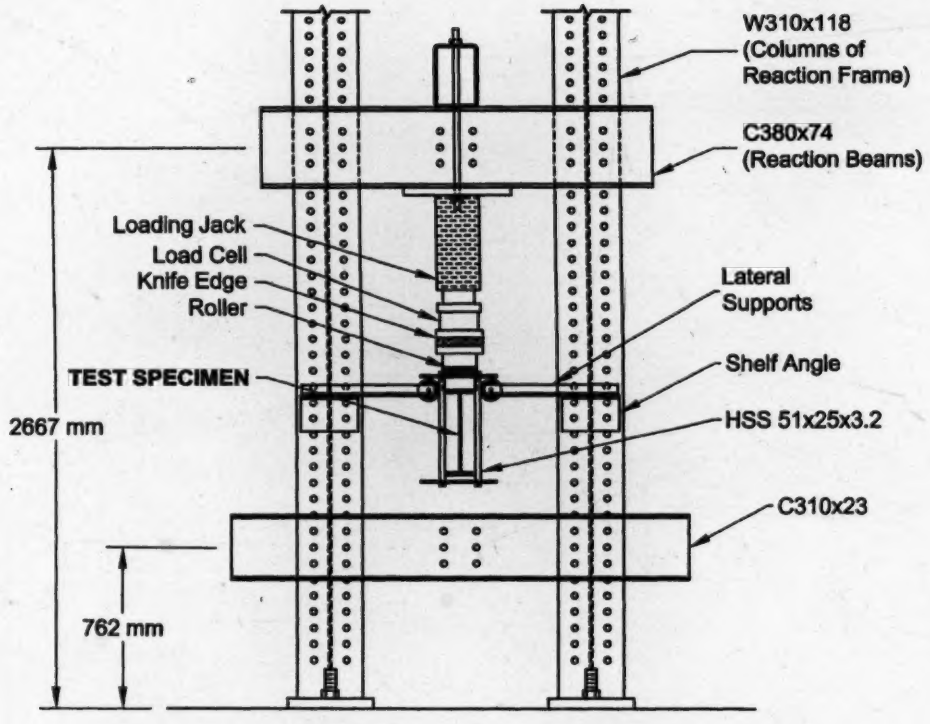

Figure 3-4: Section of Test Set-up at Loading Frame

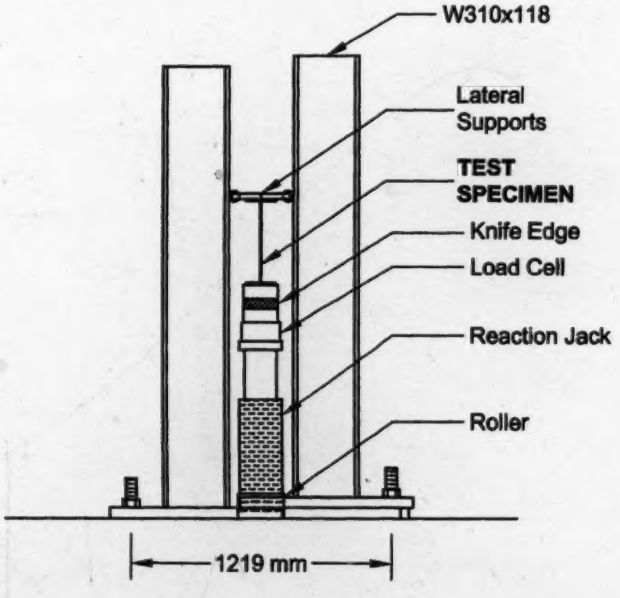

Figure 3-5: Section of Test Set-up at Reaction Frame

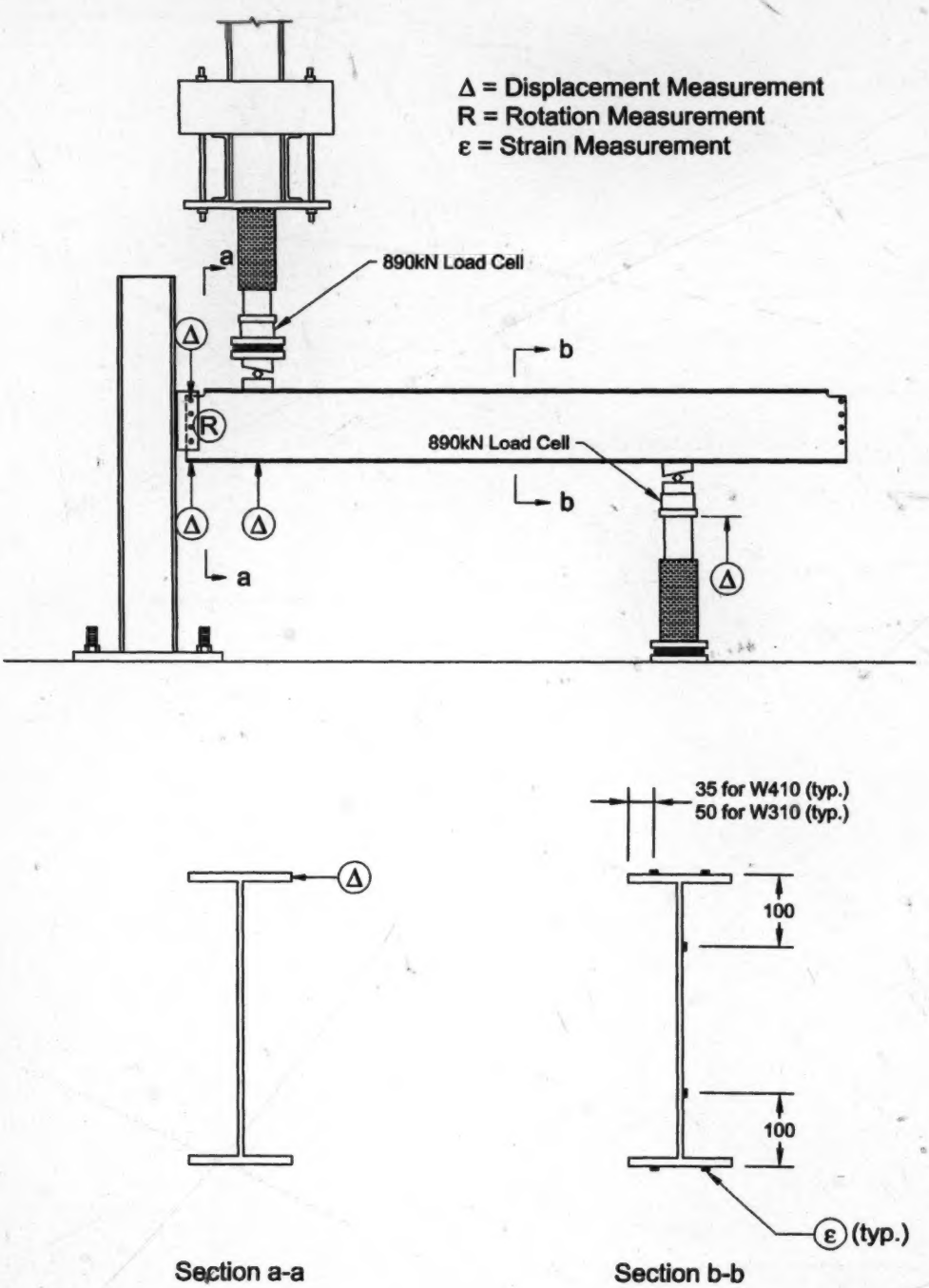

Figure 3-6: Instrumentation Layout

(a) Connection A1

(b) Connection A2

(c) Connection B1

(d) Connection B2

(e) Connection C1

(f) Connection C2

Figure 3-7: Failed Connections

(g) Connection D1

(h) Connection D2

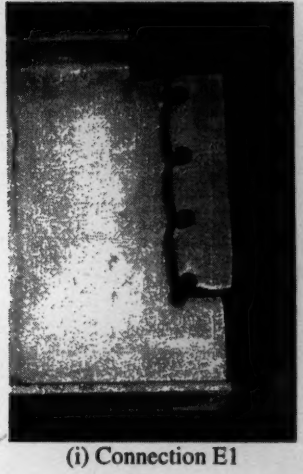

(i) Connection E1

(j) Connection E2

(k) Connection F1

Figure 3-7: Failed Connections (cont.)

(l) Connection G1

(m) Connection G2

(n) Connection H1

(o) Connection H2

(p) Connection J1

(q) Connection J2

Figure 3-7: Failed Connections (cont.)

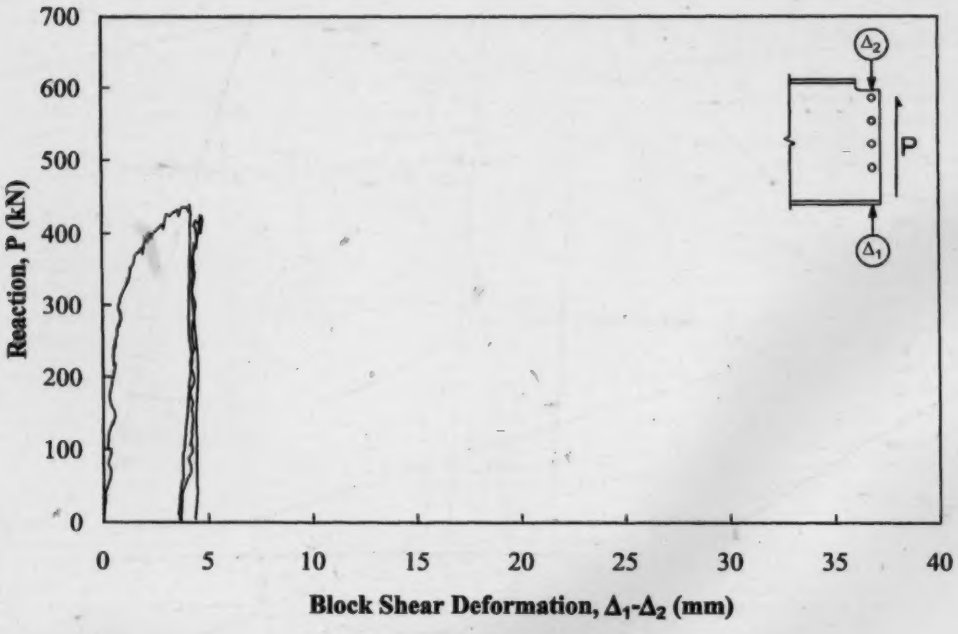

Figure 3-8: Load vs. Block Shear Deformation Curve, Test A1

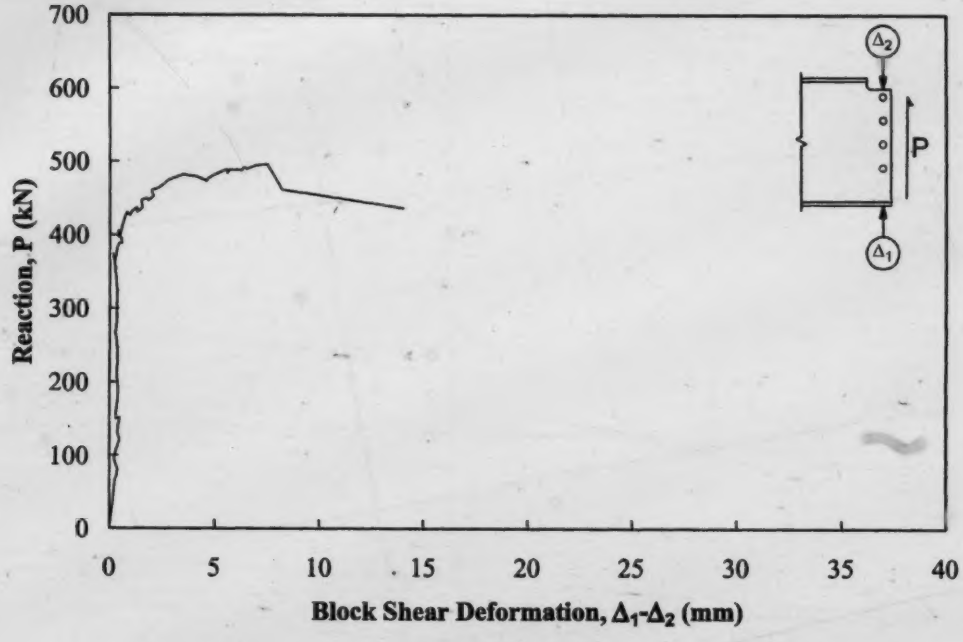

Figure 3-9: Load vs. Block Shear Deformation Curve, Test A2

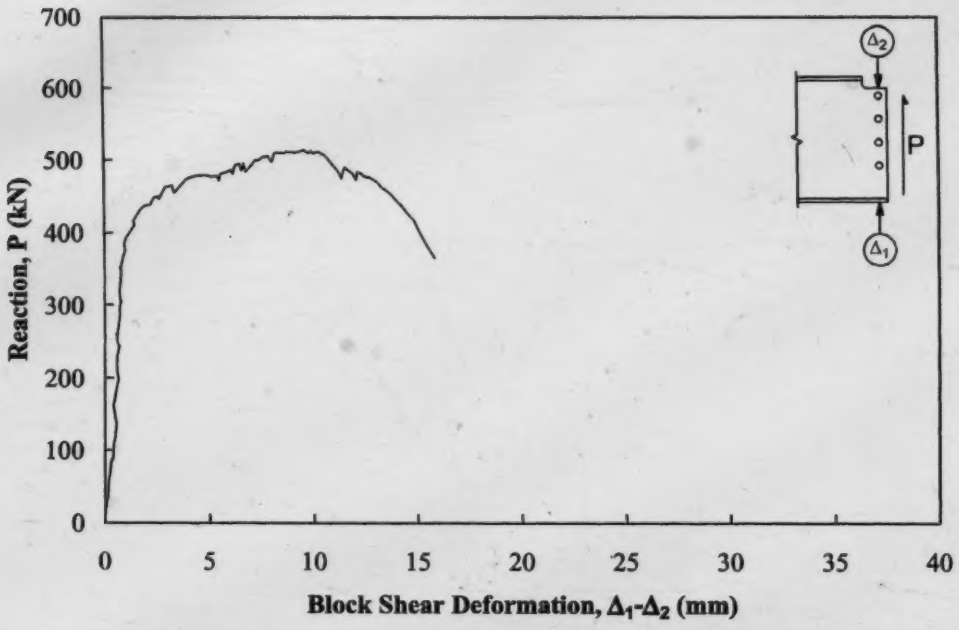

Figure 3-10: Load vs. Block Shear Deformation Curve, Test B1

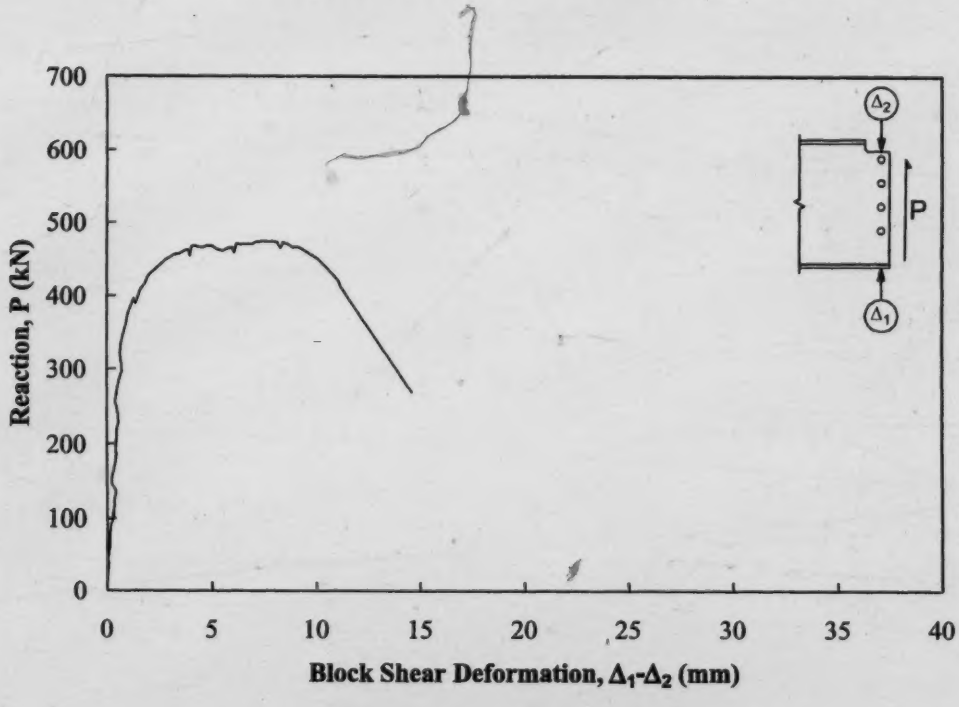

Figure 3-11: Load vs. Block Shear Deformation Curve, Test B2

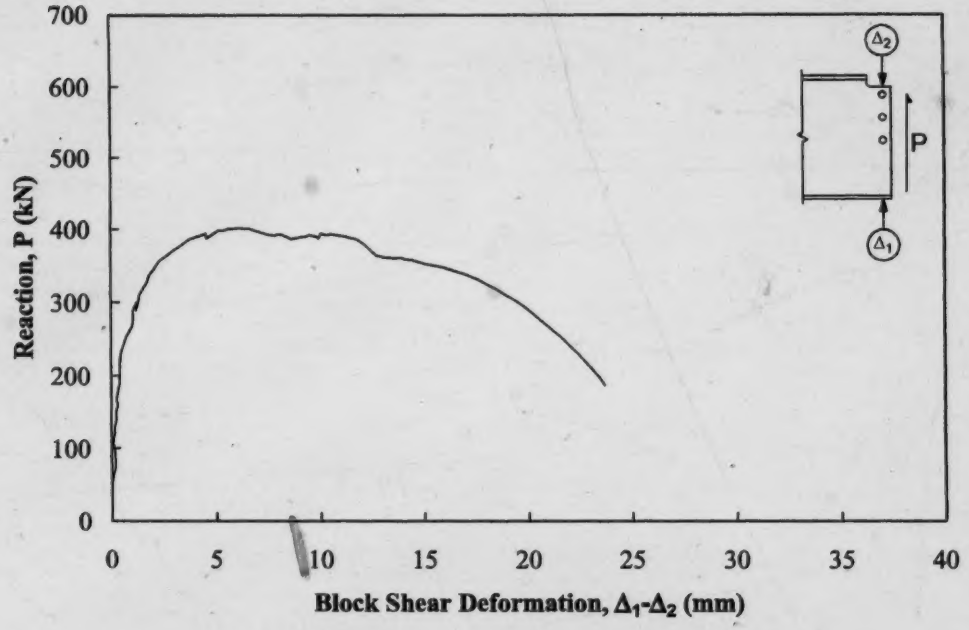

Figure 3-12: Load vs. Block Shear Deformation Curve, Test C1

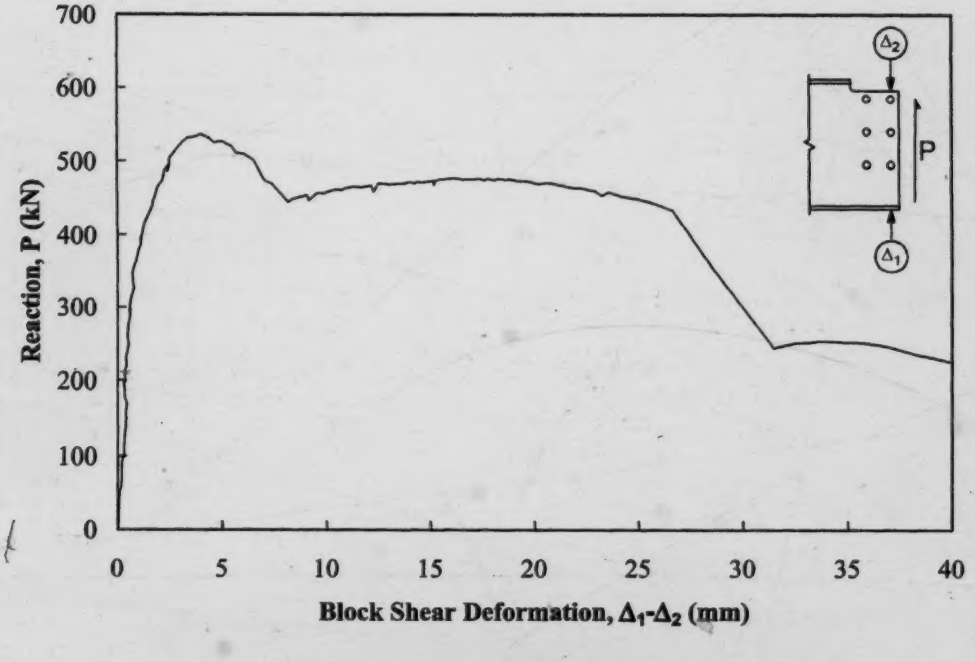

Figure 3-13: Load vs. Block Shear Deformation Curve, Test C2

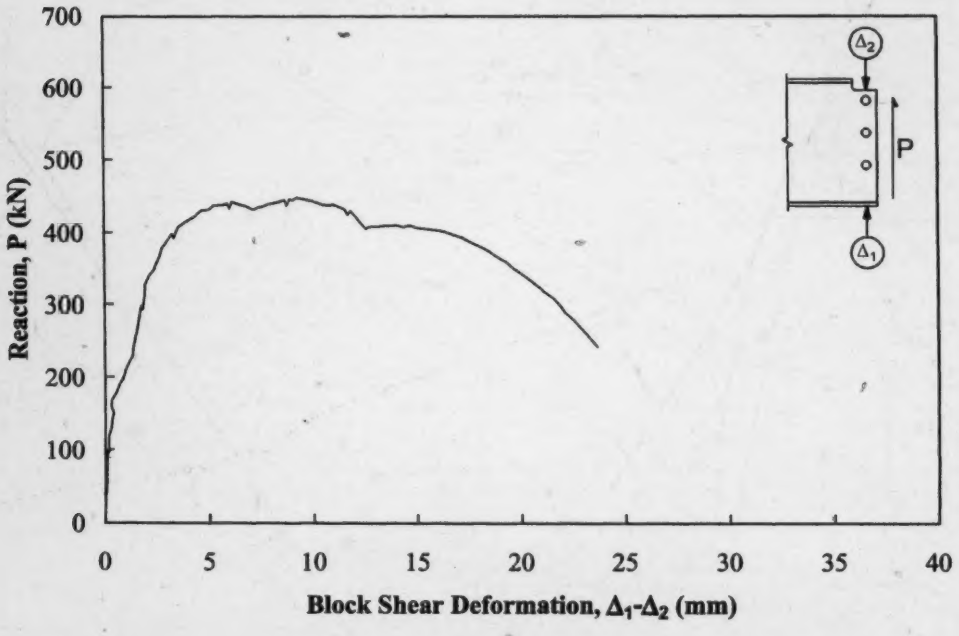

Figure 3-14: Load vs. Block Shear Deformation Curve, Test D1

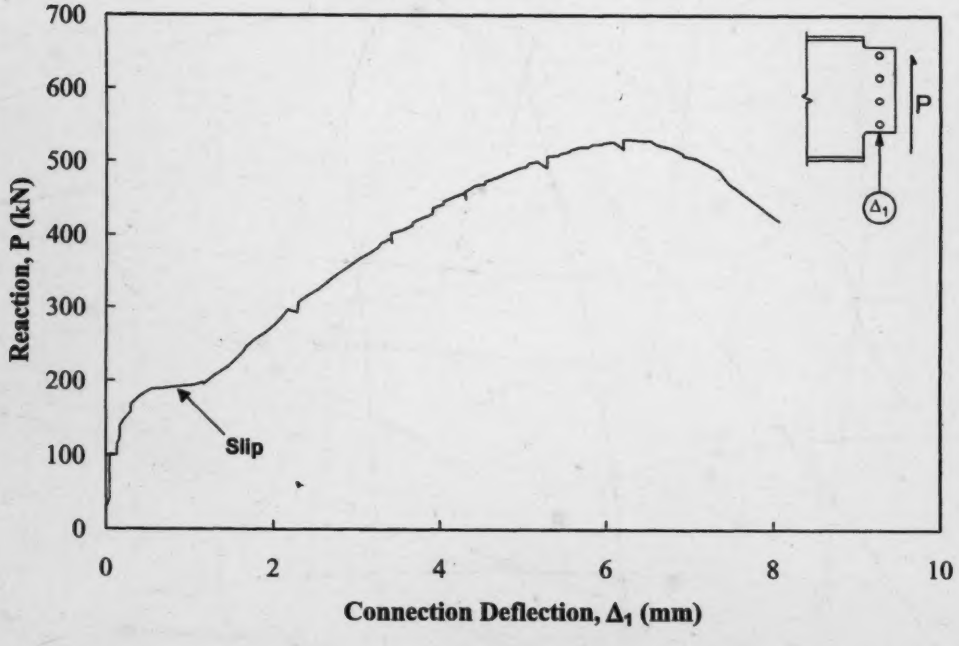

Figure 3-15: Load vs. Connection Deflection Curve, Test D2

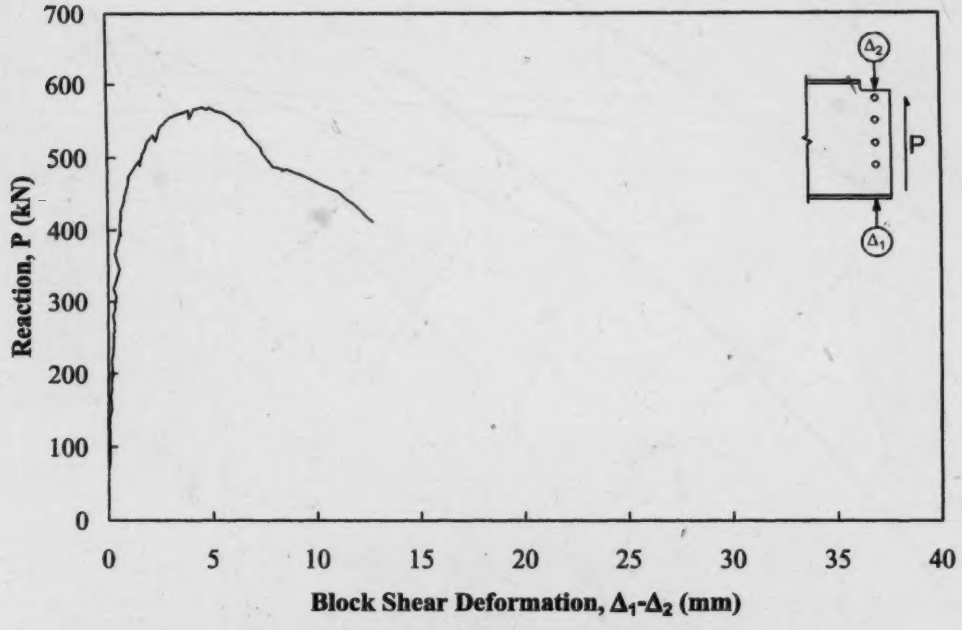

Figure 3-16: Load vs. Block Shear Deformation Curve, Test E1

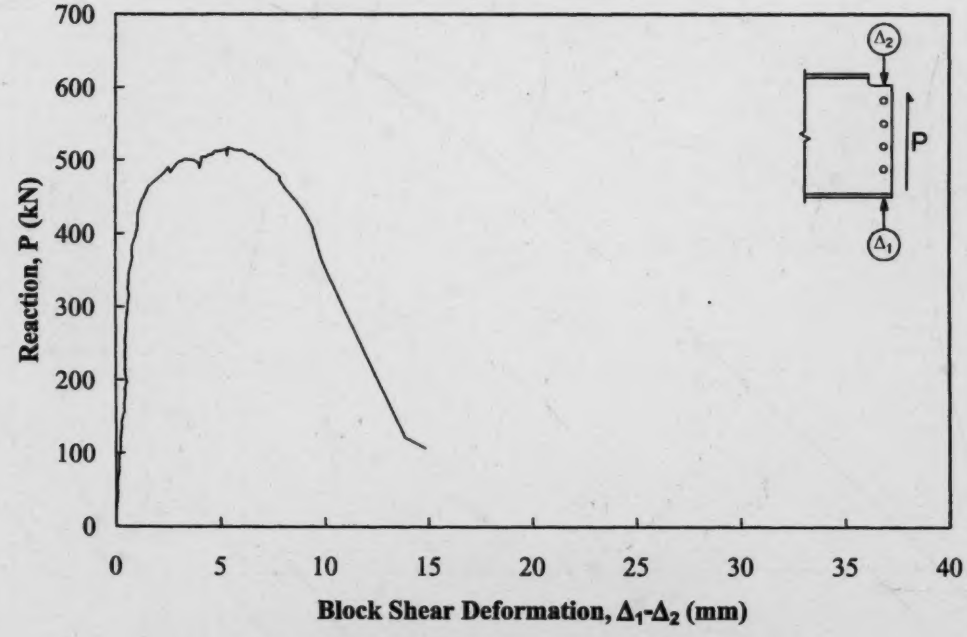

Figure 3-17: Load vs. Block Shear Deformation Curve, Test E2

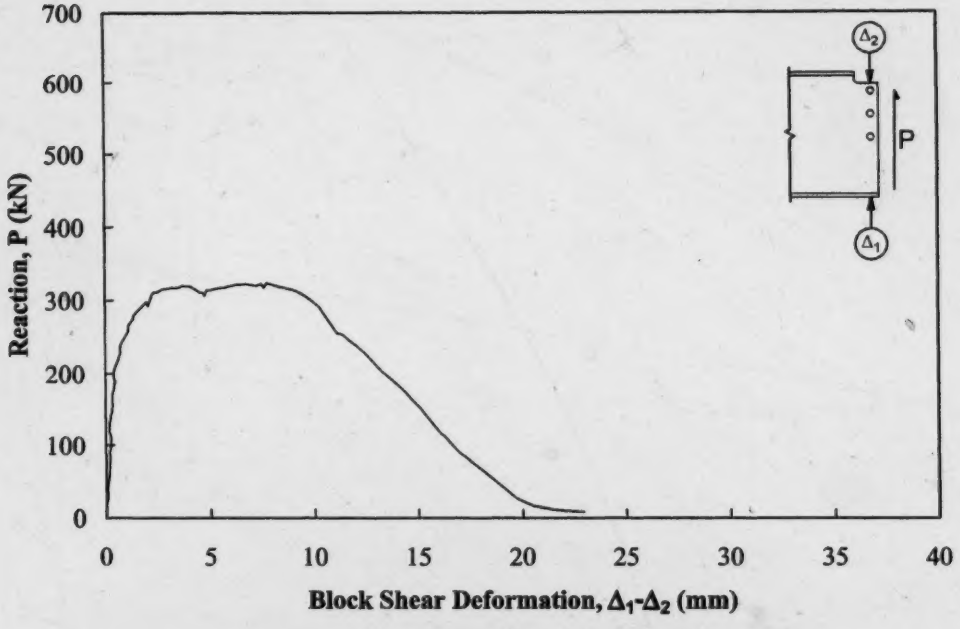

Figure 3-18: Load vs. Block Shear Deformation Curve, Test F1

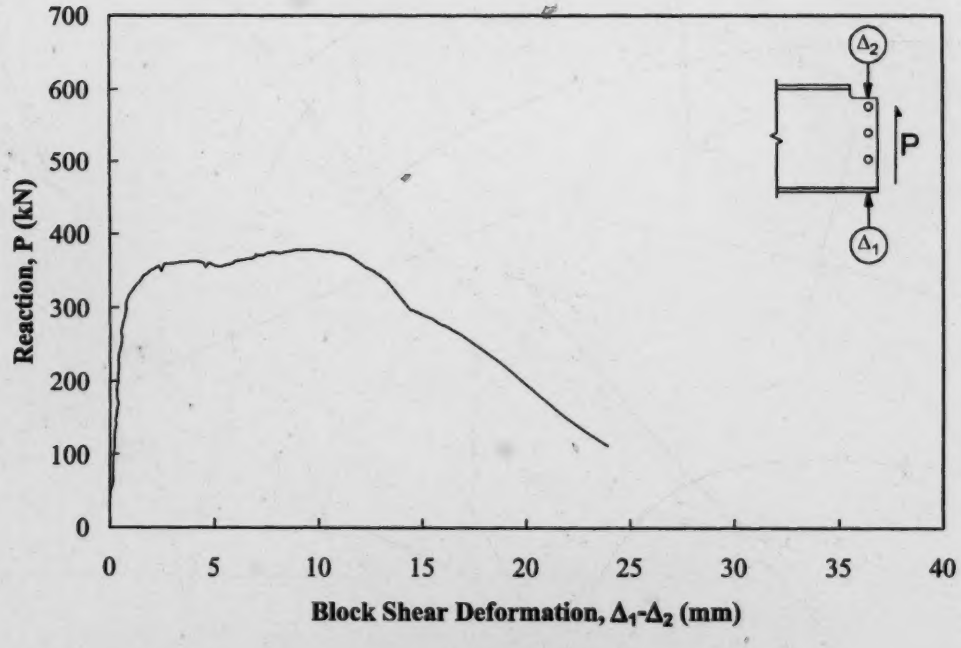

Figure 3-19: Load vs. Block Shear Deformation Curve, Test G1

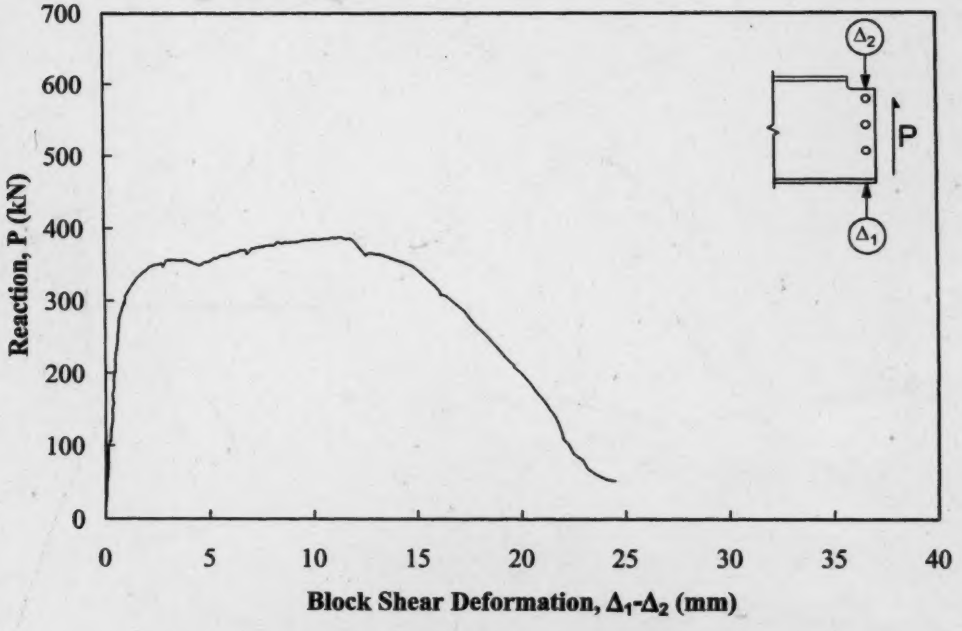

Figure 3-20: Load vs. Block Shear Deformation Curve, Test G2

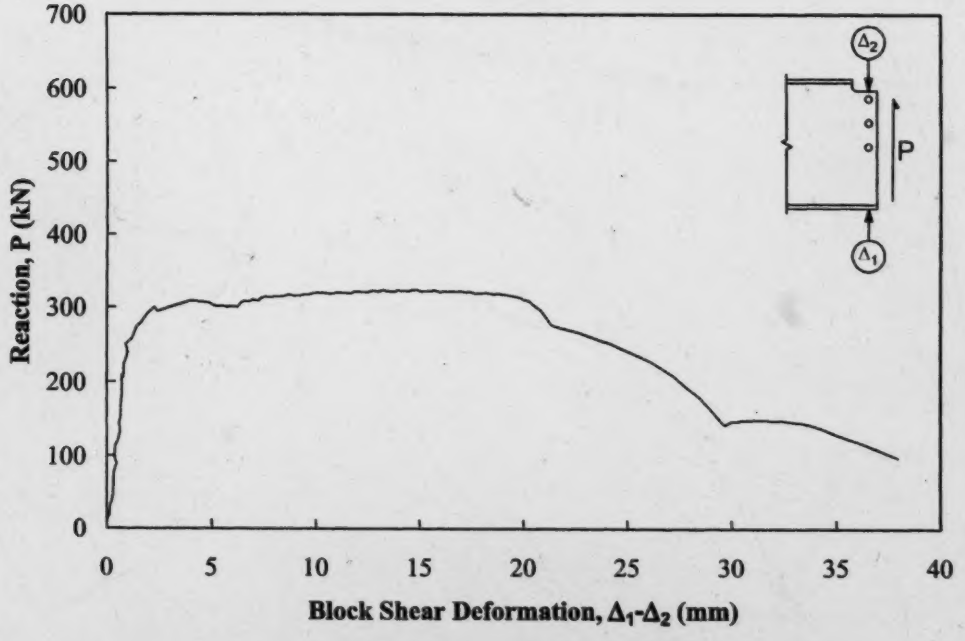

Figure 3-21: Load vs. Block Shear Deformation Curve, Test H1

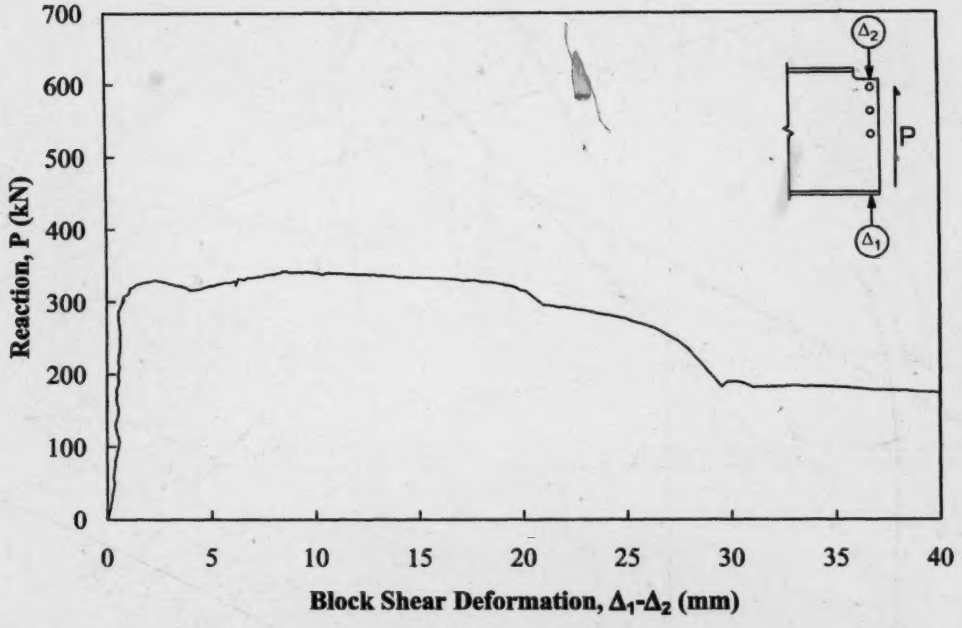

Figure 3-22: Load vs. Block Shear Deformation Curve, Test H2

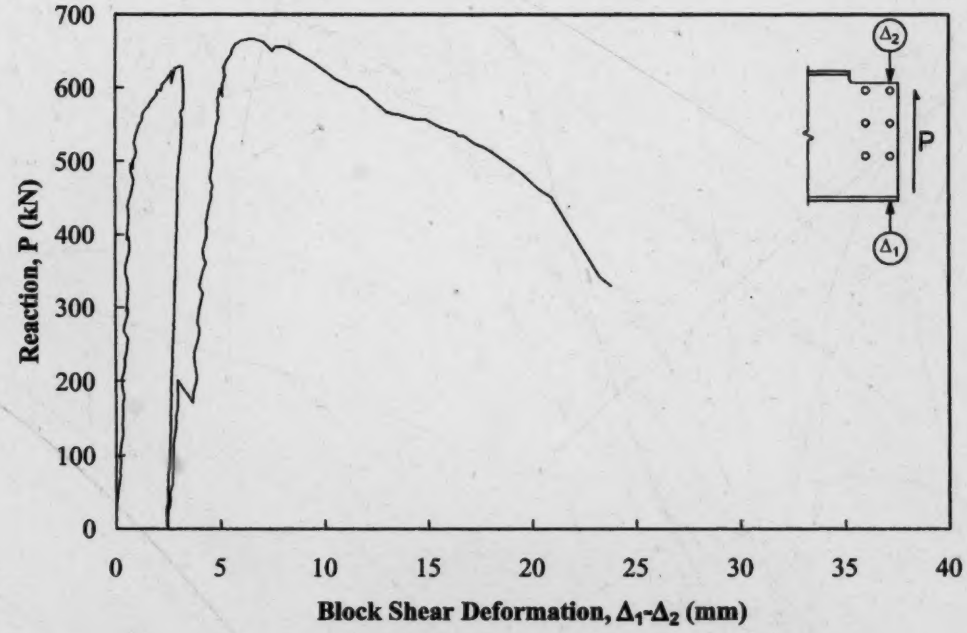

Figure 3-23: Load vs. Block Shear Deformation Curve, Test J1

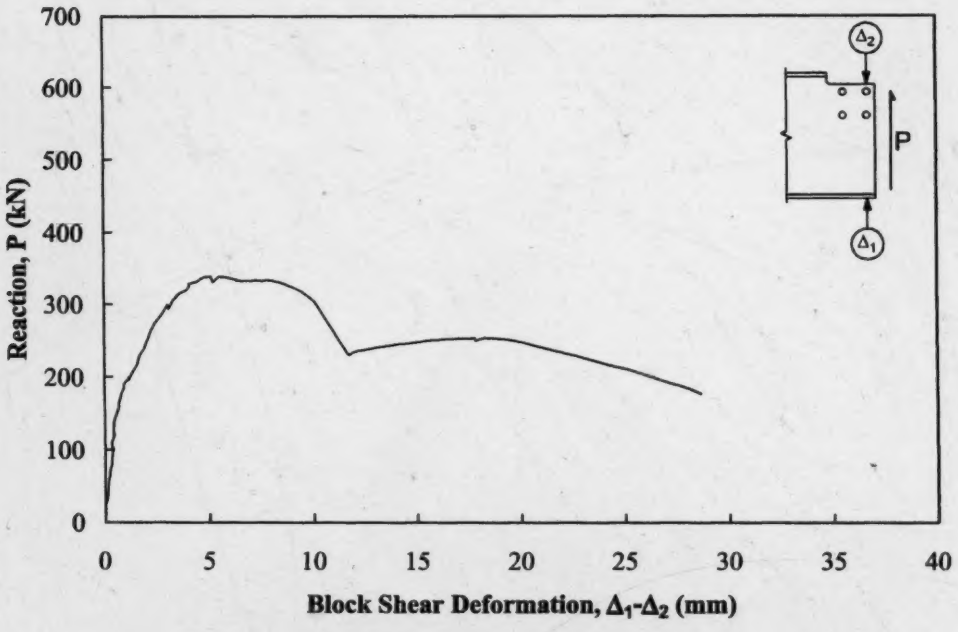

Figure 3-24: Load vs. Block Shear Deformation Curve, Test J2

4. Numerical Program

4.1 Introduction

Following full-scale physical testing, finite element analyses (FEA) of selected connections were completed to investigate some of the main features of the block shear response. The configurations chosen encompass a wide range of connection parameters including edge distance, number of rows of bolts, and number of lines of bolts. Connection end rotation was not modelled in this analysis since the laboratory test results indicated that end rotation did not have a significant effect on connection behaviour. Five models were created and analyzed using ABAQUS, a general non-linear finite element analysis program, and the resulting load vs. deformation curves were compared to the laboratory test data. Studies on the effects of the initial bolt bearing condition and incremental tension face tearing were also completed. A summary of the connection and material models, the analysis procedure, and the analysis results is presented below.

4.2 Description of Models

Models of five of the laboratory test specimens representing a wide range of connection parameters were created. Table 4-1 lists the finite element model number and its associated laboratory connection designation. Nominal connection properties of each connection are shown in Figure 3-1. Model M1 is a four-bolt, single-line connection representing a typical connection in which the connection depth is a significant portion of the section depth. The second model, M2, is a connection with a similar depth to M1, but with two lines of bolts. An increase in edge distance is investigated in Model M3. A light connection with only three bolts was modelled in M4 and, finally, M5 is a compact, two-line connection with only four bolts. These models encompass a wide range of connection variables in order to validate the finite element model.

A linear elastic finite element modelling program, S-FRAME (Softek, 2000), was used to construct the geometry and connectivity of the models because of its suitable mesh generation features. Four-node, quadrilateral shell elements were used to create models that consisted of the entire beam, including the flanges, based on

as-built dimensions. An isometric projection of a typical mesh is shown in Figure 4-1. It was found during the analyses that a very fine mesh is required in the region of the connection in order to model the localized behaviour. The mesh around the hole was defined with 16 elements along each side of a 50 mm by 50 mm area and ten elements in the radial direction. The generated mesh is somewhat finer near the hole, as shown in Figure 4-2, which provides the necessary resolution to define accurately the relatively steep strain gradients induced near the bolt holes. To reduce computational requirements, the majority of the beam web was modelled with only four elements through its depth and only two elements for each flange. This resulted in a significantly smaller total number of elements but did not affect the connection behaviour due to the small strains in the elements and their relatively large distances from the connection. A transition region was provided within the mesh to convert from approximately 100 elements through the beam depth to four, as shown in Figure 4-3.

Once the mesh was generated, the nodal co-ordinates and element definitions were imported into ABAQUS (HKS, 1998) to carry out the non-linear analysis. Four-node, reduced integration, finite strain shell elements (ABAQUS element type S4R) were selected for each of the quadrilateral elements produced by S-FRAME. As-measured thicknesses of the web and flanges were specified for the shell thicknesses. The four web elements below the load point were assigned a thickness of 30 mm to account for the effect of the stiffeners used in the laboratory tests.

Since sufficient laboratory deformation measurements were taken to isolate the beam web (block shear) deformation (*i.e.*, excluding slip, bearing, and angle deformations), it was not necessary to model the connection angles. Four methods of modelling bolt–web interaction were used. A graphical representation of these four bolt models is shown in Figure 4-4. It was initially assumed that since the bolt could bear only on the top of the hole, restraining the movement of the top of the hole and allowing the bottom of the hole to move freely was a reasonable representation. This was accomplished by fixing the translational degrees of freedom of the nodes around the top of the bolt hole in all three co-ordinate directions. The 31 nodes making up

the top half of the bolt hole were pinned in this manner (see Figure 4-4(a)). The observation that near the ultimate load the contact region was actually shorter than one-half of the hole circumference led to a second modelling method. In this case, the translation of only the top 17 of the 64 nodes (approximately ¼ of the nodes) around the bolt hole were restrained (see Figure 4-4(b)). Thereafter, a more rigorous bolt–web interaction was modelled (the third method) through the implementation of contact elements. Four-node, three dimensional, rigid elements (ABAQUS element type R3D4) were used to create a cylindrical bolt with a diameter equal to that of the nominally 19.1 mm (18.9 mm measured) bolts used in the laboratory (see Figure 4-4(c)). A simple friction model was used to represent the bolt–web interaction and a static friction coefficient of 0.7 was used, a typical value for steel-to-steel contact (Avallone and Baumeister, 1996) although this value is not expected to have a great effect on the load vs. deformation behaviour. The elements making up the bolts were fixed in space and as the load was applied, the beam web was allowed to deform around them. This was deemed to be a reasonable approximation of the laboratory conditions.

The contact element method was also used to investigate the effect of the initial bolt bearing condition. In real connections, normal fabrication tolerances result in initial conditions wherein not all of the bolts are initially in bearing. Small differences in bolt hole spacing between the angles and the beam web result in some bolts initially contacting both the angle and the web with other bolts contacting only the angles. Upon application of load on the connection, high stresses develop in the web at the contact point resulting in localized bearing deformations. As these deformations increase, the web deflects sufficiently to allow the other bolts to bear. By changing the location of the cylindrical elements in the bolt holes, the bearing condition was varied, and an investigation of its effects was completed. Another bolt–web interaction model (the fourth method) used to investigate the effect of the initial bolt bearing condition was also created by modifying the pinned node method. Rather than fixing the translation of the nodes in all directions, non-linear springs were inserted in the vertical direction (see Figure 4-4(d)). The springs were defined with no stiffness (0 kN/mm) until a specified displacement was reached, after which

the springs were given near infinite stiffness (10^{10} kN/mm). The nodes were fixed against translation in the other two co-ordinate directions. By changing the displacement required to engage the springs, different initial bolt bearing conditions could be investigated.

Other boundary conditions were modelled to represent accurately the load and support conditions of the laboratory experiments. Load was incremented through a specified displacement of the three nodes across the top flange at a distance from the connection equal to that measured to the load point in the laboratory. Lateral translation was prevented at these nodes as well, but no longitudinal restraint was included. Vertical and lateral translations were prevented at the three nodes of the bottom flange at a distance from the connection equal to that measured to the centre of the supporting jack in the laboratory. Again, no longitudinal restraint was provided. No rotational degrees of freedom in the model were restrained. Using these numerical boundary conditions, the effects of the knife edges, rollers, and lateral supports provided in the laboratory were modelled. End rotation of the connection imposed by lowering the support jack, which was a parameter in the laboratory tests, was not modelled in the numerical analyses because it was found that it did not adversely affect the coped beam capacity.

4.3 Material Model

An elastic–plastic–hardening material model was selected for the numerical analysis to represent accurately the material properties of structural steel. Using the data gathered from the three tension coupons taken from the associated test beam web, a single stress–strain response was created for each numerical model. The mean modulus of elasticity, E, from the three coupons was used to define the elastic response of the steel. For the inelastic portion of the model, the stress and strain data from the static readings taken during the coupon tests were used. Along the yield plateau, two to four static readings were taken in each coupon test and the mean of these static readings was used for the yield stress in the numerical model. The mean hardening strain from the three coupon tests defined the end of the yield plateau. Along the hardening curve, two static readings were taken in each coupon test. For

each of these points, the mean static stress and mean static strain from the three coupons were used to define a point in the model. Similarly, the mean stress and strain from the static readings at ultimate from the three coupons defined the ultimate strength. Figure 4-5 shows the stress–strain response of the three coupons from Beam J and the associated material model (up to the ultimate strength) used in the numerical analysis for Model M5. The differences among the material model curves for the five numerical analyses are relatively small.

The nominal stress, σ_{nom}, and nominal strain, ε_{nom}, evaluated from the coupon tests were converted to true stress, σ_{true}, and true plastic strain, ε^{p}_{true}, the values required as input by ABAQUS, using the following equations:

$$\sigma_{true} = \sigma_{nom}(1+\varepsilon_{nom}) \qquad [4\text{-}1]$$

$$\varepsilon^{p}_{true} = \ln(1+\varepsilon_{nom}) - \left(\frac{\sigma_{true}}{E}\right) \qquad [4\text{-}2]$$

After the ultimate load is reached in a tension coupon, the stress and strain are no longer calculated based on initial coupon dimensions, *i.e.*, load divided by initial area for stress and change in length divided by initial length for strain. As necking takes place, the length over which elongation occurs is very small and the associated cross-sectional area reduces, resulting in stresses and strains significantly different from those calculated using initial area and length. To model the stress–strain response of steel after ultimate in the material model, a material stiffness (*i.e.*, slope of the true stress–true strain curve) after ultimate was assumed. Based on numerical analyses of standard tension coupon tests by Khoo *et al.* (2000), a post-ultimate material stiffness of approximately 500 MPa was assumed (*e.g.*, see Khoo *et al.*, Table 5.6). For the tension coupons used here, the typical static ultimate stress was approximately 600 MPa (true stress) with a corresponding true plastic strain of 15%. Using the material stiffness above, the material response was extrapolated to 120% true strain resulting in a corresponding true stress of 1125 MPa. It was expected that the strain-based criterion used to eliminate elements (described in section 4.4) would dictate that elements be removed when they reach a strain less than 120% and,

therefore, the material model was extrapolated to the upper bound of this range. There was no need to extrapolate beyond this level since elements would be removed from the model prior to reaching this strain level. A summary of the material model parameters for the five numerical analyses is given in Table 4-2.

4.4 Analysis Procedure

A specified vertical displacement was applied statically to the three nodes along the top flange at a distance from the connection equal to that measured to the load point during the laboratory test. Deformations were determined in the same manner as in the laboratory tests. The displacement of the nodes at the top and the bottom of the beam directly in line with the line of bolts nearest the end of the beam were measured and the difference provided the block shear deformation.

To model the tearing behaviour of the block, a strain-based failure criterion was used. From the results of the tension coupon tests, a maximum principal strain criterion for fracture was calculated using the following equations. Assuming, first, that the volume of the coupon remains constant, it can be shown that the nominal strain at fracture, ε_{nom}^{crit}, can be calculated from the initial and final measured cross-sectional areas:

$$\varepsilon_{nom}^{crit} = \frac{A_{init}}{A_{final}} - 1 \qquad [4\text{-}3]$$

where:

A_{init} is the initial cross-sectional area of the coupon, and
A_{final} is the minimum cross-sectional area of the coupon after fracture.

The nominal strain is converted to true strain by taking the natural log of the nominal strain, as follows:

$$\varepsilon_{true}^{crit} = \ln(1 + \varepsilon_{nom}^{crit}) \qquad [4\text{-}4]$$

By substituting Equation 4-3 into Equation 4-4 and manipulating the variables, the following equation can be derived:

$$\varepsilon_{true}^{crit} = \ln\left(\frac{1}{1 - \text{Reduction of Area}}\right) \qquad [4\text{-}5]$$

This value is the true strain in the tension coupon at rupture, and, since the loading in a tension coupon is uniaxial, this is the maximum principal strain at fracture. Reduction of Area, as defined in ASTM A370 (ASTM, 1997), is the difference in the initial cross-sectional area of the coupon and the final cross-sectional area expressed as a fraction of the initial area:

$$\text{Reduction of Area} = \frac{A_{init} - A_{final}}{A_{init}} \qquad [4\text{-}6]$$

The Reduction of Area for each coupon set is shown in Table 3-4. As the connection was loaded, the maximum principal strains along the tension face were monitored. A sixth order polynomial regression was fit to the data from the integration points of the ten elements in a radial line extending out from the bolt hole and extrapolated to the hole edge. At the load increment at which this extrapolated strain reached $\varepsilon_{true}^{crit}$ (considered to represent the onset of tearing at the hole), the maximum and minimum principal strains at the hole edge, $\varepsilon_{pr,max}$ and $\varepsilon_{pr,min}$, respectively, were recorded. To reflect the fact that ductile fracture is a shear phenomenon, the point of tearing of subsequent elements was determined using a shear strain criterion. Using the theory of strain transformation, the maximum shear strain, γ_{max}, at the integration points of the elements along the tension face was calculated using the following equation:

$$\gamma_{max} = \varepsilon_{pr,max} - \varepsilon_{pr,min} \qquad [4\text{-}7]$$

The shear strain at the element edge was then determined using the extrapolation method outlined above. This shear strain was used as the critical shear strain, γ_{max}^{crit}, for failure of any element in the model. The critical principal strains at the hole edge

(onset of tearing) and the corresponding critical shear strains (used as the general tearing failure criterion) for each model are shown in Table 4-3.

As load was applied to the model, the maximum shear strain for all elements in the connection was monitored. The element in the model with the largest γ_{max} at the integration point was located and the maximum shear strain at the element edge was determined by extrapolation. If this strain was larger than γ_{max}^{crit}, then the element was removed from the model. This process was continued until all elements with an edge shear strain greater than γ_{max}^{crit} were removed. Along the shear face, only those elements with a shear strain at the element edge exceeding the critical strain were removed at any given load increment. This approach assumes that the crack tip would blunt because of extensive yielding in the region around the crack tip. Although significant plastic deformation is expected to take place at the crack tip due to the high ductility of the steel in the test specimens, the extent of crack blunting in a real crack is probably not as large as the one modelled by element removal. Along the tension face, the elements were removed in a more abrupt manner. For single-line connections, the entire tension face was removed when the shear strain at the hole edge exceeded γ_{max}^{crit}, while the tension face was removed in two sections for two-line connections. The area between the two bolt lines was treated as one section and the area from the bolt line nearest the beam edge to the beam edge was treated as another, each being removed when the shear strain at the hole edge along that section exceeded γ_{max}^{crit}. Although removing the entire tension face at once may not accurately represent the actual failure, it provides a conservative result. This topic is discussed further in section 4.5. Once all elements exceeding γ_{max}^{crit} were removed, the vertical displacement of the nodes along the top flange at the load point was incremented. The connection load, therefore, increased and all elements were re-checked and removed if required. This process was continued until the connection load had decreased significantly, at which point the analysis was terminated. The web block was not completely torn from the beam web at the end of the analysis.

4.5 Analysis Results

The first set of analyses used the bolt model in which approximately one-half of the nodes were pinned, a method found by Epstein and Chamarajanagar (1996) and Huns *et al.* (2002) to produce acceptable results. This method gave reasonable predictions of load vs. deformation, but the connection initial stiffness was significantly higher in the model than in the laboratory tests. In an attempt to improve this, the rigid cylindrical bolt model with surface contact was implemented. These analyses resulted in slightly improved predictions of connection stiffness, although improvements were still required. A series of models intended to improve this further were completed in which the bolt initial bearing condition was varied. The cylindrical elements were lowered slightly inside the bolt hole to represent bolts that were not initially in bearing. Various bolt bearing conditions were modelled and it was found that the initial connection stiffness could easily be manipulated through this method. A reasonable bolt bearing condition was found for models M1 and M2 that resulted in acceptable approximations of connection stiffness. Upon continuing these contact element analyses past tension face rupture, it was found that shear tearing could not be modelled with reasonable effort. The removal of elements along the hole edge also removed a part of the contact surface, and as the connection was loaded further, the cylindrical bolt element attempted to contact web elements not defined in the contact surface interaction. This could only be resolved by redefining the contact surface at each step in which elements were removed, a process that would have made modelling times unreasonable. The contact element models were, therefore, not pursued past the initial bearing condition trials.

Examination of the contact element results showed that only a small portion of the bolt was in contact with the beam web at high loads. The method of pinning the nodes on the hole edge was reinvestigated, but with only ¼ of the nodes pinned. This method resulted in load vs. deformation behaviour similar to that obtained from the contact element models. It was, therefore, concluded that this method was a reasonable approximation of the bolt–web interaction. All models were analyzed using this bolt model and load vs. deformation plots for all five are shown in

Figures 4-6 through 4-10. The nature of the modelling process results in load vs. deformation behaviour that exhibits sharp decreases in capacity with the discrete removal of elements. Furthermore, immediately prior to the removal of elements, the capacity tends to be somewhat overestimated. The process, therefore, provides a bound of load vs. deformation behaviour, with the lower and upper peaks representing the lower and upper bounds of behaviour, respectively. The true load vs. deformation behaviour lies somewhere between these two bounds. Table 4-4 summarizes the ultimate vertical connection reaction and block shear deformation at ultimate for each model. In each case, the ultimate reaction from the analysis is compared to the ultimate reaction from the associated laboratory test in the form of a test to predicted ratio.

All five models failed in a block shear mode with the tension face, or a portion of it in the two-line connections, being removed first. For both of the two-line connections, Models M2 and M5, the portion of the tension face between the two lines failed initially, with the remaining portion failing after some tearing of the shear face had already taken place. After tension rupture, the connections showed gradual shear tearing vertically upwards from the bolt holes. The combination of tensile and shear tearing indicates that a block shear type failure was predicted by the analysis.

The effect of the initial bolt bearing condition was also investigated using the ¼-pinned models through the use of non-linear springs. Similar patterns of bolt bearing conditions as were used in the contact element models were analyzed using this method. Note that the results of Figures 4-6 to 4-10 are for an initial bearing condition where all of the bolts are initially in contact with the top of the hole, a condition that may not occur in practice due to normal fabrication tolerances. The two models selected for the bolt bearing investigation were Models M1 and M2, which did not show particularly good agreement in initial stiffness with the experimental response for the case of full bolt contact. For Model M1, two additional bearing conditions are presented in Figures 4-11 and 4-12. The maximum stagger case, Model M1-B-Max, had the topmost bolt pinned at the beginning of the test, with the remaining bolts modelled with non-linear springs requiring different

displacements to engage the high stiffness springs. The displacements required were 0.67 mm, 1.33 mm, and 2.00 mm for the second, third, and fourth bolt rows, respectively, with the last case representing a bolt at the bottom of the hole. The intermediate stagger case, Model M1-B-Int, had the topmost bolt pinned with the second, third, and fourth bolt rows requiring 0.17 mm, 0.33 mm, and 0.50 mm, respectively, to engage the springs. For Model M2, only one staggered case is presented in which the topmost row of bolts was pinned and the second and third rows were engaged after 1.00 mm and 2.00 mm of displacement, respectively. The load vs. deformation behaviour for Model M2-B-Max is shown in Figure 4-13. Models M1-B-Int and M2-B-Max gave reasonable approximations of the connection stiffness of their respective laboratory test specimens. Note that the initial curves—Figures 4-6 and 4-7—and the maximum stagger curves—Figures 4-11 and 4-13—demonstrate the large range of stiffness that can be achieved merely by varying the initial bearing condition. A summary of the data from the bearing condition investigation analyses is shown in Table 4-4. The results indicate that, although the bolt bearing condition affects connection stiffness, the ultimate load is not greatly affected, as shown by the similar ultimate loads of the tests with varying bolt bearing conditions.

One series of analyses was completed to investigate the effect of progressive tension tearing. In all previous analyses, the tension face of the block was removed in a single step when the strain at the hole edge exceeded the critical shear strain. Based on observations of block shear failure of gusset plates tested by Huns (2002), this was considered to be a reasonable approximation. However, in coped beams, the stress distribution along the tension face is less uniform than in gusset plates, with high stresses near the hole edge and lower stresses towards the end of the beam. As such, the tension tear likely does not occur all at once, but probably occurs progressively. Analysis of the normal stress distributions along the tension face of each of the five models showed that Model M3 exhibited a more non-uniform distribution than any of the others, likely due to the increased edge distance. Moreover, this model showed the largest error in ultimate load when compared to the test results, a result that may be improved through more refined modelling of the tension face tearing process. As such, this connection configuration was used in the incremental tearing analysis series

and designated Model M3-I. The analysis was completed using the ¼-pinned node bolt model. Rather than removing the entire tension face at once, the elements were removed one at a time in the same manner as the shear tears. It should be noted, however, that this method is not a true representation of the tension tearing process, since the width of a crack tip is infinitely small and the modelled crack tip had the finite with of the adjacent remaining element. Nevertheless, the fineness of the mesh provided a reasonable crack tip condition. It was believed, therefore, that this was a more representative method than removal of the entire tension face in a single step. The load vs. deformation behaviour of this model is shown in Figure 4-14. At the peak connection load, only two of the 18 elements along the tension face had been removed, and the ultimate connection reaction showed a significant increase over Model M3, as seen in Table 4-4.

4.6 Summary

Non-linear finite element analyses were completed on five connections from the laboratory experiments to explore some of the main features of the connection response. The configurations chosen encompassed a wide range of connection parameters including number of bolt rows, number of bolt lines, and edge distance, and were used to validate the finite element model for future use. A variety of modelling procedures were used to predict the load vs. deformation behaviour recorded in the laboratory tests. Four methods were used to represent the restraining effect of the bolts on the connection that utilized pins, non-linear springs, and surface contact elements. Non-linear material models based on tension coupon test data were created to represent the elastic–plastic–hardening behaviour of structural steel. The results show that due to the complexity of the behaviour, the load vs. deformation response of coped beams cannot yet be predicted accurately in all respects by finite element analysis.

The methods used in this research program may not accurately represent the propagation of the tears by which block shear failure occurs. In particular, the blunt crack propagation that is used in this method does not accurately represent the condition that exists at the crack tip. The analyses revealed, as well, that the

connection initial stiffness is highly dependent on the initial bolt bearing condition and that a reasonable bearing condition exists that gives good agreement with the experimental stiffness. However, it was also found that the ultimate connection capacity is not as significantly affected by this parameter. Although the finite element models did not predict well the load vs. deformation behaviour of the laboratory connections over their full range, they do provide a significant advancement toward the development of a strength model for block shear failure of coped beams over those that have been described in the literature.

Table 4-1: Analysis–Laboratory Test Associations

FEA Model Number	Associated Laboratory Connection Designation
M1	B2
M2	C2
M3	E1
M4	F1
M5	J2

Table 4-2: Material Properties Summary

Model M1		Model M2		Model M3		Model M4		Model M5	
E = 203 500 MPa		E = 210 600 MPa		E = 201 200 MPa		E = 207 500 MPa		E = 205 400 MPa	
σ_{true} (MPa)	ε^{p}_{true}	σ_{true} (MPa)	ε^{p}_{true}	σ_{true} (MPa)	ε^{p}_{true}	σ_{true} (MPa)	ε^{p}_{true}	σ_{true} (MPa)	ε^{p}_{true}
368	0.000	367	0.000	371	0.000	368	0.000	379	0.000
374	0.017	373	0.018	377	0.016	374	0.016	388	0.024
442	0.035	442	0.027	458	0.036	452	0.035	446	0.037
501	0.062	505	0.059	512	0.059	505	0.059	515	0.067
590	0.137	592	0.135	602	0.140	598	0.143	607	0.161
1125	1.20	1125	1.20	1125	1.20	1125	1.20	1125	1.20

Table 4-3: Critical Strains Summary

Model Number	$\varepsilon^{crit}_{true}$	γ^{crit}_{max}
M1	0.56	0.70
M2	0.51	0.70
M3	0.56	0.70
M4	0.48	0.70
M5	0.86	1.30

Table 4-4: Finite Element Analysis Results Summary

Model Number	Ultimate Connection Vertical Reaction (kN)	Displacement of Bottom of Connection at Ultimate (mm)	Displacement of Top of Connection at Ultimate (mm)	Block Shear Deformation† at Ultimate (mm)	Laboratory Ultimate Connection Vertical Reaction (kN)	Test to Predicted Ratio††
M1	432	6.2	0.5	5.7	475	1.10
M2	513	1.2	0.2	1.0	537	1.05
M3	415	5.8	0.5	5.3	568	1.37
M4	276	3.9	0.4	3.5	324	1.17
M5	364	2.1	0.4	1.7	338	0.93
M1-B-Max	400	5.7	0.5	5.2	475	1.19
M1-B-Int	401	4.7	0.4	4.3	475	1.18
M2-B-Max	540	3.3	0.6	2.7	537	0.99
M3-I	473	3.1	0.4	2.7	568	1.20

† Block Shear Deformation is the difference between Bottom of Connection Displacement and Top of Connection Displacement

†† Test to Predicted Ratio = P_{LAB} / P_{FEA}

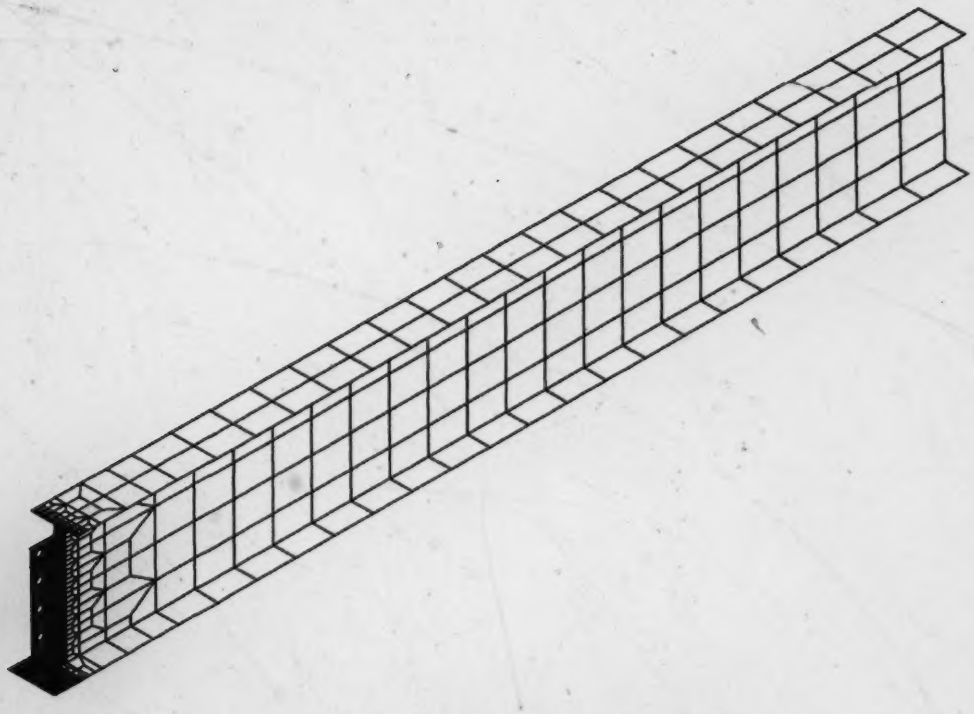

Figure 4-1: Typical Beam Mesh, Isometric

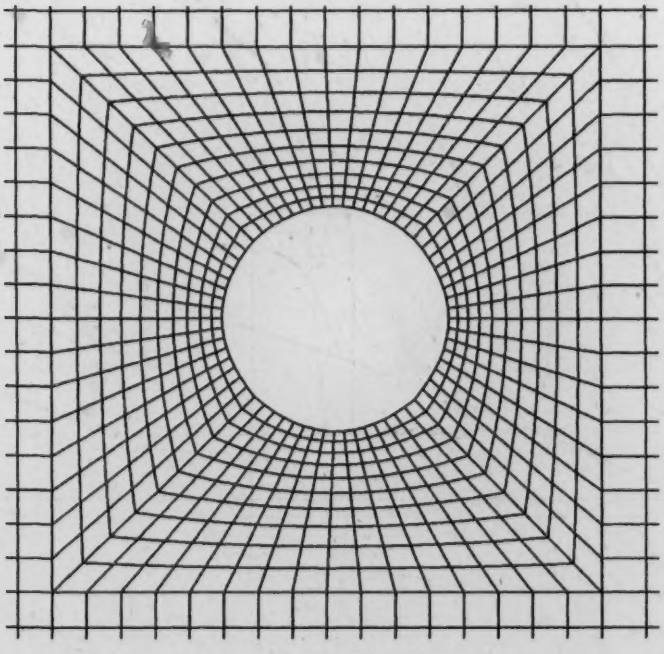

Figure 4-2: Typical Bolt Hole Mesh Detail

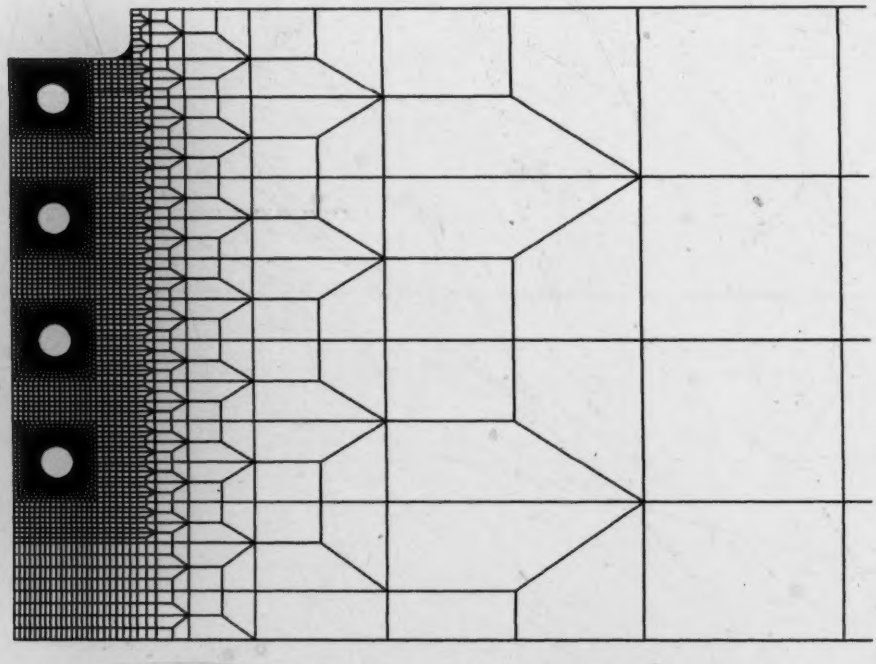

Figure 4-3: Typical Transition Mesh Detail

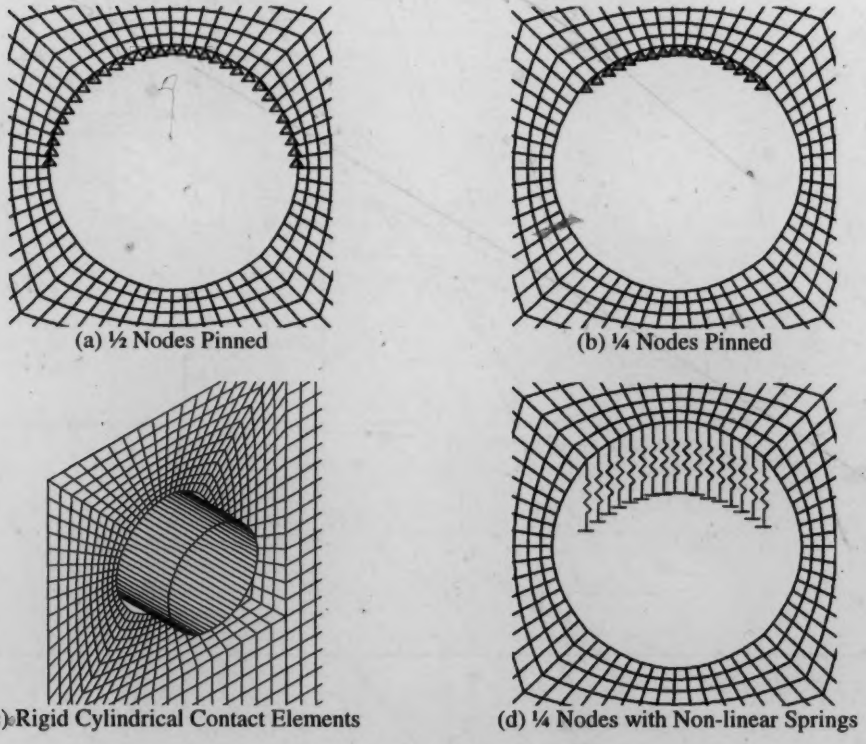

Figure 4-4: Bolt Modelling Methods

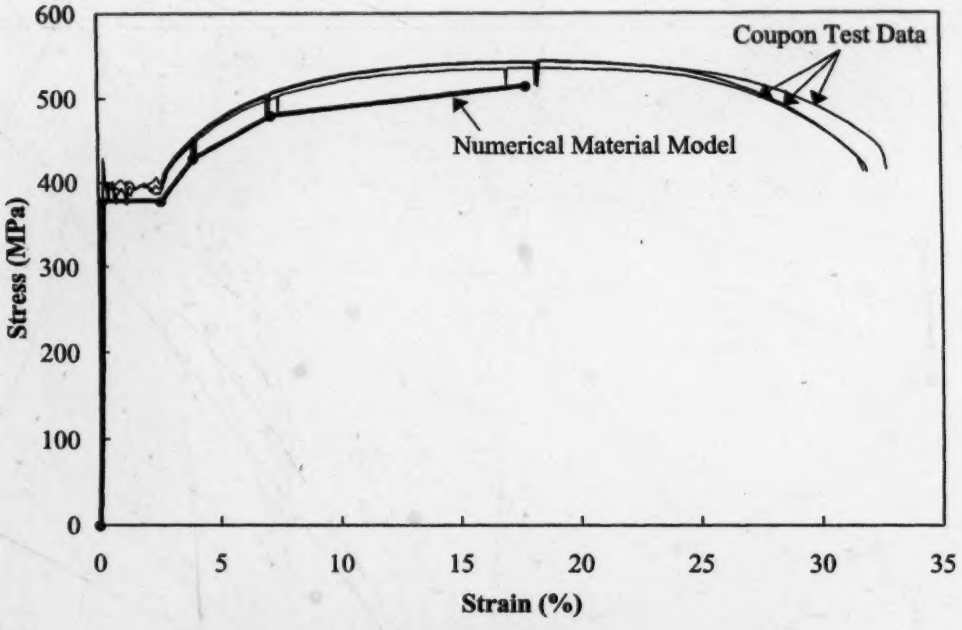

Figure 4-5: Material Model Definition, Model M5

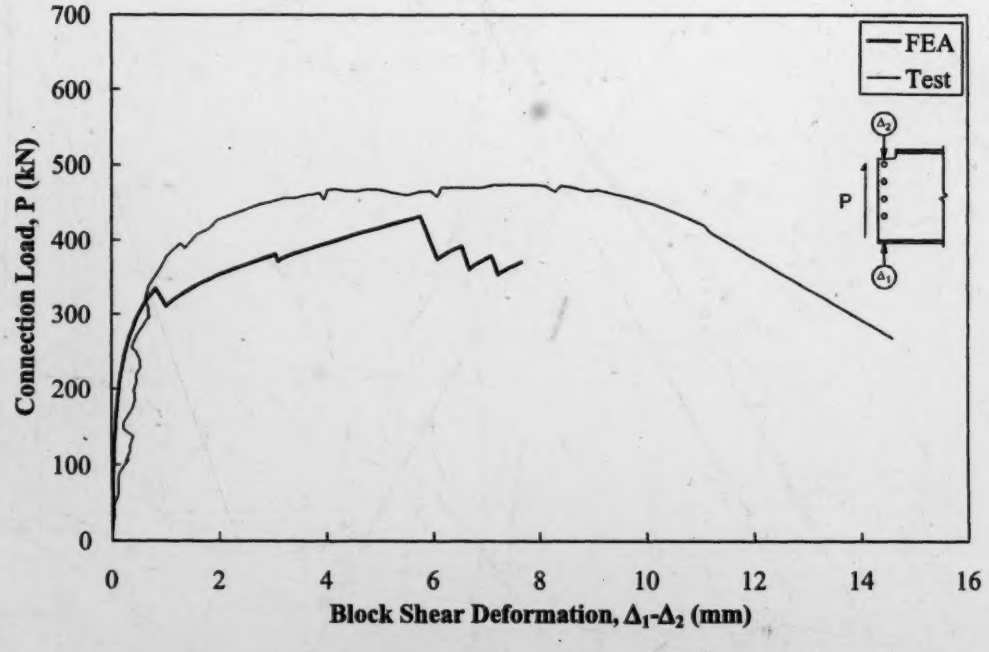

Figure 4-6: Load vs. Block Shear Deformation Curve, Model M1

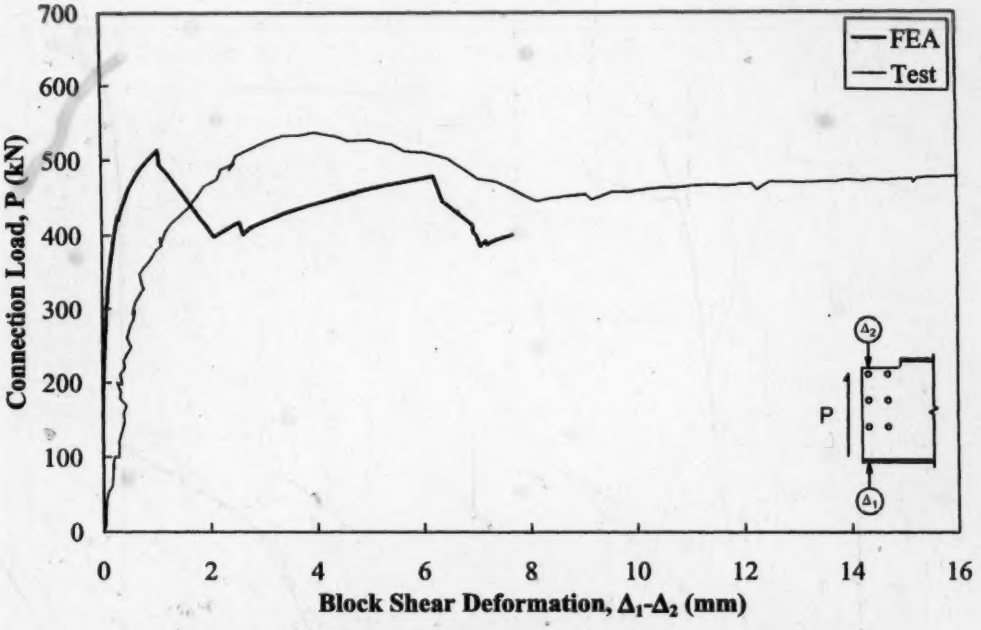

Figure 4-7: Load vs. Block Shear Deformation Curve, Model M2

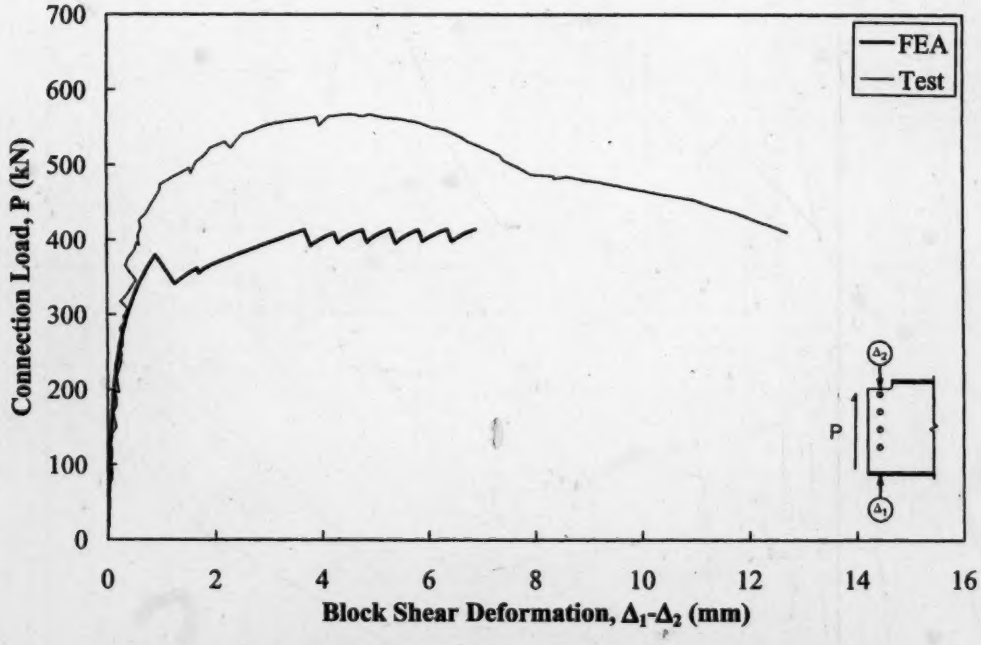

Figure 4-8: Load vs. Block Shear Deformation Curve, Model M3

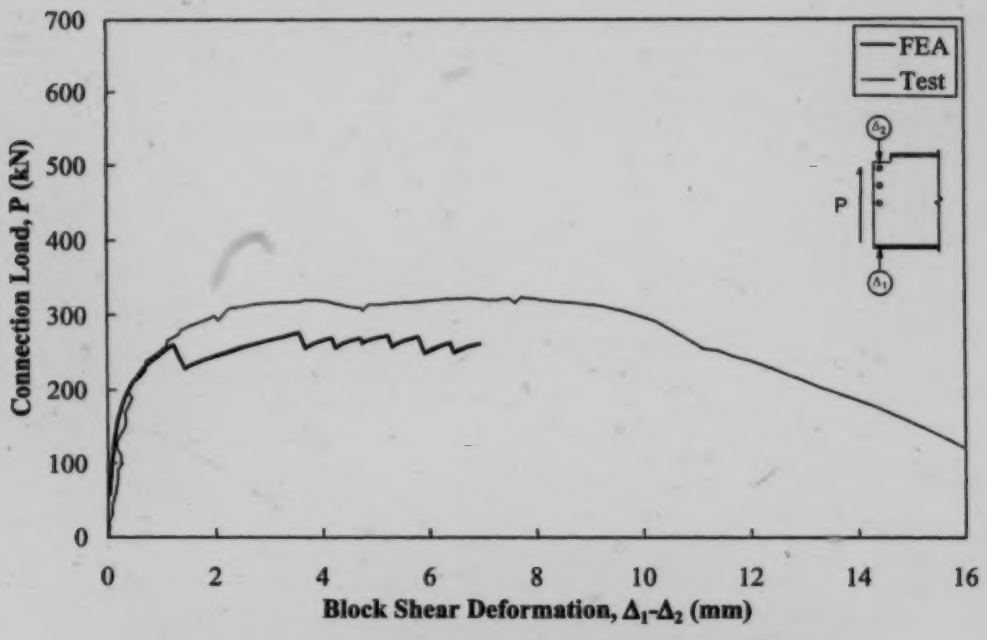

Figure 4-9: Load vs. Block Shear Deformation Curve, Model M4

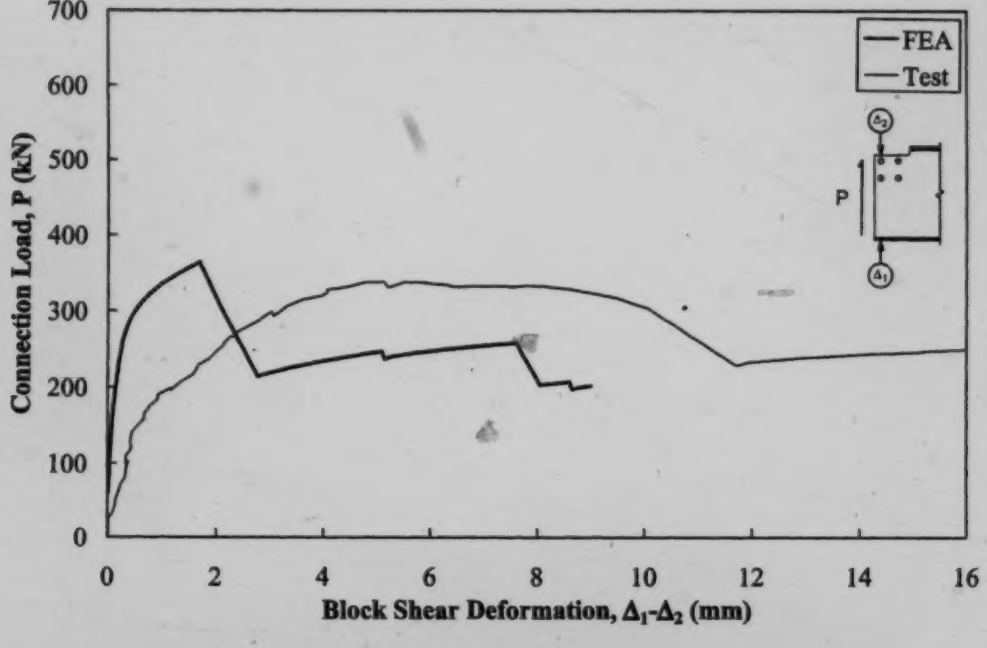

Figure 4-10: Load vs. Block Shear Deformation Curve, Model M5

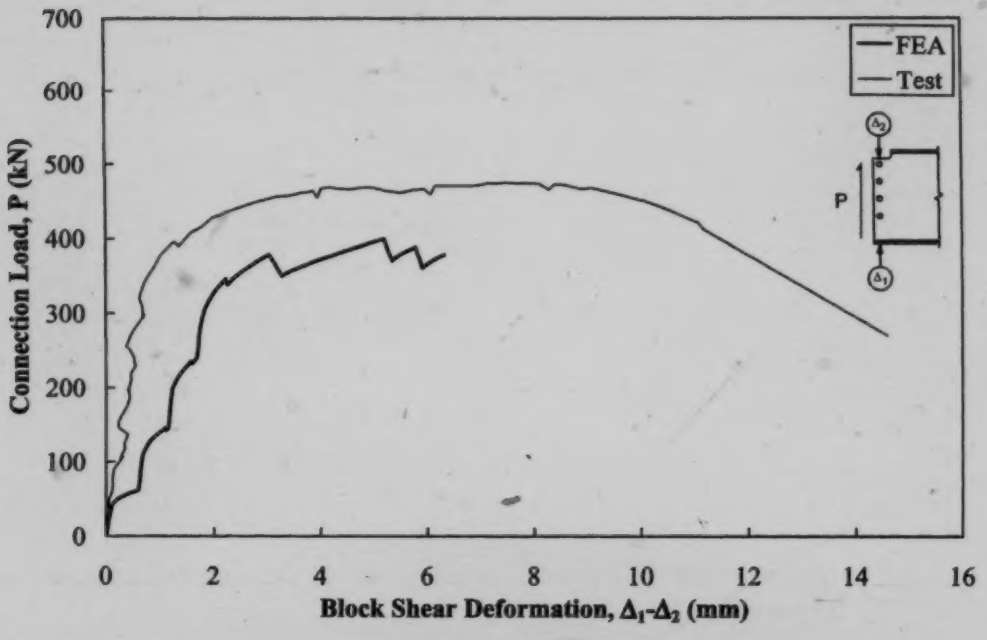

Figure 4-11: Load vs. Block Shear Deformation Curve, Model M1-B-Max

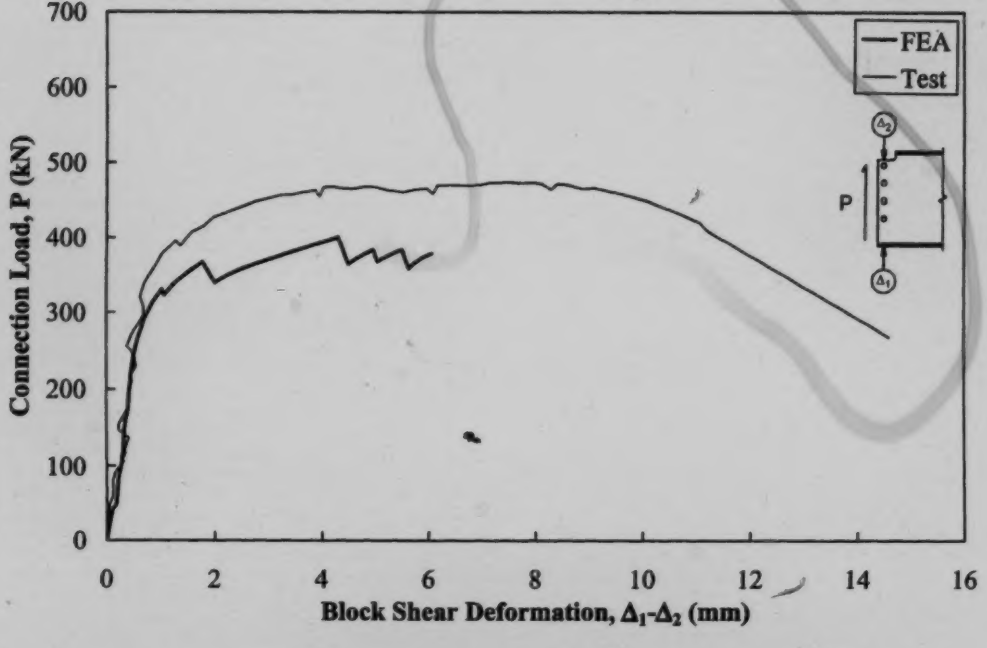

Figure 4-12: Load vs. Block Shear Deformation Curve, Model M1-B-Int

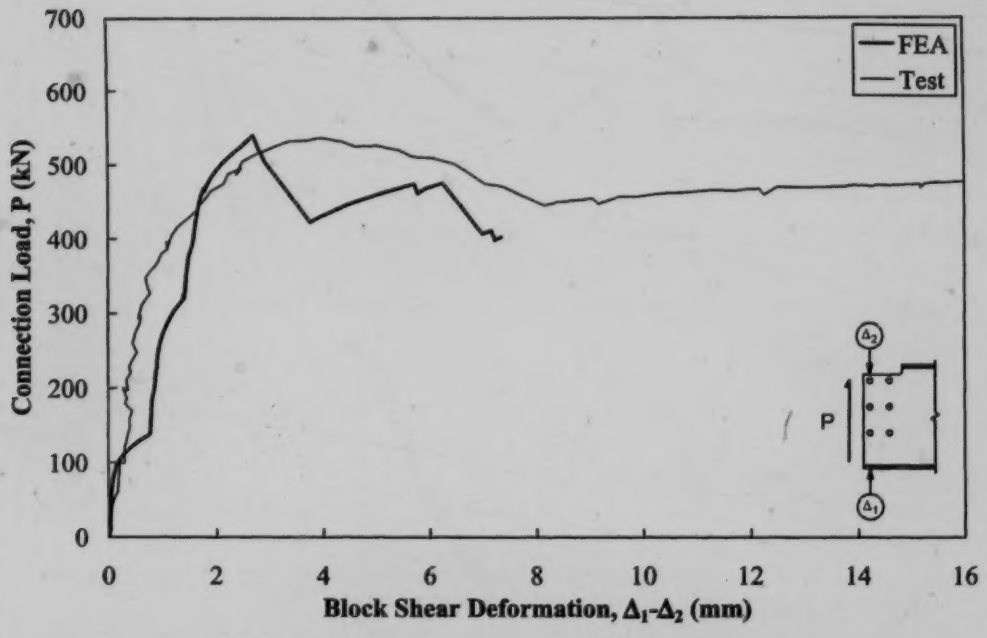

Figure 4-13: Load vs. Block Shear Deformation Curve, Model M2-B-Max

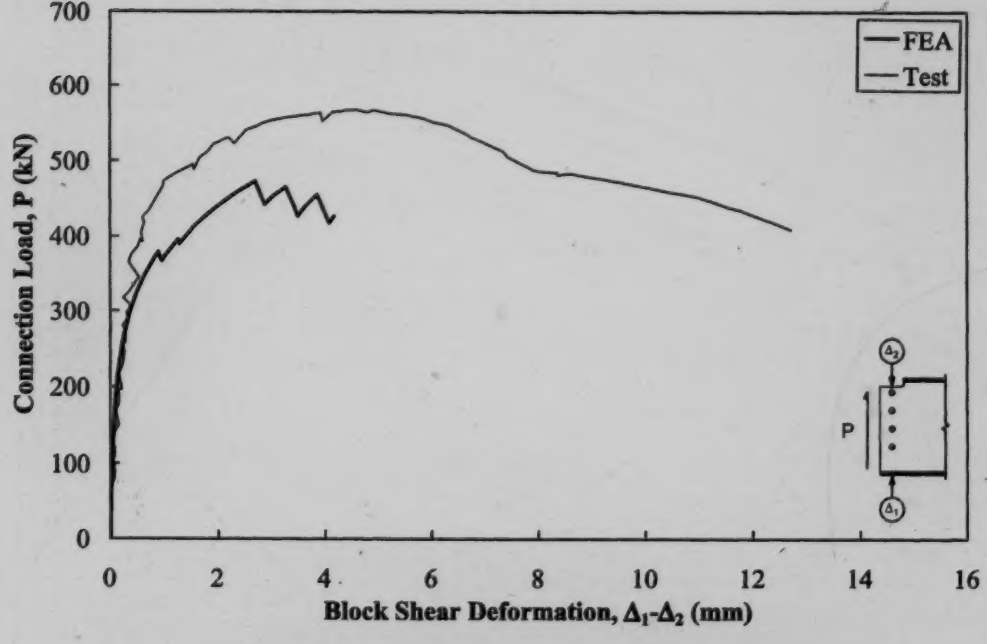

Figure 4-14: Load vs. Block Shear Deformation Curve, Model M3-I

5. Discussion

5.1 Introduction

A discussion of the laboratory tests and numerical analyses is presented below. Each of the 11 parameters explicitly investigated in the laboratory tests is examined and conclusions on their effects on block shear behaviour are drawn. Additionally, the numerical analyses are critically examined and conclusions on load vs. deformation behaviour, initial bolt bearing condition, and connection stiffness are reached. Following this, existing design standards are assessed for their accuracy and consistency in predicting block shear failure, and three potential new design equations are presented. All of these models are then assessed by calculating the resistance factor required to provide an adequate level of safety. It is found that the models presented in the current Canadian and American standards do not provide adequate levels of safety for all connection configurations. A new design model is proposed for prediction of block shear capacity of coped beams.

5.2 Laboratory Tests

From the laboratory test results, many conclusions regarding the behaviour and capacity of coped beam connections failing by block shear can be drawn. In the discussion below, comparisons are made among the ultimate capacities of the various connections tested. In order to avoid biasing the conclusions toward a particular capacity equation, the experimental capacities presented have not been normalized to account for variations in material properties. The yield and tensile strengths of the nine beam webs did not vary significantly, as shown in Table 3-4, although the tensile strengths of beams G and H were slightly lower than those of the other beams. Where significant differences occur, the relative material strengths are considered in the interpretation of the results and are included in the discussion below. For each test parameter (see Table 3-3), load vs. deformation curves of the relevant connection tests are presented on a single plot. These are shown in Figures 5-1 through 5-12.

Effect of End Rotation

Three series of tests examining the effect of end rotation were completed, the results of which are shown in Figures 5-1 to 5-3. In all cases, the ultimate load was not adversely affected by rotation, and, in fact, the beams to which a rotation was applied tended to achieve somewhat higher capacities, particularly in two-line connections. In the second series (Figure 5-2), the lower material strength of the web of beam H amplifies this conclusion further. The effect of end rotation on connection ductility is more difficult to determine. In the first series, Tests B2, B1, and A2, the connection ductility was not significantly affected by end rotation, as shown by the nearly identical load vs. deformation behaviour of these connections in Figure 5-1. For the second series, the ductility of Connections H1 and H2 was significantly higher than for Test F1. This is attributed to the change in failure mode from a classical tear-out (Test F1 with no rotation) to a partial tear-out (Tests H1 and H2). As the load was increased, the tensile crack opened further, rather than the web block tearing out, resulting in higher block shear deformation readings. In the third end rotation series, Tests C2 (no rotation) and J1 exhibited partial tear-out and classical tear-out, respectively. Since the high ductility exhibited by some of these connections can be accounted for by the mode of failure, it is concluded that end rotation does not have a significant effect on connection ductility. As end rotation was shown to have no adverse effect on connections failing in block shear, the remaining tests were completed with no applied end rotation.

Effect of Gross Shear Area

Connections B2 and C1 were fabricated with identical net tension and net shear areas but with a different number of bolt rows. This required an increase in bolt row spacing for Connection C1 (3 bolts) over Connection B2 (4 bolts), but resulted in a reduced gross shear area. Connection B2 showed 18% higher capacity, and therefore it is apparent that the shear portion of the block shear capacity must be developed over an area greater than the net shear area. However, this does not necessarily imply that the resistance is developed over the gross shear area. Observations of the failed

specimens showed that the fracture surfaces actually intersect a small portion of the bolt holes, implying that the governing shear area lies somewhere between the gross area and net area, although it appears to be very close to the gross area (see Figure 3-7). The bolts force the shear failure plane to pass through the edge of the hole rather than through the hole centre, where the shear area is minimum. The net tension area and material properties for the two connections are nearly identical, and the increase in strength is more than can be attributed simply to the increase in gross shear area. It is not known why the capacity of Connection B2 was somewhat higher than expected.

Effect of End and Edge Distance

Tests with increased end or edge distance (Figure 5-5) demonstrated anticipated changes in load vs. deformation behaviour. For the test with increased edge distance, Connection E1, the capacity was 20% higher than that of a similar connection, Connection B2, having the minimum edge distance prescribed by CSA–S16–01. The net tension area of Connection E1 was 68% larger than that for B2. For comparison, the equation proposed by Ricles and Yura (1983), presented as Equation 2-1, is used to calculate an expected increase in capacity. The capacity for Connection E1 is expected to be 12% higher than that for Connection B2, which is significantly lower than the observed difference in capacity. This may be due, in part, to the inherent assumption in Equation 2-1 that the stress distribution varies linearly along the tension face, which may not be correct. If the factor 0.5 in Equation 2-1 is changed to 0.9, then the predicted increase in capacity for these tests is 20%. This suggests that the stress distribution along the tension face may not vary linearly from zero to F_u, as assumed by Ricles and Yura. Test E2 had increased end distance, resulting in a 9% increase in gross shear area over Test B2, which had the minimum permissible end distance, and the capacity of Connection E2 was 9% higher than that of Test B2. Equation 2-1 predicts an increase in capacity, in this case, of 10%, which is very close to the observed increase. This observation supports the shear portion of this equation, which assumes that shear yield stresses act over the gross shear area. It is seen that a 25 mm increase in edge distance (tension area) more effectively increases capacity

than the same increase in end distance (shear area), as would be expected based on the fact that the ultimate tensile stress is higher than the ultimate shear stress. These results support similar conclusions made by Ricles and Yura. Neither end distance nor edge distance is shown to have a significant effect on connection ductility.

Effect of Bolt Diameter

One test was completed with 25.4 mm (1 ") bolts while all others used 19.1 mm (3/4 ") bolts. This test, Connection D1, had the same number of bolt rows and the same net shear area as Connection C1. Both connections were fabricated with minimum end and edge distances and were on opposite ends of the same beam, effectively removing any variation due to material properties. As shown in Figure 5-6, Test D1 exhibited an 11% increase in ultimate capacity over Test C1. This is attributed to a 14% increase in net tension area, due to the slightly larger edge distance, and a 3% increase in gross shear area, due to the slightly larger bolt row spacing. Using the equation proposed by Ricles and Yura (Equation 2-1), the expected increase in load due to these changes in area is 7%. Since the difference is relatively small, it is not believed that bolt diameter has a significant effect on capacity. The two connections had nearly identical ductility showing that the bolt diameter does not affect connection behaviour.

Effect of Section Depth

Identical three-bolt connections on two section sizes were tested. Connection F1 was on a W410x46 section while Connections G1 and G2 were on opposite ends of the same W310x60 beam. The load vs. deformation behaviour of the three tests was nearly identical with the connection ductility varying little, as shown in Figure 5-7. The capacity of Connection F1 was 15% to 16% lower than that of the connections on the W310 section, but this can be largely attributed to a 12% to 13% difference in as-measured web thickness between the two sections. The tensile strength, F_u, of these two beams was different, but it is not believed that this had a significant impact on the connection capacity. It has been shown, above, that the shear portion of the capacity is generated by shear yielding over the gross shear area,

and, in this case, the yield strength of the two beams was nearly identical. Since the net tension area is small compared to the gross shear area, the difference in tensile strength had minimal impact on the connection ultimate load.

Effect of Connection Depth

Connections C1 and F1 were both three-bolt connections on W410x46 beams with the bolt row spacing as the only variable. The connection depth represented approximately 62% and 48%, respectively, of the section depth remaining at the cope. As seen in Figure 5-8, Connection F1 exhibited a 19% lower capacity than C1, an effect that is largely due to the 24% smaller gross shear area of this connection. The expected decrease in capacity, as calculated using Equation 2-1, is 22%, which is close to the observed decrease of 19%. The depth of the connection does not seem to affect significantly connection capacity apart from the effect of the increase in gross shear area. The behaviour of the two connections was very similar with slightly less ductility in the shallower connection (F1).

Effect of Number of Bolt Rows

The number of bolt rows was varied between Connections B2 and F1, while the bolt spacing was identical for the two tests. The three-bolt connection, Test F1, had 32% less capacity than the four-bolt connection, B2, as shown in Figure 5-9. The gross shear area of Connection F1 was 30% lower than that of B2, to which the change in capacity is largely attributed. Using Equation 2-1, the expected decrease in capacity for these two connections is 29%, which is close to the observed decrease. The connection behaviour is nearly identical in the two cases with the ultimate load being reached at similar displacements. The number of bolt rows does not affect the connection capacity apart from the effect of the associated change in gross shear area.

Effect of Number of Bolt Lines

Connections C1 and C2 compared one-line and two-line connections with all other connection parameters remaining constant. The bolt line spacing for Connection C2 was nominally 75 mm, and, as expected, the two-line connection had

more capacity, as shown in Figure 5-10. The 351% increase in net tension area produced a 34% increase in connection strength. Again, using Equation 2-1, the expected increase, here, is 25%. As described above with the edge distance series, the implicit assumption in this equation that the tension stress varies linearly along the tension face may not be correct. In this case, replacing the 0.5 factor with 0.7 results in an expected increase in capacity of 34%, the same as that observed. This supports the conclusion that the stress may not vary linearly from zero to the ultimate tensile strength along the tension face. The change in failure mode for Connection C2 to the partial tear-out makes assessment of the effect on ductility difficult, as described in the discussion of the end rotation series. The deformation at the ultimate load is similar in the two connections, but past the ultimate load, the partial tear-out failure produced high values of block shear deformation in Connection C2.

Effect of Double Cope

The double-coped connection, Test D2, had identical connection parameters to Test E1 except for the relatively deep cope of the bottom flange, which provided nominally equal top and bottom end distances. Connection D2 was designed to fail in pure shear, which is considered to be a special case of block shear. The change in failure mode—which effectively replaces the tension face resistance with that of an extension of the shear face—resulted in only a 7% loss in capacity with the deflection at the ultimate load being somewhat lower in the double-coped connection, as shown in Figure 5-11. Equation 2-1 predicts a 6% loss in capacity, in this case. An edge distance greater than the minimum permissible was selected to emphasize the effect of losing the tension face resistance and to ensure the shear failure mode in D2. The edge distance in Connection E1 was approximately twice the bottom end distance of D2. The test results demonstrate that a significant portion of the connection capacity can be developed by the shear component of the resistance. Examination of the deformed specimen shows that the manner in which deflections were measured did not capture the block shear deformation well (see Figure 3-7(h)), and it is, therefore, difficult to comment on the effect of the double cope on connection ductility.

Repeatability

The variability of the test procedure was examined with two identical connections having identical material properties, Tests G1 and G2, on the opposite ends of the same W310x60 beam. The load vs. deformation behaviour of the two tests is nearly identical, as shown in Figure 5-12, and only a 2% difference in capacity occurred. This verifies that the tests were conducted in a similar manner and that the results of all the tests are, in themselves, directly comparable.

The effects of the test parameters discussed above on connection capacity can be largely attributed to the associated changes in tension and shear areas. None of these parameters was shown in and of itself to have a significant effect on connection behaviour or ductility. An exception is the end rotation series, where end rotation was shown to increase the connection capacity, particularly for two-line connections. Due to the difficulty in predicting the degree of end rotation at the ultimate load, and the variability in the amount of increase observed, it is recommended that this effect be neglected in design. Nevertheless, it was demonstrated that no reduction in capacity need be considered to account for the effects of end rotation. Therefore, of the parameters investigated in this research program, only the magnitude of the net tension area and gross shear area are found to affect significantly coped beam connections.

Although many test parameters have been investigated in this laboratory program and the pool of experimental data has been significantly increased, further full-scale testing is required to improve the understanding of certain aspects of the behaviour of these connections. The effect of variables such as block aspect ratio and in-plane eccentricity have not yet been explicitly investigated and the effects of double copes and number of bolt lines need to be investigated further.

5.3 Numerical Analysis

The finite element analyses carried out in this research program, while not being developed to the point where the full load vs. deformation response can be predicted, did provide useful insights into important aspects of the connection behaviour. The

method used in this research program was shown by Huns *et al.* (2002) to produce reasonable estimations of connection behaviour in bolted gusset plates. Attempts to adapt the procedure of Huns *et al.* to account for the differences in the connection conditions of coped beams were made, including varying the bolt model and the tearing method, but the laboratory connection behaviour could not be reliably reproduced by the analysis.

One limitation of the finite element analysis is the method of modelling block tearing. The process used is not truly representative of the behaviour and may not provide accurate results. As shown in the incremental tension face tearing investigation, the process of eliminating the entire tension face at once does not provide accurate results, although this method gives a conservative estimation of capacity. If a progressive failure occurs, some resistance will remain after the initiation of the block tear. Removal of the tension face in one step, however, eliminates all load resistance provided by that portion of the block, resulting in less connection resistance. The incremental tearing analysis, however, did not accurately represent the true tearing behaviour either. By eliminating elements in the model, blunt crack propagation is modelled, while tearing in the real connection is a sharp crack propagation process. Blunt cracks do not exhibit the same high strain concentrations that exist at the tip of a sharp crack and, therefore, the critical strain criteria used will not be reached at the appropriate load step. Further development of the finite element model would likely resolve these issues and allow for accurate prediction of block shear in coped beams. A more rigorous approach to block tearing is likely the key to accurate prediction of load vs. deformation behaviour.

Two of the test parameters studied in the laboratory tests were also studied within the five finite element models. These were the effect of the number of bolt rows and the effect of edge distance. Even though the finite element analysis cannot, using the current procedure, accurately predict the ultimate capacity of a coped beam connection, it may still be useful in predicting the relative capacities of two connections. Comparing only within the analytical results, the decrease in the number of bolt rows from four to three (Models M1 and M4, respectively) resulted in a 36%

reduction in capacity. The associated laboratory tests (Connections B2 and F1) showed a 32% reduction in capacity. Although the ultimate capacities of these two connections are not well predicted by the finite element analysis, their relative capacities are. The increase in edge distance from 25 mm to 50 mm resulted in a 9% increase in capacity in the numerical analyses (Models M1 and M3-I), while the laboratory tests showed a 20% increase in capacity for the associated connections (Tests B2 and E1). In this case, the relative capacities are reasonably predicted although there is still a significant difference.

The finite element analysis revealed that the initial bolt bearing condition has a strong effect on connection stiffness and that the connection stiffness could perhaps be reasonably predicted if the bolt bearing condition were known. The bearing condition was examined for Models M1 and M2. An upper bound stiffness was found when all bolts were in bearing at the beginning of the test. The bearing condition with the top row of bolts initially in bearing, the lowest row initially in contact with the bottom of the hole, and the intermediate rows varying linearly in between (*i.e.*, a staggered condition) showed the lowest stiffness of the configurations examined. The finite element analysis was used to estimate the range of connection stiffnesses within which the real connection stiffness lies. The analysis also showed that the initial bearing condition has a minimal effect on the predicted ultimate load of the connection, and, therefore, even if the initial bearing condition is not known, the finite element analysis should be capable of predicting connection capacity.

The distribution of stress along the tension and shear areas determined from the finite element analysis can be assessed to indicate how the connection load is being resisted. However, since the load vs. deformation behaviour has not yet been accurately modelled and the stress concentrations at the crack tips have not been accurately represented, these results may not be reliable. Nevertheless, the stress distributions were examined to determine the trends in normal tensile stress along the tension face immediately prior to tension face rupture. These stress distributions are shown in Figures 5-13 and 5-14 for one- and two-line connections, respectively. The stress is normalized by the maximum stress along the tension face, thus removing any

bias between the individual analyses due to the magnitude of the stresses. The horizontal axis represents the length along the block from the edge of the beam and is normalized by the distance from the beam edge to the bolt hole furthest from the edge. In Figure 5-14, the discontinuity in the stress distribution between 16% and 40% of the tension face distance represents the bolt hole in the bolt line nearest the beam edge. In general, for the one-line connections with minimum edge distance (Models M1 and M4), the normal stress along the tension area was approximately uniform, except very near the beam edge. For the two-line connections (Models M2 and M5) and the one-line connection with increased edge distance (Model M3), the normal stress distribution was non-uniform with the stresses being highest near the bolt holes and somewhat lower away from the bolts. This does not support the conclusion made by Ricles and Yura (1983), based on linear elastic analyses, that the stress distribution can be approximated as a linearly varying stress across the tension area with a stress equal to F_u at the beam edge and zero at the line of bolts furthest from the beam edge.

Further development in the tear propagation method and an extension of the investigation into the effect of the bolt bearing condition should lead to more accurate predictions of the full load vs. deformation response. Once the model is refined and validated using existing test results, a parametric study should be completed in which connection parameters outside those examined in the laboratory are analyzed to increase the data pool. As well, block stress distributions could be used to quantify the effects of many connection parameters on the load carrying mechanism of these connections. These data would provide valuable input to the development of design equations that better reflect the true failure mode of coped beams failing in block shear.

5.4 Current Design Standards

An analysis of current design standards from North America, Europe, and Japan shows that an adequate and uniform level of safety is not being provided against block shear failure in coped beams (Kulak and Grondin, 2000, 2001). The design equations

for these standards, CAN/CSA–S16.1–94, CSA–S16–01, AISC LRFD 1999, EC3 ENV 1993–1–1, and AIJ 1990, are presented in Chapter 2.

The professional factor is defined as the ratio of the connection capacity determined experimentally to the predicted capacity as calculated from a design equation using measured dimensions and material properties and a resistance factor equal to 1.0. A professional factor of 1.0 indicates that the equation predicts the observed capacity exactly, while values greater than unity represent the case where the equation provides a conservative prediction of capacity and those less than unity represent an unconservative prediction. Table 5-1 lists the mean professional factors for each of these standards for all 36 full-scale tests completed (both in this research program and those reported in the literature) on coped beams. Also presented parenthetically is the coefficient of variation of the professional factor, indicative of the variability of the factor. A coefficient of variation approaching zero indicates better agreement between the design equation and the test capacity. For CAN/CSA–S16.1–94, the factor 0.85 is considered to be part of the resistance factor and therefore is not included in the capacity prediction calculations. Graphical representations of the professional factors for each test for each standard are shown in Figures 5-15 through 5-19 in the form of test vs. predicted capacity plots. The diagonal line on each graph represents a professional factor of 1.0. Points above this line indicate conservative results, while points below indicate unconservative results.

All standards provide a mean professional factor greater than one when all test results are considered, although their abilities to predict the capacity of the various connection configurations varies widely. The mean professional factor is closer to unity for CAN/CSA–S16.1–94 (Equation 2-2) than for any of the other standards presented. This equation assumes that the stresses reach ultimate on both the tension and shear areas. However, the professional factor for this standard has a large variability, as indicated by the coefficient of variation of 0.20 and as identified in the test vs. predicted capacities plot (Figure 5-15). Examination of the mean professional factors indicates that the equation is, in general, much less conservative for two-line connections than for one-line connections, and the standard also exhibits the lowest

professional factor for any test under any standard, 0.59 (a two-line connection), representing a significant over-estimation of capacity. The mean professional factor for this standard for all of the two-line connections conducted was 0.76, with a coefficient of variation of 0.18. Kulak and Grondin (2001) identified this over-prediction of strength, as well as the large variability, and the standard has since been revised.

The current edition of the Canadian standard, CSA–S16–01 (Equations 2-3 and 2-4), reduces the contribution of the tension component to the connection capacity by one-half and provides an additional limit to the shear component of the yield stress on the gross area. This provides significantly more conservative results than the previous edition of the standard, with a mean professional factor of 1.23. In fact, as seen in Figure 5-16, only two of the 36 predictions are unconservative, with professional factors of 0.89 and 0.96. Equations 2-3 and 2-4 govern in 17 and 19 test cases, respectively. As well, the variability of the results has been reduced, as indicated by the coefficient of variation of 0.12. The standard implies that the effective stress acting over the net tension area is 0.5 F_u for all connections. This is consistent with the observations of the numerical analyses wherein the tension face normal stress distribution is non-uniform, especially for two-line connections. However, a magnitude of this factor other than 0.5 may be more appropriate and provide more consistent results.

The AISC LRFD 1999 standard (Equations 2-5 and 2-6) employs three capacity equations representing three failure modes. Based on the relative ultimate strengths of the tension area and shear area, the equations combine either ultimate strength on the net tension area with yielding on the gross shear area or yielding on the gross tension area with ultimate strength on the net shear area. Both equations are limited to the combination of ultimate strength on both the net tension and net shear areas. The combination of ultimate stress in tension with the yield stress in shear is logical and is supported by test observations. However, the qualifying statement that the tension ultimate strength must be greater than the shear ultimate strength is rarely achieved in practice, and of the 36 coped beam tests, this equation governs for only

one. For the remaining cases, the combination of tensile yield and shear ultimate is applicable for 12 tests, and the rupture cut-off governs for 23. The standard provides slightly more conservative and less variable results than CAN/CSA–S16.1–94. However, for the two-line connections, the equations are largely unconservative, with professional factors as low as 0.59, as shown in Figure 5-17. The mean professional factor for this standard for all of the two-line connections tested was 0.78, with a coefficient of variation of 0.17. The three equations used here do not provide better results than the single equation used in CAN/CSA–S16.1–94, and, as such, the increased complexity is not justified. Furthermore, the standard does not describe the failure mode observed in the tests.

The set of equations presented in Eurocode 3 ENV 1993–1–1 (simplified to Equation 2-7) provides results similar to those provided by CSA–S16–01. The equations combine yielding of the gross shear area with a reduced stress acting over the tensile area. The reduction of $1/\sqrt{3}$ for the normal stress provides a reduction similar to the 0.5 factor used in CSA–S16–01, although the value appears to be derived from the von Mises shear yield criterion and is not applicable to the tension portion of the model. Eurocode 3 uses the net tensile area for one-line connections but reduces the net tension area for two-line connections by one bolt hole, the basis for which is unknown. The professional factors for this standard are, in general, conservative with only two unconservative results. The standard also provides the least variability of any of the standards investigated with a coefficient of variation of 0.11. The equations provide similar results for both one- and two-line connections.

The method outlined by the Architectural Institute of Japan (Equations 2-8 and 2-9) is, in theory, a conservative approach to block shear, combining shear and tensile strengths acting over net areas. One of the stresses is assumed to be at yield while the other reaches ultimate, with the lower of the two combinations governing the design. It is generally accepted that yield stresses can develop over gross areas, so the use of a reduced area should provide conservative results. In general, the standard provides professional factors greater than one, sometimes by a large margin, but also leads to several unconservative results, which can be seen graphically in Figure 5-19.

Professional factors as high as 1.90 and as low as 0.78 are observed, and the coefficient of variation of the results is higher for this standard than for any of the others at 0.23. The two-line tests conducted by Ricles and Yura (1983) show the most unconservative results, and the mean professional factor for this standard for all of the two-line connections tested was 0.96, with a coefficient of variation of 0.16. The AIJ 1990 method appears not to be representative of the actual failure mechanism for block shear in coped beams.

Many strength models for block shear in coped beams have been proposed. Of those examined above, few consistently provide a reasonable estimation of capacity. In particular, the differences in the ability to predict one- and two-line connections can be significant. Not only are many of these models inconsistent, but also they are often highly unconservative, and, therefore, an adequate level of safety is not yet being provided in all standards. A new design approach may better represent the observed failure mode of block shear in coped beams.

5.5 Proposed Capacity Equations

Three connection strength models were created in an attempt to represent better the connection failure mode. The first model presented, herein referred to as Proposed 1, includes only the first equation of the two used in CSA–S16–01:

$$P = 0.5A_{nt}F_u + 0.6A_{gv}F_y \qquad [5\text{-}1]$$

This single equation was originally proposed for use in the newest Canadian standard but the second equation (Equation 2-4), limiting the capacity to rupture on both the net tension and net shear areas, was added for consistency with the procedure used for gusset plates. The combination of rupture on the net tension area with yielding on the gross shear area is consistent with test observations. Mean professional factors for each dataset using this equation are shown in Table 5-2. This model makes a small improvement in the mean professional factor for both one- and two-line connections over CSA–S16–01 but makes no improvement on the coefficient of variation. Figure 5-20, which shows the test vs. predicted capacity data for this model, indicates that the equation provides generally conservative results.

The second model, herein referred to as Proposed 2, involves a modification to the model presented in CSA–S16–01 by applying a reduction factor for the tension contribution that is different for one- and two-line connections, as shown in the following three equations:

$$P = R_t A_{nt} F_u + 0.6 A_{gv} F_y \qquad [5\text{-}2]$$

$$P = R_t A_{nt} F_u + 0.6 A_{nv} F_u \qquad [5\text{-}3]$$

where:

$$R_t = \begin{cases} 1.0 & \text{for one-line connections} \\ 0.5 & \text{for two-line connections} \end{cases} \qquad [5\text{-}4]$$

The connection capacity is the lesser of Equations 5-2 and 5-3. For the test data available, Equations 5-2 and 5-3 govern in 17 and 19 cases, respectively. Based on the numerical analysis, it was found that the normal stress distribution along the tension face in one-line connections was nearly uniform and, for two-line connections, the tension face stress was significantly non-uniform. Therefore, a different reduction factor, R_t, was calculated for each case. A quasi-Newton method was used to find the reduction factors that minimized the coefficient of variation of the professional factors calculated using the equations. The values 1.0 and 0.5 for one- and two-line connections, respectively, were found to minimize the variation in the results. The factors can be interpreted as representing a uniform stress of F_u acting over the tension area in the case of one-line connections, and an average stress of $0.5\,F_u$ in the case of two-line connections. When compared to the predictions by CSA–S16–01, this model provides predictions that are closer to the test capacities, as indicated by the mean professional factor of 1.14, and less variable, as indicated by the coefficient of variation of 0.10. Figure 5-21 shows the test vs. predicted capacities for this design model and reveals that the Proposed 2 model reduces the variability in the professional factors over CSA–S16–01. This method may be more representative of the true block shear failure mode.

Analysis of the level of safety provided by these equations, which is dependent upon both the professional factor and its variability as discussed in section 5.6, indicated that a consistent level of safety was not being provided by Proposed 2 when comparing one- and two-line connections. It was found that the equations provided reasonable safety for one-line connections but not for two-line connections. To improve the level of safety, as well as its consistency, the values of R_t were changed such that an adequate safety index was provided for both one- and two-line connections. The new magnitudes for R_t are combined with Equations 5-2 and 5-3, which are re-presented below, to create model Proposed 3:

$$P = R_t A_{nt} F_u + 0.6 A_{gv} F_y \qquad [5\text{-}2]$$

$$P = R_t A_{nt} F_u + 0.6 A_{nv} F_u \qquad [5\text{-}3]$$

where:

$$R_t = \begin{cases} 0.9 & \text{for one-line connections} \\ 0.3 & \text{for two-line connections} \end{cases} \qquad [5\text{-}5]$$

Again, the lesser of Equations 5-2 and 5-3 is taken as the connection capacity. In this case, Equation 5-2 governs for 17 of the tests and 5-3 governs for the remaining tests. This model provides more conservative results than Proposed 2, with a mean professional factor of 1.20, and comparable variation in the results, with a coefficient of variation of 0.11. Figure 5-22 shows that all of the predictions using this model are conservative and that the scatter has been reduced compared to CSA–S16–01.

Although some improvements on the mean professional factor, which reflects the ability of the equation to predict block shear capacity correctly in an average sense, and the coefficient of variation, which reflects the associated variability, have been made using these equations, these parameters do not in themselves indicate the level of safety in the connection as designed. The level of safety is quantified by the safety index, which can be set to the desired level through the judicious selection of the resistance factor.

5.6 Resistance Factor Assessment

The level of safety a design model provides can be assessed by statistical methods. In general, an appropriate safety index, β, directly related to the probability of failure, is selected and the associated resistance factor, ϕ, determined therefrom. These parameters are affected by both the mean professional factor for the model as well as its variability. The resistance factor is calculated using the following equations:

$$\phi = \Phi_\beta \rho_R \exp(-\alpha_R \beta V_R) \qquad [5\text{-}6]$$

where:

$$\rho_R = \rho_M \rho_G \rho_P \qquad [5\text{-}7]$$

$$V_R = \sqrt{V_M^2 + V_G^2 + V_P^2} \qquad [5\text{-}8]$$

The variables in the equations above are defined as follows:

Φ_β is the modification factor,
α_R is the separation variable,
β is the safety index,
ρ_M is the ratio of mean measured to nominal material strength,
ρ_G is the ratio of mean measured to nominal connection geometric properties,
ρ_P is the mean professional factor,
V_M is the coefficient of variation of ρ_M,
V_G is the coefficient of variation of ρ_G, and
V_P is the coefficient of variation of ρ_P.

The bias coefficient for the resistance, ρ_R, represents the ratio of the mean to the nominal connection capacity, the latter being based on nominal material and geometric properties. V_R is the coefficient of variation of this ratio. The variability of relevant material properties is represented by the factor ρ_M, the mean ratio of

measured to nominal material properties. For block shear failure of coped beams, the relevant properties are the yield and ultimate tensile strengths of the beam web material. Geometric variabilities, related to both rolling and connection fabrication, are represented by the factor ρ_G, which is the mean value of the ratio of the measured relevant geometric properties to the nominal values. For block shear, the relevant geometric properties are the tensile and shear areas of the block, which are related to both the web thickness and the placement of the bolt holes. The coefficients of variation of the two ratios ρ_M and ρ_G are represented by V_M and V_G, respectively. The values of the material and geometric parameters selected for this analysis are summarized in Table 5-3 and discussed below. Ravindra and Galambos (1978) recommend that the separation variable, α_R, be taken as 0.55. The quantity Φ_β is a modification factor for ϕ, discussed below. The safety index, β, represents the probability of failure of the structural element.

Schmidt and Bartlett (2002) showed, based on 20 295 samples, that for typical rolled steel shapes, the material factor, ρ_M, for the flange dynamic yield plateau stress is 1.11, with a coefficient of variation, V_M, of 0.063. To adjust this factor to web static yield strength, two corrections are required. First, the authors suggest that the web yield strength bias coefficient be taken as 1.02 times the flange yield strength bias coefficient and that the coefficient of variation remain the same. Next, the authors suggest that the static yield stress be taken as 29.3 MPa lower than the dynamic yield plateau stress. Applying these two corrections to the values above results in a material factor of 1.05 and a coefficient of variation of 0.068. For the ultimate strength, the authors propose that a value of 1.13 for the material factor with a coefficient of variation of 0.044 be used for both flanges and webs. When corrected to static ultimate strength in the same manner as above, the values become 1.06 and 0.047, respectively. Due to the complexity of including material factors for both yield and ultimate strength in the assessment of resistance factors, a single material factor is used, herein. The factor for the web yield strength has a lower mean and a larger variability than the factor for ultimate strength, providing conservative resistance

factor results. Therefore, the material factor for web yield stress is used for both yield and ultimate strengths.

The geometric factor was calculated based both on data from this research program as well as work by Kennedy and Gad Aly (1980). For each connection configuration in this research program, net tension and gross shear lengths were calculated based on both nominal and as-measured properties. The mean geometric factor, ρ_G, for this aspect of the connection geometry was calculated to be 1.00 with a coefficient of variation, V_G, of 0.004. The second aspect of the geometry in these connections is the web thickness. Kennedy and Gad Aly indicate, based on 352 measurements, that the mean geometric factor for web thickness is 1.017, with a coefficient of variation of 0.0384. These statistics were combined to give an overall mean geometric factor of 1.017, with a coefficient of variation of 0.039 for these connections. More recently, Scmidt (2000) evaluated the web thickness bias coefficient, although the sample size was significantly smaller than the work by Kennedy and Gad Aly. Furthermore, the bias coefficients from the two sources are similar, indicating that changes in rolling practices have had little effect on the geometric factor. Therefore, the data from Kennedy and Gad Aly was used to assess the geometric factor.

Errors in measurement of connection properties, most notably the placement of the holes in the connection, were not included in this analysis. It was found that the inclusion of this parameter did not significantly affect the calculated resistance factors, although exclusion of the measurement errors results in slightly unconservative estimates of the resistance factor. The discretization factor, of consequence only in the selection of a suitable web thickness from standardized shapes, has also been excluded from this analysis, as it is expected to have a relatively small impact on the resistance factor and its omission leads to slightly conservative results. Neglecting the two factors will likely have little effect on the calculated resistance factor, since individually their effects are relatively small and they tend to offset one another.

The factors ρ_P and V_P represent the mean professional factor for the strength model and its coefficient of variation, respectively. These values, for the existing and proposed strength models, are listed in Tables 5-1 and 5-2 and are taken as the values for all existing test results. The safety index, β, represents the probability of failure of a given structural element considering both the variability of loads and resistances; a higher safety index indicates a lower probability of failure, and, hence, a higher level of safety. In the capacity design approach used in North American standards, it is desirable to have a higher safety index for connections than for structural members, such as beams. As such, members are usually assigned a safety index of about 3.0, while connections are assigned a value of approximately 4.5 (Ravindra and Galambos, 1978).

Due to the interdependence of the resistance factor and the load factor, it has been shown by Fisher *et al.* (1978) that the use of a safety index other than 3.0 in Equation 5-6 requires that a modification factor be applied to the resistance factor. This factor, denoted as Φ_β herein, takes values less than one for safety indices greater than 3.0 and greater than one for safety indices less than 3.0. Using the procedure outlined by Fisher *et al.*, values for Φ_β were calculated for safety indices ranging from 1.5 to 5.0 using mean live load to mean dead load ratios ranging from 0.5 to 2. It was found that Φ_β varied little between the two values of the live load to dead load ratio, and that using a ratio of 1.0 provided representative modification factors. The calculated values of Φ_β using a live load to dead load ratio of 1.0 are shown in Table 5-4 along with the load factors required in the calculation. The parameters γ_E, γ_D, and γ_L, are the load factors representing analysis uncertainties, dead load, and live load, respectively, as defined in Fisher *et al.* A second order polynomial regression analysis was applied to this data (with a correlation coefficient of 1.000) to approximate the relationship between the modification factor, Φ_β, and the safety index, β:

$$\Phi_\beta = 0.0062\beta^2 - 0.131\beta + 1.338 \qquad [5\text{-}9]$$

The modification factor calculated using Equation 5-9 is within 2.0% of the factor calculated using the procedure of Fisher *et al.* over the full range of live load to dead load ratios and safety indices examined. (It is to be noted that for a safety index of 3.0 for the resistance factor calculation, the modification factor is not a function of the live to dead load ratio and is equal to 1.0. However, as the safety index deviates from 3.0, the error resulting from the use of Equation 5-9 for live to dead load ratios other than 1.0 increases. For this reason, extrapolation beyond the range of safety indices considered here should be critically examined.)

For each design model presented in sections 5.4 and 5.5, the resistance factor required to provide a safety index of 4.5 is shown in Table 5-5. The safety index provided by each equation using the resistance factor prescribed in the respective standard is presented in Table 5-6. The resistance factor itself is also shown in Table 5-6 for convenience. (The resistance factor given in the table for CAN/CSA–S16.1–94 includes the coefficient 0.85.) For the three proposed models, the basic Canadian resistance factor of 0.90 is assumed. In both tables, the results for one-line and two-line tests are also presented separately. Due to the demonstrated differences in behaviour between these two types of connections, it is appropriate to consider the safety indices separately. The prescribed resistance factor for AIJ 1990 is not known and, therefore, this standard is not included in Table 5-6. It can be seen that, in general, a consistent level of safety is not being provided between one- and two-line connections. For the Canadian and American standards, an adequate level of safety is being provided for one-line connections, with safety indices of at least 4.2. However, for two-line connections, CSA–S16–01 provides a safety index of only 2.9 using the basic resistance factor of 0.90, and the current American standard, AISC LRFD 1999, provides a safety index of only 1.6, both of which would be considered by most to represent an unacceptable level of safety for connections. Eurocode 3 provides the most consistent results between one- and two-line connections with nearly equal safety indices. The level of safety for two-line connections is higher in this standard than for any of the others due, in part, to the reduction of the net tension length by one bolt hole diameter, thereby reducing the tension contribution to connection capacity.

Proposed 1 does not provide adequate safety for either one- or two-line connections using the basic resistance factor of 0.90. The safety indices are also inconsistent between the two connection types, indicating that this does not represent the actual failure mode. Likewise, Proposed 2 provides inconsistent levels of safety for one- and two-line connections, with a safety index of only 3.1 for two-line connections. To address this inconsistency, the values of R_t were modified until a consistent level of safety was provided, resulting in model Proposed 3, as discussed in section 5.5. Using the basic Canadian resistance factor of 0.90, Proposed 3 provides a safety index of 3.9 for both one-line and two-line connections. Although this is lower than the target value of 4.5, it may be a reasonable level of safety for connections. If an increased level of safety is desired, a reduction to the resistance factor could be provided within the block shear design equation, as was done in CAN/CSA–S16.1–94 where this factor was 0.85. In this case, an additional reduction factor of 0.90 would result in a safety index for all connections of 4.5.

A consistent level of safety is not being provided by current design standards, especially when considering two-line connections. In most cases, safety indices much lower than those required to ensure an acceptable probability of failure are being provided. It is, therefore, recommended that a new design model, Proposed 3 (Equations 5-2, 5-3, and 5-5), that addresses the apparent differences in behaviour between one- and two-line connections and results in a relatively small dispersion of the professional factor for both cases be used. Model Proposed 3 also consistently provides an adequate level of safety for coped beam connections and is therefore suitable for use in design standards.

5.7 Summary

The results of the laboratory tests indicate that, of the parameters investigated in this research program, only the magnitudes of the tension and shear areas have a significant effect on connection capacity. Although there was a concern that end rotation might adversely affect block shear behaviour, it was found that the lowest ultimate load was produced in the case where no end rotation was applied, with the most marked differences occurring for two-line connections. It is, therefore, not

necessary to include end rotation as a parameter in block shear capacity prediction. The numerical analyses were not capable of accurately predicting the full load vs. deformation behaviour of these connections. However, the analysis revealed a strong dependence of the connection stiffness on the initial bolt bearing condition. Fortunately, this did not appear to affect the connection ultimate load. Further development of the finite element model, focused on tear propagation, are likely to produce reasonable predictions of behaviour.

Using the laboratory data from this research program as well as that completed by others, existing design standards from North America, Europe, and Japan were examined. Professional factors were calculated for each data set for each standard and examined for accuracy and consistency. Three new design equations were presented in an attempt to represent better the block shear failure mode in coped beams, and resistance factors required to ensure an adequate level of safety were calculated for each strength model. Examination of these results shows that existing design standards provide varying levels of safety and that, in general, current standards do not provide an adequate level of safety for two-line connections. Current Canadian and American standards are found to be unconservative in the prediction of capacity for two-line connections by a considerable margin. To address this, three potential new design models have been presented. It is found that a consistent and sufficient level of safety can be provided by model Proposed 3, defined by Equations 5-2, 5-3, and 5-5. Using the basic Canadian resistance factor of 0.90, a safety index of 3.9 is provided for both one- and two-line connections, which is likely adequate. However, if an additional reduction factor of 0.90 were to be applied, the overall safety index would be increased to 4.5. Since the design model is consistent in its prediction of block shear capacity for both one- and two-line connections, with relatively low variability, it is believed that it is more representative of the actual failure mechanism than any of the models in the existing design standards.

Table 5-1: Professional Factors for Existing Design Standards

Source	Number of Tests	Professional Factor Mean (Professional Factor Coefficient of Variation)				
		CAN/CSA–S16.1–94	CSA–S16–01	AISC LRFD 1999	EC3 ENV 1993–1–1	AIJ 1990
Birkemoe and Gilmor	1	0.95 (—)	1.18 (—)	0.98 (—)	1.18 (—)	1.29 (—)
Yura *et al.*	3	1.07 (0.11)	1.22 (0.13)	1.07 (0.11)	1.25 (0.13)	1.64 (0.11)
Ricles and Yura	7	0.69 (0.09)	1.04 (0.09)	0.72 (0.11)	1.13 (0.06)	0.88 (0.07)
Aalberg and Larsen	8	1.16 (0.07)	1.37 (0.09)	1.16 (0.07)	1.21 (0.19)	1.38 (0.17)
Franchuk	17	1.11 (0.13)	1.24 (0.09)	1.11 (0.13)	1.21 (0.07)	1.47 (0.14)
All One-line Tests	26	1.14 (0.10)	1.28 (0.10)	1.14 (0.10)	1.20 (0.12)	1.49 (0.13)
All Two-line Tests	10	0.76 (0.18)	1.10 (0.12)	0.78 (0.17)	1.19 (0.10)	0.96 (0.16)
All Tests	36	1.03 (0.20)	1.23 (0.12)	1.04 (0.19)	1.20 (0.11)	1.34 (0.23)

Note: Professional factors greater than unity are conservative. All resistance factors are taken as 1.0.

Table 5-2: Professional Factors for Proposed Design Equations

Source	Number of Tests	Professional Factor Mean (Professional Factor Coefficient of Variation)		
		Proposed 1	Proposed 2	Proposed 3
Birkemoe and Gilmor	1	1.18 (—)	1.01 (—)	1.04 (—)
Yura *et al.*	3	1.22 (0.13)	1.16 (0.13)	1.17 (0.13)
Ricles and Yura	7	1.04 (0.09)	1.04 (0.09)	1.20 (0.11)
Aalberg and Larsen	8	1.21 (0.20)	1.17 (0.07)	1.20 (0.07)
Franchuk	17	1.17 (0.06)	1.17 (0.09)	1.22 (0.12)
All One-line Tests	26	1.18 (0.11)	1.15 (0.09)	1.18 (0.09)
All Two-line Tests	10	1.09 (0.12)	1.10 (0.12)	1.26 (0.13)
All Tests	36	1.16 (0.12)	1.14 (0.10)	1.20 (0.11)

Note: Professional factors greater than unity are conservative.

Table 5-3: Parameters for Resistance Factor Calculations

Parameter	Value
ρ_M	1.05
V_M	0.068
ρ_G	1.017
V_G	0.039
α_R	0.55
β	4.5

Table 5-4: Load Factors and Modification Factors

Safety Index, β	γ_E	γ_D	γ_L	Φ_β †
1.5	1.04	1.05	1.20	1.16
2.0	1.06	1.06	1.26	1.10
2.5	1.07	1.08	1.33	1.05
3.0	1.09	1.09	1.39	1.00
3.5	1.10	1.11	1.46	0.96
4.0	1.12	1.12	1.52	0.91
4.5	1.13	1.14	1.59	0.87
5.0	1.15	1.16	1.66	0.84

† Based on live load to dead load ratio of 1.0

Table 5-5: Resistance Factors Required for Safety Index of 4.5

Design Standard	One-Line Tests			Two-Line Tests			All Tests		
	ρ_R	V_R	ϕ	ρ_R	V_R	ϕ	ρ_R	V_R	ϕ
CAN/CSA–S16.1–94	1.21	0.15	0.72	0.81	0.27	0.36	1.10	0.21	0.57
CSA–S16–01	1.36	0.13	0.86	1.17	0.17	0.67	1.31	0.15	0.80
AISC LRFD 1999	1.22	0.15	0.73	0.83	0.26	0.38	1.11	0.21	0.58
EC3 ENV 1993–1–1	1.28	0.14	0.79	1.27	0.12	0.81	1.28	0.14	0.80
AIJ 1990	1.60	0.18	0.89	1.02	0.28	0.44	1.44	0.24	0.69
Proposed 1	1.26	0.14	0.79	1.16	0.14	0.72	1.24	0.15	0.75
Proposed 2	1.23	0.12	0.80	1.17	0.15	0.71	1.22	0.13	0.78
Proposed 3	1.26	0.12	0.82	1.35	0.15	0.81	1.28	0.13	0.81

Table 5-6: Safety Indices Provided by Design Equations

Design Standard	Resistance Factor	Safety Index Provided		
		One-Line Tests	Two-Line Tests	All Tests
CAN/CSA–S16.1–94	0.77	4.2	1.4	3.1
CSA–S16–01	0.90	4.2	2.9	3.8
AISC LRFD 1999	0.75	4.3	1.6	3.2
EC3 ENV 1993–1–1	0.91	3.6	3.8	3.7
Proposed 1	0.90	3.7	3.1	3.4
Proposed 2	0.90	3.7	3.1	3.6
Proposed 3	0.90	3.9	3.9	3.8

Note: Resistance factor for AIJ 1990 is not known and therefore this standard has been excluded

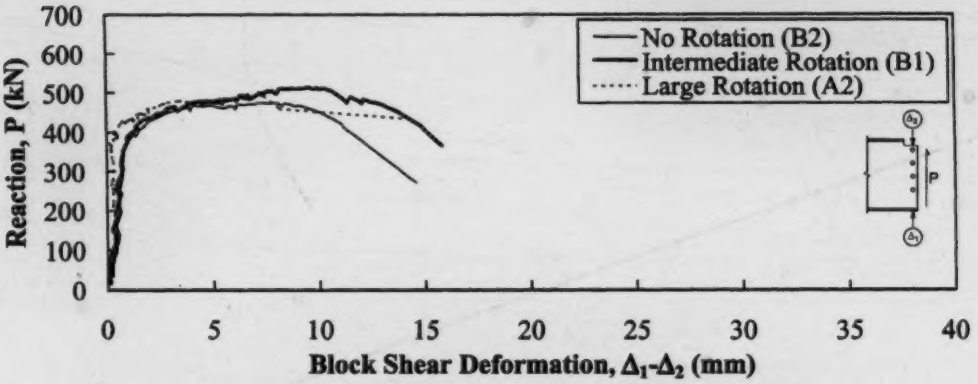

Figure 5-1: Load vs. Deformation Results, End Rotation Series 1

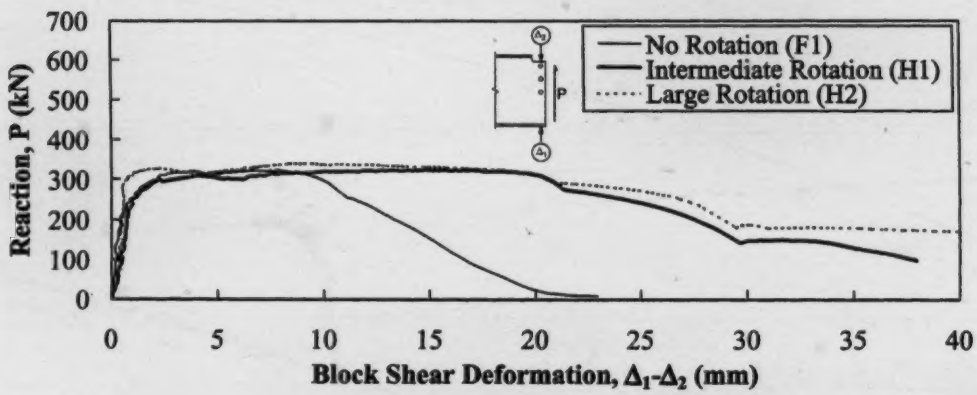

Figure 5-2: Load vs. Deformation Results, End Rotation Series 2

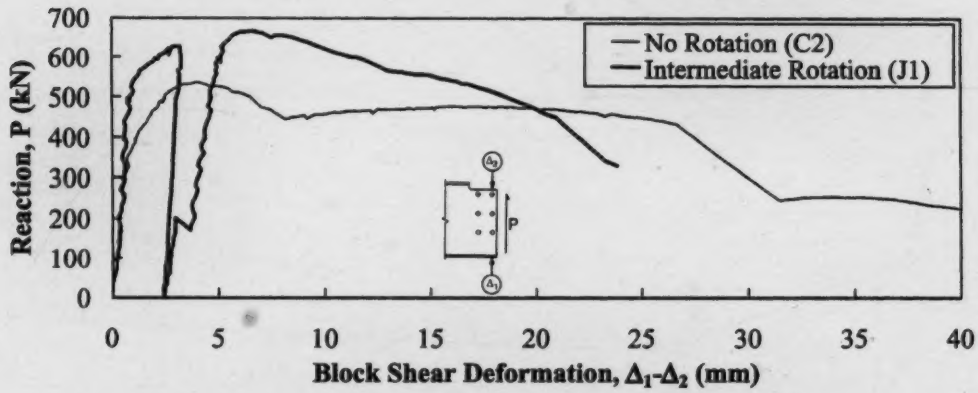

Figure 5-3: Load vs. Deformation Results, End Rotation Series 3

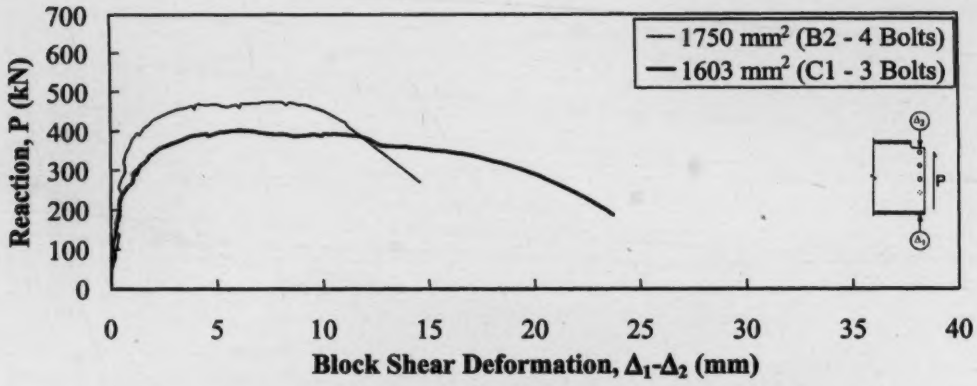

Figure 5-4: Load vs. Deformation Results, Gross Shear Area Series

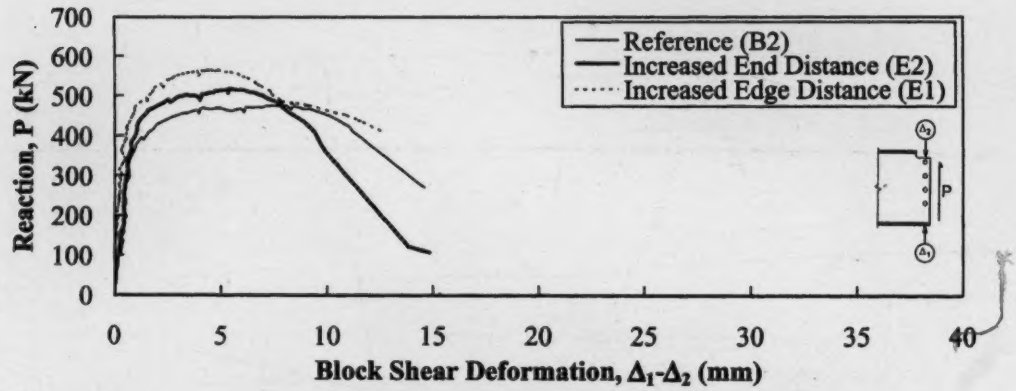

Figure 5-5: Load vs. Deformation Results, Edge / End Distance Series

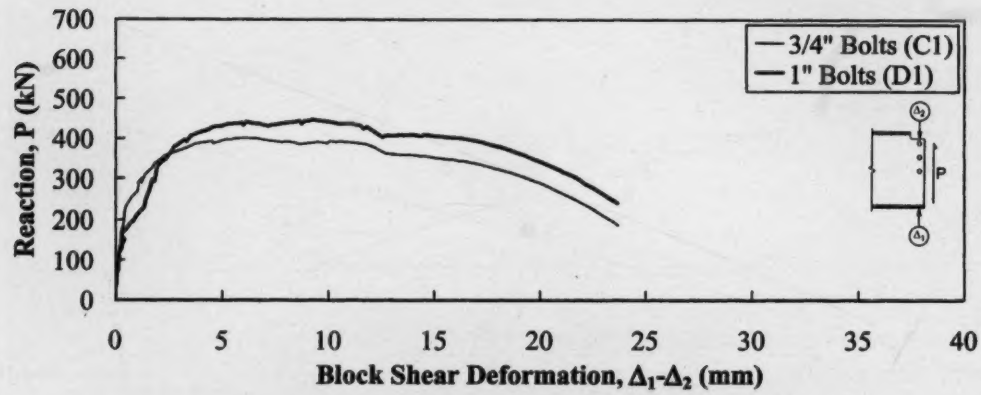

Figure 5-6: Load vs. Deformation Results, Bolt Diameter Series

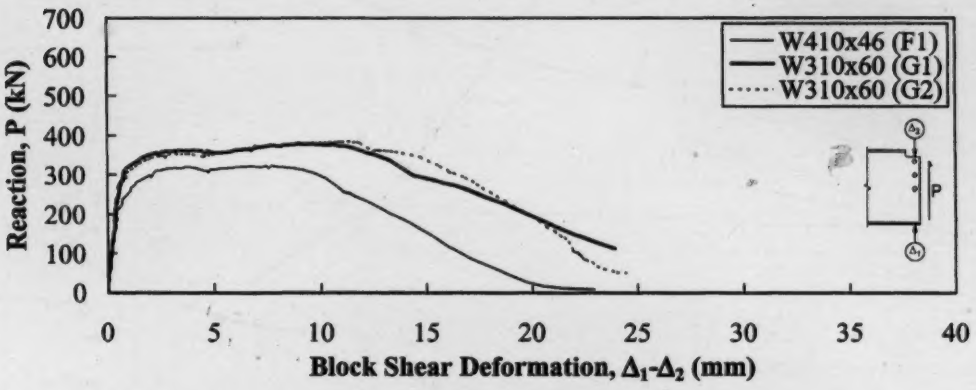

Figure 5-7: Load vs. Deformation Results, Section Depth Series

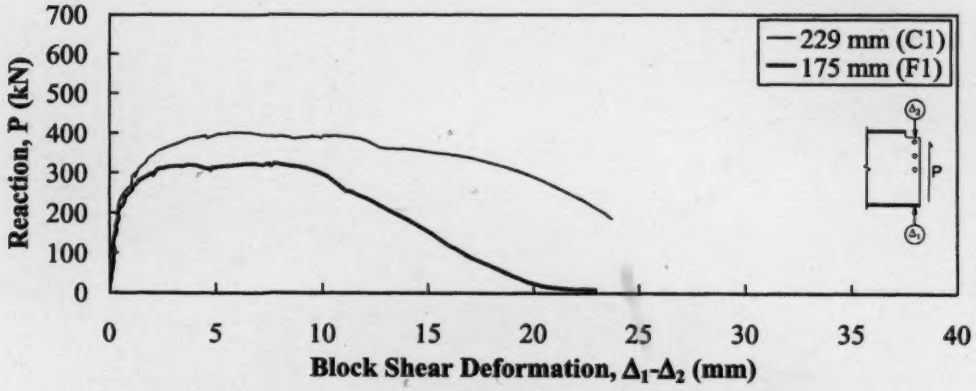

Figure 5-8: Load vs. Deformation Results, Connection Depth Series

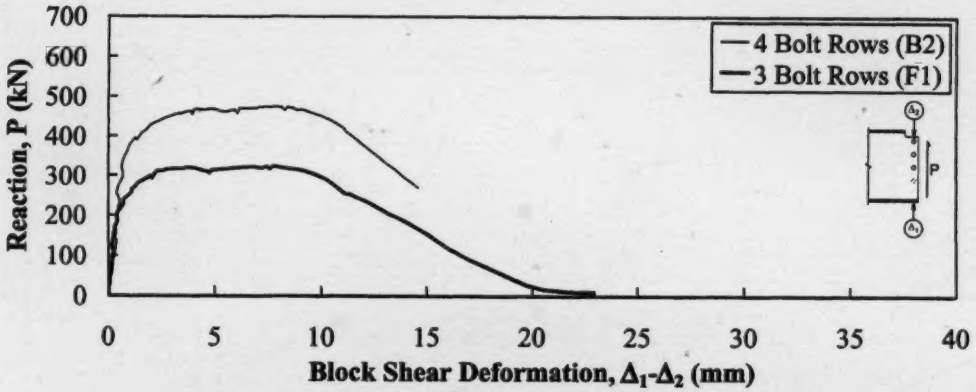

Figure 5-9: Load vs. Deformation Results, Number of Bolt Rows Series

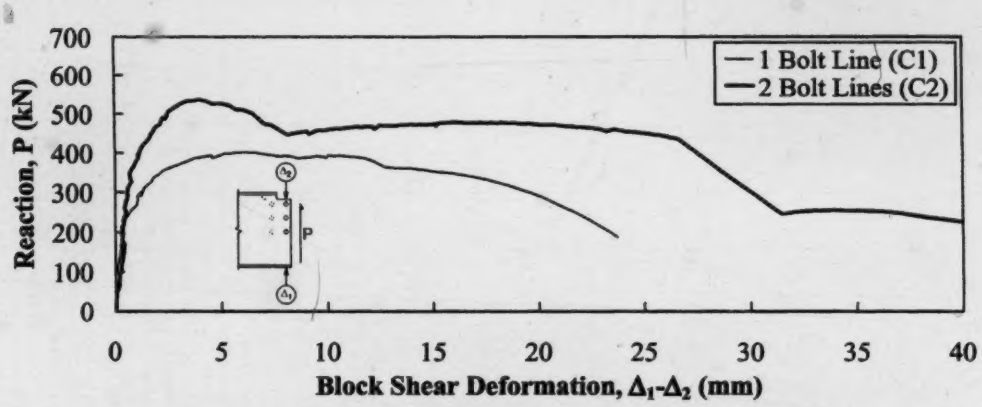

Figure 5-10: Load vs. Deformation Results, Number of Bolt Lines Series

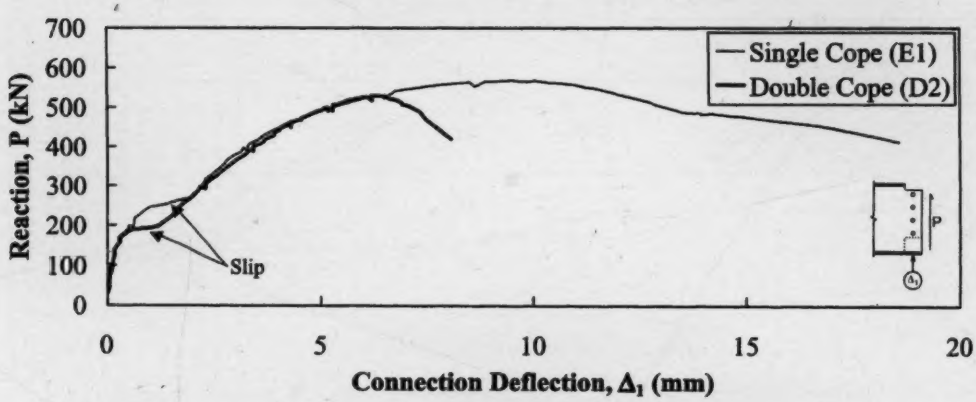

Figure 5-11: Load vs. Deformation Results, Double Cope Series

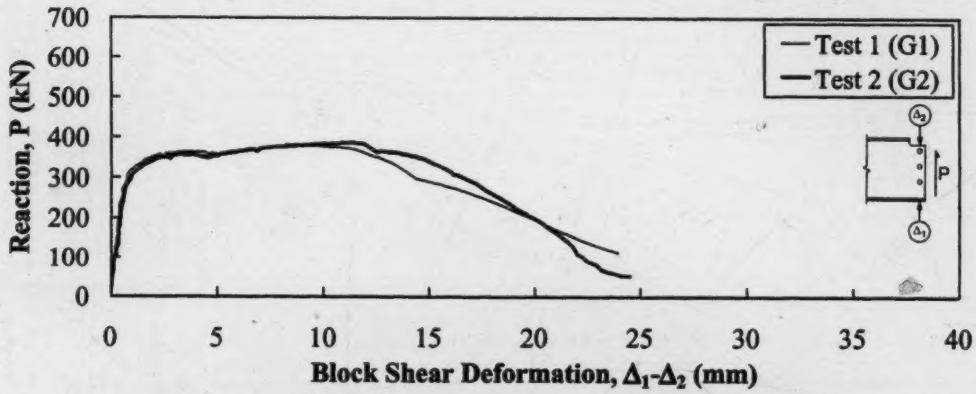

Figure 5-12: Load vs. Deformation Results, Repeatability Series

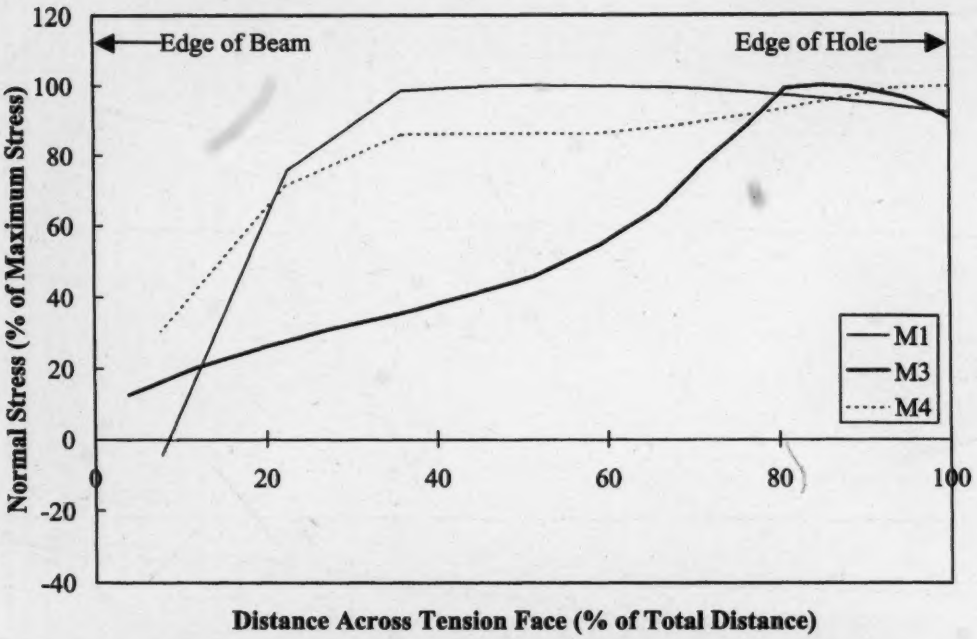

Figure 5-13: Tension Face Stress Distributions, One-line Connections

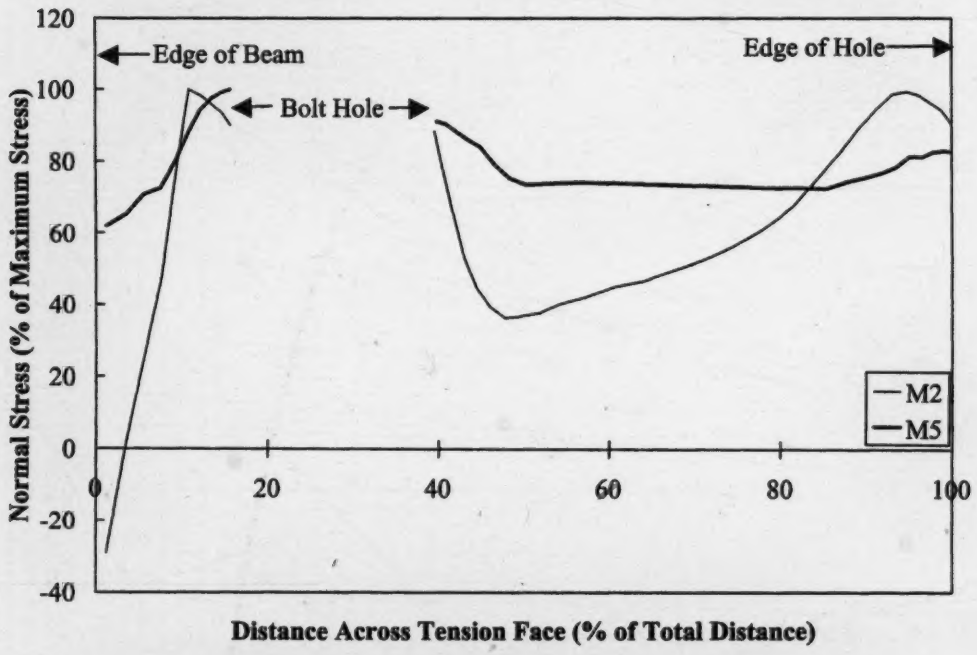

Figure 5-14: Tension Face Stress Distributions, Two-line Connections

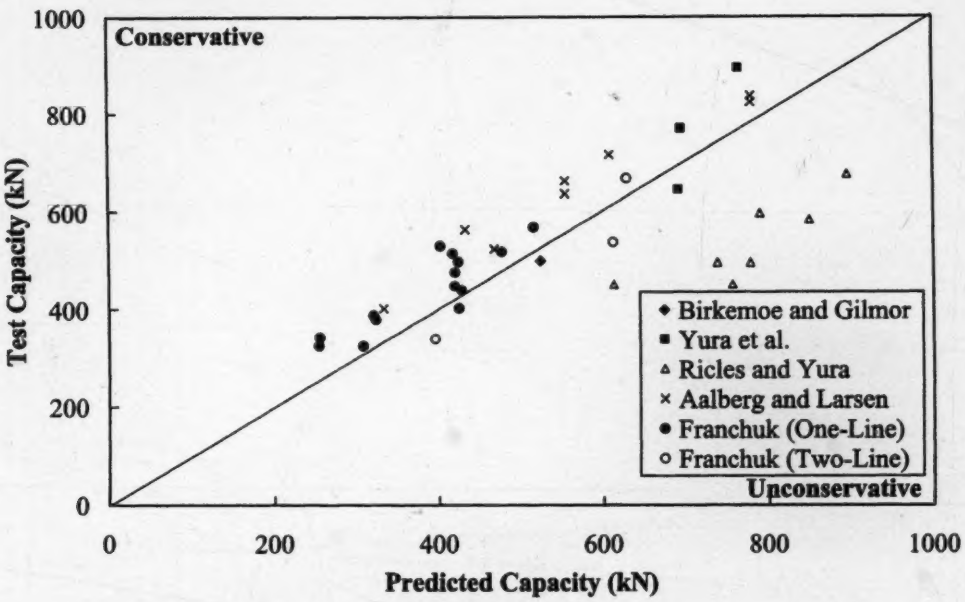

Figure 5-15: Test vs. Predicted Capacities, CAN/CSA–S16.1–94

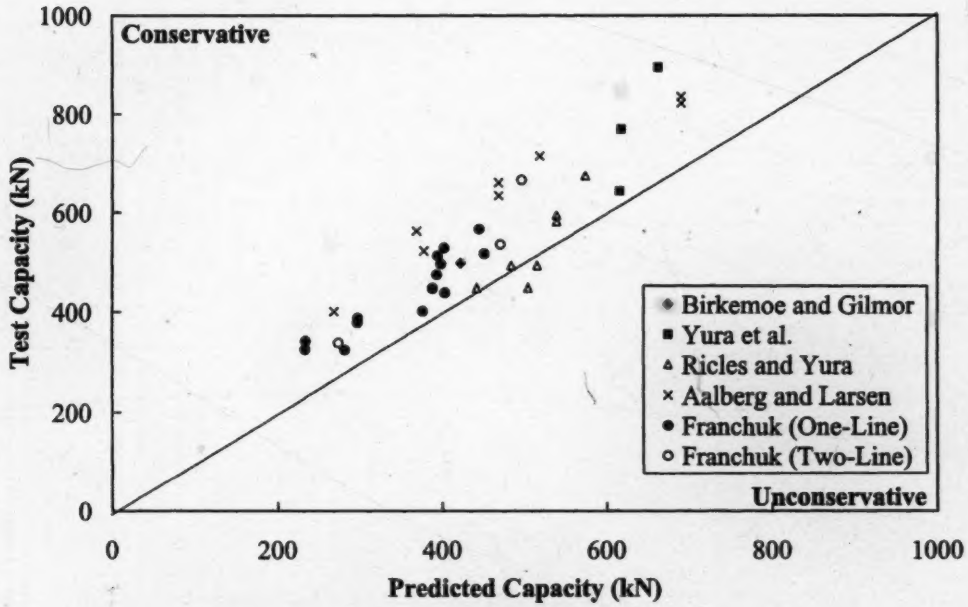

Figure 5-16: Test vs. Predicted Capacities, CSA–S16–01

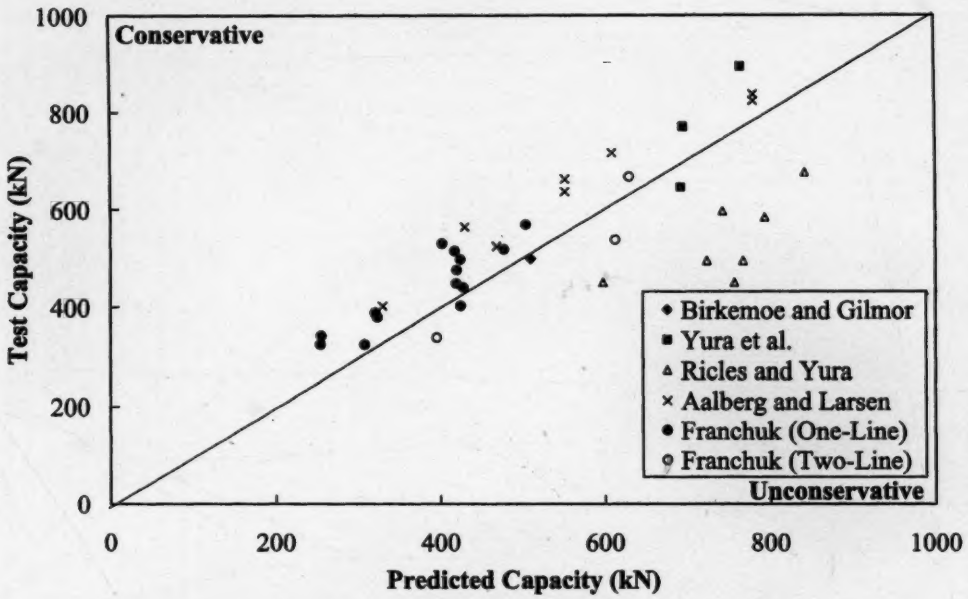

Figure 5-17: Test vs. Predicted Capacities, AISC LRFD 1999

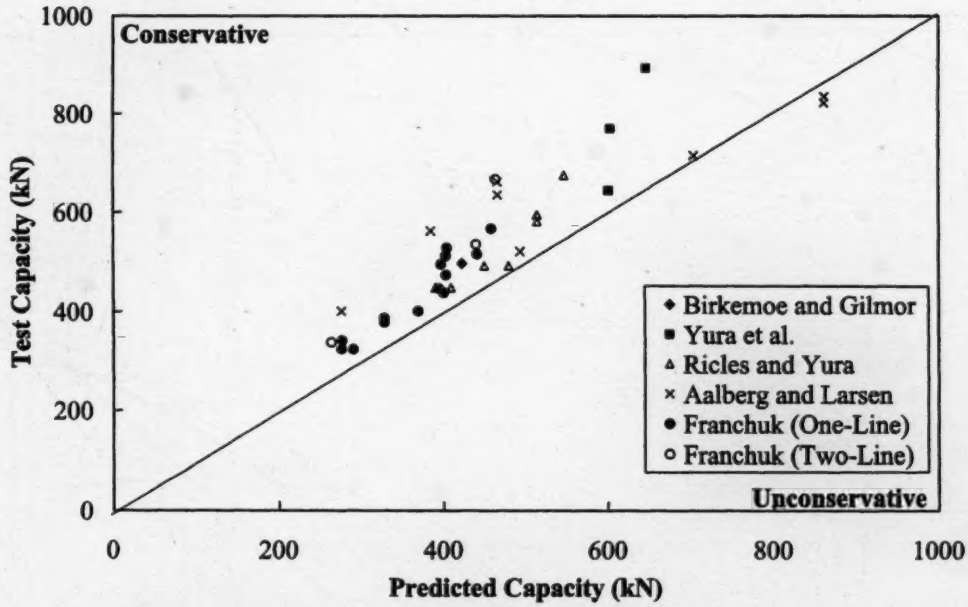

Figure 5-18: Test vs. Predicted Capacities, Eurocode 3 ENV 1993-1-1

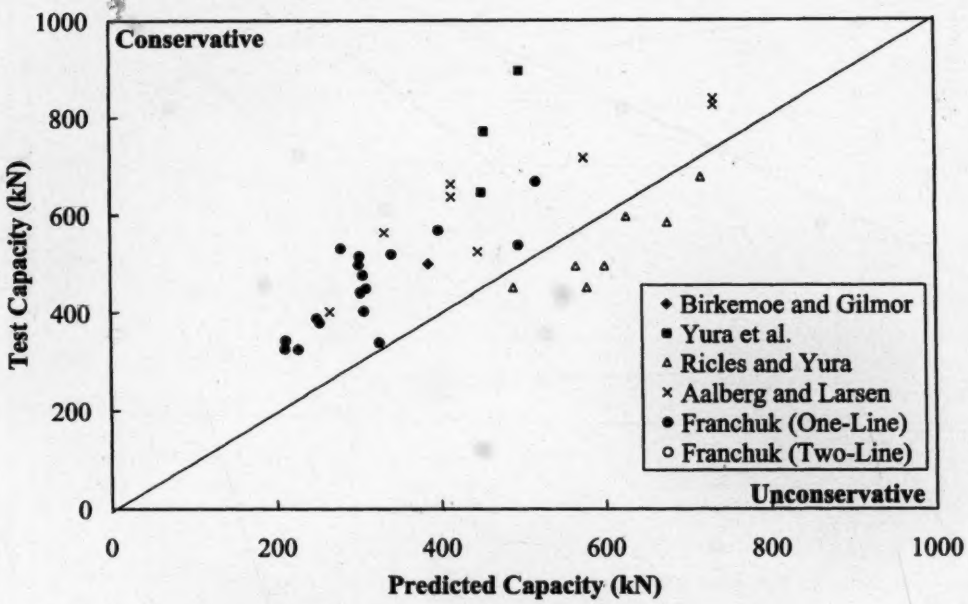

Figure 5-19: Test vs. Predicted Capacities, AIJ 1990

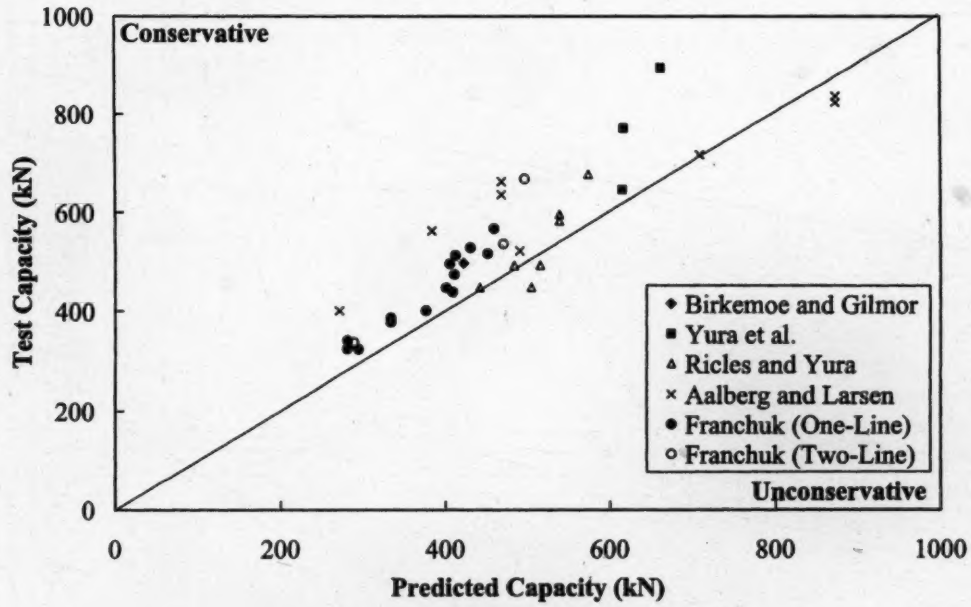

Figure 5-20: Test vs. Predicted Capacities, Proposed 1

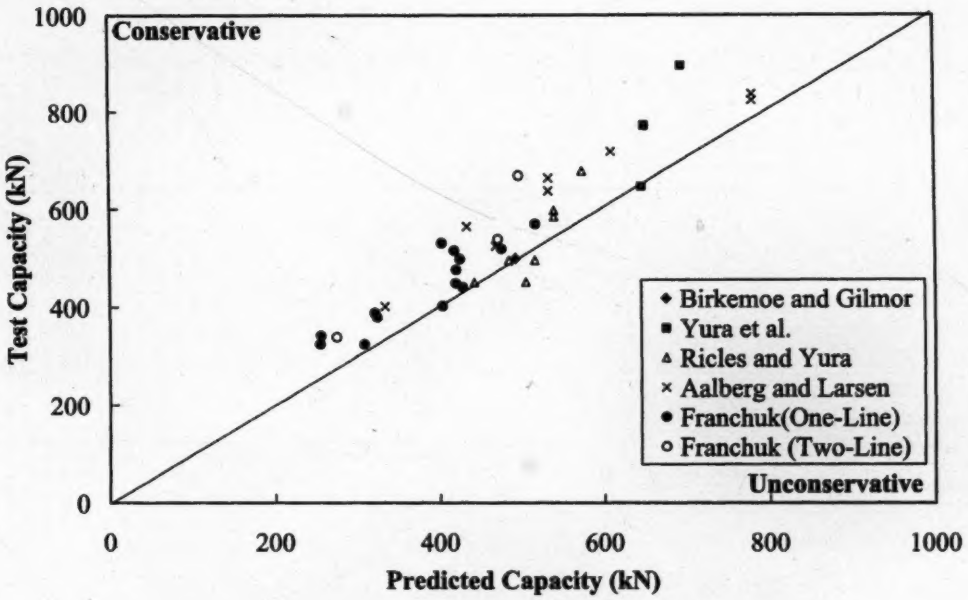

Figure 5-21: Test vs. Predicted Capacities, Proposed 2

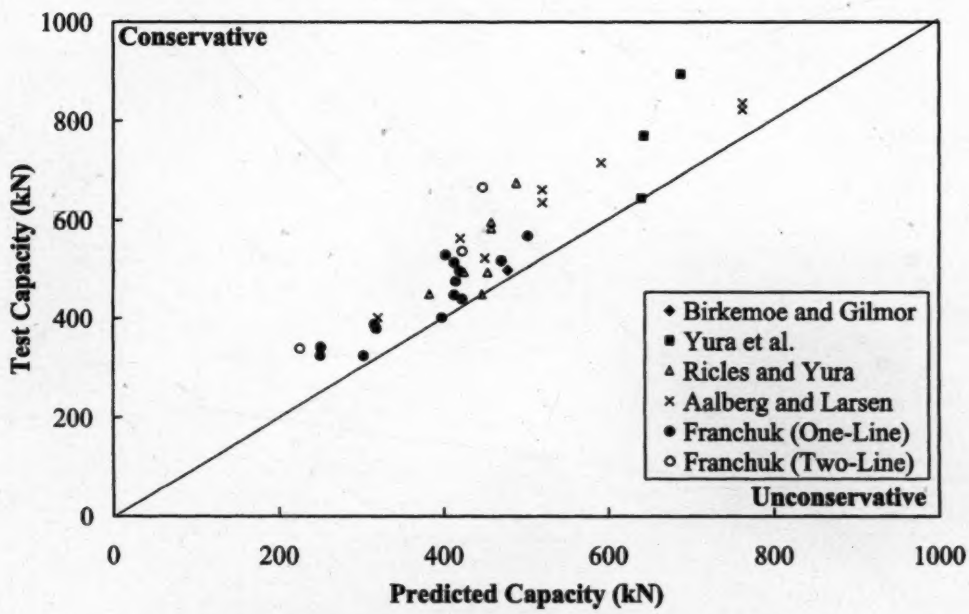

Figure 5-22: Test vs. Predicted Capacities, Proposed 3

6. Summary, Conclusions, and Recommendations

6.1 Summary

Equations currently in use to predict block shear capacity of coped beams have been shown to provide inconsistent and often unconservative results (Kulak and Grondin, 2000, 2001). Furthermore, few full-scale laboratory tests have been completed on the subject resulting in capacity equations largely based on block shear failure of bolted gusset plates, and only linear elastic finite element analyses have been carried out. To ensure that an appropriate level of safety is being provided by standards from North America, Europe, and Japan, a comprehensive research program consisting of full-scale tests and finite element analyses was carried out.

The research program commenced with full-scale testing of 17 coped beam connections. Test parameters examined included end and edge distances, bolt layout, double cope, and end rotation. The last parameter had not been investigated previously, with all tests being completed with the beam held horizontal during loading. To better reflect the loading condition in real connections, a rotation was applied to some specimens as load was increased. Analysis of the load vs. deformation results showed that none of the parameters investigated significantly affected connection capacity apart from the associated changes in tension and shear areas. Although perhaps counter-intuitive, the application of end rotation was found to increase capacity, particularly for two-line connections.

Non-linear finite element analyses were completed on five of the connections tested in the laboratory. The configurations were chosen to encompass a wide range of connection parameters including bolt layout, edge distance, and number of bolt lines. In general, it was found that the complete load vs. deformation response from the laboratory tests could not be predicted with the method used. Various bolt models and tear propagation models were used in attempts to refine the analysis and better predict the laboratory results, although the model is not yet developed to the point where the full response curve can be predicted reliably. The bolt bearing condition, *i.e.*, the location of the bolts in the holes at the beginning of the test, was varied in an investigation into connection stiffness. It was found that the stiffness is highly

dependent on the bearing condition. Fortunately, it was also shown that this did not significantly affect the connection ultimate load. Furthermore, the tearing propagation model used in this analysis is not truly representative of the actual process. Here, a blunt crack propagation model was used while a tear is, in fact, significantly smaller at the crack tip than that modelled by element removal. Although this method was found by Huns *et al.* (2002) to predict reasonably the load vs. deformation response of bolted gusset plates, it did not do so for coped beams.

A statistical analysis of current standards from North America, Europe, and Japan was completed through assessment of resistance factors and safety indices. In general, few of these standards consistently provide an adequate level of safety for all coped beam connections. Most provide a sufficient level of safety for one-line connections, but for two-line connections, a level of safety significantly lower than that desired is being provided. Only Eurocode 3 is found to provide a consistent level of safety between one- and two-line connections.

In an attempt to improve the disparity in predictions between one- and two-line connections, three new design models were presented. Again, a statistical analysis of resistance factors and safety indices was completed, and these results were compared to those for the existing standards. It was found that by reducing the contribution of the tension area to the connection capacity, a consistent level of safety could be provided for both one- and two-line connections. Model Proposed 3 was found to provide a safety index of at least 4.2 for both connection types using the basic Canadian resistance factor of 0.90. To increase the safety index for all connections to 4.5, the conventional target index for connections, a reduction to the resistance factor could be applied; in this case, a reduction of 0.95 would be sufficient.

6.2 Conclusions and Recommendations

The number of laboratory tests completed on block shear failure of coped beams has been substantially increased. Many connection parameters were investigated in this research program, but it was found that only the magnitudes of the tension and shear areas significantly affect the connection capacity. End rotation, a parameter that

had not been examined prior to this research, was found to increase the capacity of these connections. Due to the variabilities in end rotation that exist in real connections and the difficulty in assessing this parameter, it is recommended that end rotation not be considered in the prediction of capacity for coped beams. Therefore, only the tension and shear areas need be considered in a design equation to reasonably represent this failure mode.

The numerical analysis carried out in this research program was not capable of accurately predicting the full load vs. deformation behaviour of these connections. One limitation of the analysis used is the tear propagation model, and further development of this may result in accurate predictions. In this analysis, it was assumed that the tear propagates across the tension face instantaneously. However, as the incremental tearing analysis showed, this may not be the case; the tear likely progresses slowly, initiating at the bolt hole in the line furthest from the beam edge and propagating toward the end of the beam. A method that accurately defines the stress concentrations at a crack tip would likely lead to accurate predictions of load vs. deformation behaviour. The connection initial stiffness was found to be dependent on the initial bearing condition of the bolts, although this does not appear to affect connection capacity. Connection stiffness is seldom a parameter for design, so this effect may not need to be investigated further, although, if in future numerical work the full response curve is sought, this aspect must be considered. It should be noted that the bearing condition wherein all of the bolts in the connection are in bearing with the web prior to the application of load results in the upper bound of connection stiffness. With further development of the finite element analysis, focused on the propagation of tears, block stress distributions could be determined, from which the effects of the various connection parameters could be further evaluated.

An examination of current design standards shows that few consistently provide an adequate level of safety for coped beam connections. In particular, the capacity of two-line connections is poorly represented. As such, changes to these standards may be warranted, either in the form of a reduced resistance factor or a change in the design model. In any case, the probability of failure for these connections is currently

unacceptable. The new design model referred to as Proposed 3 is recommended for the prediction of capacity for coped beam connections. The model addresses the issue of over-prediction of capacity of two-line connections by reducing the contribution of the tension face to connection capacity. With this model, a consistent level of safety is provided for both one- and two-line connections. Using the basic Canadian resistance factor of 0.90, a sufficiently low probability of failure can be ensured, indicated by a safety index of 4.2. If a safety index of 4.5 is desired, an additional reduction factor of 0.95 must be applied to the current resistance factor. Based on its ability to consistently predict the capacity of a wide variety of connection configurations, this model appears to represent better the actual failure mode of block shear failure in coped beams than those currently in use.

Although this research has substantially increased the number of full-scale tests and numerical analyses completed on the subject of block shear in coped beams, the total number of tests is still small. More research on the subject would contribute further to the understanding of these connections. Many connection parameters remain to be systematically investigated in the laboratory, including block aspect ratio and the number of bolts in each bolt line. The numerical analysis also requires further development, and, once fully developed and validated using the laboratory test data, a parametric study can be completed to investigate connection parameters outside those examined in the laboratory. Block stress distributions, available from numerical analyses, could be used to quantify further the effects of these parameters. Although the understanding of block shear failure of coped beams has been furthered through this research program, more work is required to fully comprehend the complex failure mechanism.

References

Aalberg, A., and Larsen, P.K. (2000). "Strength and Ductility of Bolted Connections in Normal and High Strength Steels," *Proceedings of The Seventh International Symposium on Structural Failure and Plasticity*, Melbourne, Australia.

Avallone, E.A., and Baumeister, T. (1996). *Marks' Standard Handbook for Mechanical Engineers*, 10th Edition, McGraw-Hill, New York, NY, USA, pp. 3-23.

AISC (1999). *Load and Resistance Factor Design Specification for Structural Steel Buildings*, American Institute for Steel Construction, Chicago, IL, USA.

ASTM (1997). *A370-97 Standard Test Methods and Definitions for Mechanical Testing of Steel Products*, American Society for Testing and Materials, Philadelphia, PA, USA.

AIJ (1990). *Standard for Limit States Design of Steel Structures (Draft)*, Architectural Institute of Japan, Tokyo, Japan.

Birkemoe, P.C., and Gilmor, M.I. (1978). "Behavior of Bearing Critical Double-Angle Beam Connections," *Engineering Journal*, AISC, Vol. 15, No. 4, pp. 109-115.

CSA (1994). *CAN/CSA–S16.1–94 Limit States Design of Steel Structures*, Canadian Standards Association, Toronto, ON, Canada.

CSA (1998). *CAN/CSA–G40.21–98 Structural Quality Steel*, Canadian Standards Association, Toronto, ON, Canada.

CSA (2001). *CSA–S16–01 Limit States Design of Steel Structures*, Canadian Standards Association, Toronto, ON, Canada.

Cunningham, T.J., Orbison, J.G., and Ziemian, R.D. (1995). "Assessment of American Block Shear Load Capacity Predictions," *Journal of Constructional Steel Research*, Elsevier Science Ltd., Vol. 35, pp. 323-338.

Epstein, H.I., and Chamarajanagar, R. (1996). "Finite Element Studies for Correlation with Block Shear Tests," *Computers & Structures*, Elsevier Science Ltd., Vol. 61, No 5, pp. 967-974.

ECS (1992). *ENV 1993-1-1 Eurocode 3: Design of Steel Structures*, European Committee for Standardization, Brussels, Belgium.

Fisher, J.W., Galambos, T.V., Kulak, G.L., and Ravindra, M.K. (1978). "Load and Resistance Factor Design Criteria for Connectors," *Journal of the Structural Division*, ASCE, Vol. 104, No. ST9, pp. 1427-1441.

Hardash, S.G., and Bjorhovde, R. (1985). "New Design Criteria for Gusset Plates in Tension," *Engineering Journal*, AISC, Vol. 22, No. 2, pp. 77-94.

HKS (1998). *ABAQUS/Standard,* Version 5.8, Hibbitt, Karlsson & Sorenson, Inc., Pawtucket, RI, USA.

Huns, B.B.S. (2002). *Block Shear Failure of Gusset Plates*, Master of Science Thesis, Department of Civil and Environmental Engineering, University of Alberta, Edmonton, AB, Canada.

Huns, B.B.S., Grondin, G.Y., and Driver, R.G. (2002). "Block Shear Failure of Bolted Gusset Plates," *Proceedings of the 4th Structural Specialty Conference of the Canadian Society for Civil Engineering*, Montréal, QC, Canada.

Kennedy, D.J.L., and Gad Aly, M. (1980). "Limit States Design of Steel Structures—Performance Factors," *Canadian Journal of Civil Engineering*, NRCC, Vol. 7, No. 1, pp. 45-77.

Khoo, H.A., Cheng, J.J.R., and Hrudey, T.M. (2000). *Ductile Fracture of Steel*, Structural Engineering Report No. 232, Department of Civil and Environmental Engineering, University of Alberta, Edmonton, AB, Canada.

Kulak, G.L., and Grondin, G.Y. (2000). "Block Shear Failure in Steel Members – A Review of Design Practice," *Proceedings of Connections in Steel Structures IV: Steel Connections in the New Millennium*, Roanoke, Virginia, USA.

Kulak, G.L., and Grondin, G.Y. (2001). "Block Shear Failure in Steel Members – A Review of Design Practice," *Engineering Journal*, AISC, Vol. 38, No. 4, pp. 199-203.

Ravindra, M.K., and Galambos, T.V. (1978). "Load and Resistance Factor Design for Steel," *Journal of the Structural Division*, ASCE, Vol. 104, No. ST9, pp. 1337-1353.

Ricles, J.M., and Yura, J.A. (1983). "Strength of Double-Row Bolted-Web Connections," *Journal of Structural Engineering*, ASCE, Vol. 109, No. 1, pp. 126-142.

Softek Services Ltd. (2000). *S-FRAME for Windows (Professional Edition)*, Version 5.1, Softek, Richmond, BC, Canada.

Schmidt, B.J. (2000). *Review of Resistance Factor for Steel*, Master of Science Thesis, Department of Civil and Environmental Engineering, University of Western Ontario, London, ON, Canada.

Schmidt, B.J., and Bartlett, F.M. (2002). "Review of resistance factor for steel: data collection," *Canadian Journal of Civil Engineering*, NRCC, Vol. 29, No. 1, pp. 98-108.

Yura, J.A., Birkemoe, P.C., and Ricles, J.M. (1982). "Beam Web Shear Connections: An Experimental Study," *Journal of the Structural Division*, ASCE, Vol. 108, No. ST2, pp. 311-325.

Appendix A: Single-Angle Connections with Slotted Holes

A. Single-Angle Connections with Slotted Holes

A.1 Introduction

The current Canadian steel standard, CSA–S16–01 (CSA, 2001), requires that for connections with long slotted holes—*i.e.*, having slot lengths up to 2.5 times the bolt diameter—in the outer plies of the joint, a plate washer must be installed to prevent pull-out of the bolts. A plate washer is a washer built from plate 8 mm or greater in thickness that is large enough to cover completely the slot after installation and can be provided individually or in a continuous bar. Pull-out occurs in a connection without plate washers when the slotted holes deform sufficiently to allow the bolt head or nut to pull through the hole. In order to economize fabrication and installation costs, it is desirable not to use plate washers. No testing has been completed to show that pull-out of the bolts does, in fact, occur in these connections. As such, five tests on single-angle connections with slotted holes and without plate washers were conducted. The eccentricity inherent in single-angle connections makes them susceptible to failure by pull-out of the bolts. A description of the test specimens, set-up, instrumentation, and results is presented below. Conclusions and recommendations for future work are also presented.

A.2 Description of Test Specimens

Five single-angle connections with slotted holes and without plate washers were fabricated using L102x102x6.4 angles. The connection parameters investigated were bolt location in the slot, length of the slot, number of bolt rows, and bolt diameter. Nominal connection configurations are shown in Figure A-1 and as-built dimensions are listed in Table A-1. Test I was the baseline test and represented a typical connection in which the depth is a significant portion of the beam section depth. Minimum end and edge distances and standard 19.1 mm (3/4") bolts were used. Slot dimensions of 21 mm x 32 mm were used since this is the standard slot size used by the fabricator who supplied the specimens, and the bolts were installed in the middle of the slots. Test II was completed on an identical connection angle to Test I, but the bolts were installed at the end of the slot away from the support column. This increased the flexibility of the connection due to the larger eccentricity of the

connection centre of resistance from the support column. The effect of slot length was investigated through Test III, which had all connection dimensions equal to those of Test I and used 19.1 mm bolts but had 45 mm long slots. This represents a slot length of 2.4 d_b, which is near the upper limit permitted by CSA–S16–01 (CSA, 2001). Test IV was a three-bolt connection using 19.1 mm bolts and had a larger bolt spacing (102 mm) with 21 mm x 32 mm slots. Again, the connection depth is a significant portion of the beam section depth but, in this case, only three bolts were used resulting in higher bearing stresses at the bolts. Larger diameter bolts (25.4 mm) were used in Test V with the same bolt spacing as Test IV. The fabricator's standard slots for 25.4 mm bolts, with dimensions of 27 mm x 42 mm, were used. Minimum end and edge distances were used for this connection, as well. All slots tested are long slots, as defined by CSA–S16–01 and AISC LRFD 1999, and A325 bolts were used for all connections.

The angles were connected to the reaction column through two 25.4 mm (1") A325 high strength bolts. A 12.7 mm (1/2") thick cover plate was attached to the angles on the column-side leg to reduce the angle deformation. The connections were designed such that shear failure of the outstanding (connection-side) leg of the angle was the governing failure mode, as per CSA–S16–01.

The angles were produced from CAN/CSA–G40.21–98 350W steel (CSA, 1998), although material property tests (*e.g.*, tension coupon tests) were not completed and mill reports were not available. Although the nominal tensile strength for this steel grade is 450 MPa, a value of 500 MPa is assumed herein, which has been shown to be typical for 350W steel.

The beams for all tests were W410x46, and the same beam was used for Tests I, II, and III. Its connection configuration was identical to that of Connection A1 from the block shear tests, shown in Figure 3-1, except for increased end and edge distances of 50 mm and 40 mm, respectively. These were used, rather than minimum distances, so that the beam would have only minor damage at the end of each test and could be re-used. For Tests IV and V, beam connections identical to those of

Connections C1 and D1, respectively, were used. All holes on the beams were standard sized, round holes and were punched. The beam web thickness was greater than the angle thickness to ensure that failure would occur in the angles.

A.3 Description of Test Set-up

The basic test set-up for this research program was nearly identical to that used in the block shear tests, which is described in section 3.4. Figures 3-2 through 3-5 show the basic test set-up, although in the slotted angle test series, some modifications were made. At the load point, the knife edge was replaced by a small-diameter spherical bearing to accommodate any beam twisting that might occur. This bearing assembly allows rotation in all directions. Additional lateral support was provided for all tests to both sides of the top flange of the beam at the cope using an assembly similar to that used at the load point. This was added to approximate the restraining effect of a metal or concrete deck attached to the beam top flange. Another support was added to the bottom flange at the end of the beam away from the tested connection to restrain beam twisting. Rollers identical to those used on the top flange at this location were used at the bottom flange on both sides of the beam. This represented the effect of beam-to-beam bracing typically found in structures.

A.4 Instrumentation

All instrumentation used in the block shear tests, as described in section 3.5 and shown in Figure 3-6, was also used in these tests. This includes measurements of load in both the loading and reaction jacks, vertical displacements at four locations (bottom flange and top of web at the connection, the load point, and the reaction point), rotation of the connection, and strain distribution at mid-span. Additional instrumentation was added to investigate other connection parameters in the slotted hole tests. A graphical representation of this instrumentation is shown in Figure A-2. Vertical displacement of the top and bottom of the connection angle were measured to assess angle deformations. Lateral displacements in the connection were measured at four locations—two each on the angle and the beam—by cable transducers attached to the connection in line with the row of bolts, directly above the topmost bolt and directly below the bottom bolt. These displacements were also used to assess the

twist of the connection about the axis of the beam. The connection twist was calculated using the difference in the displacements at the top and the bottom of the connection and the linear distance between the two measurements. This quantity assumes that the angle and the beam rotate as rigid bodies and that no localized deformations occur. Although this is not a true representation of the connection twist, it provides a reasonable estimate up to near the ultimate load.

A.5 Specimen Installation and Test Procedure

The test angles with cover plates were first attached to the reaction column and the bolts were tightened by the turn-of-nut method, as described in CSA–S16–01 (CSA, 2001). The test beam was then moved into the test apparatus, levelled, and attached to the connection angle. New 19.1 mm (3/4") or 25.4 mm (1") bolts were installed and tightened to the snug-tight condition. The bolts were installed with the head on the beam side of the connection and the nut on the angle side with a single standard hardened washer placed between the angle and the nut. The threads were not in the shear plane. The loading assembly (roller and spherical bearing) was then placed in the apparatus and the four lateral supports were installed.

The loading procedure is described in section 3.6. As the load was applied to the connection, data readings were taken at regular intervals. Electronic readings of load, displacement, rotation, and strain were taken at 10 kN load increments or 0.25 mm displacement increments. Connection deflection was increased until either the angle had completely fractured or the connection load had decreased significantly. No end rotation was imposed on these connections by lowering of the reaction jack.

A.6 Test Results

Two failure modes were observed in the five connection tests. Tests I, II, and III all failed by shear failure of the connection angles, as depicted in Figure A-3. For each test, a load vs. deflection curve is presented to show the response of the connection. These are shown in Figures A-5 through A-7. The vertical axis of these graphs is the connection vertical reaction and the horizontal axis is the deflection of the bottom flange of the beam directly in line with the line of bolts. Table A-2 lists

the connection ultimate load and the displacement and twist of the connection at ultimate for each test. In Test II, the connection was unloaded and re-loaded at a connection deflection of approximately 20 mm. For Test I and for the first part of Test II, a knife edge was used in the loading assembly to prevent unwanted rotational restraint at that location. However, it was noted during Test II that the beam had slightly twisted about its axis causing a stability problem in the loading assembly. To mitigate this problem, the connection was unloaded and the knife edge was replaced by a small-diameter spherical bearing, which allows rotation in all directions. The test was continued with this bearing and the connection was loaded to failure. The remaining tests were completed using the spherical bearing.

The connection failure mechanism was similar in these three tests. Failure initiated with small tears propagating downwards from the bottom bolt hole to the end of the angle, first observed at a connection load of 85% to 90% of the connection ultimate load. Small tears then formed at the second bolt from the bottom of the connection followed by total shear failure of the angle. Little deformation of the beam occurred during these tests.

For Tests IV and V, shear failure did not take place. Rather, a combined angle and beam failure occurred involving tilting of the bolts about the axis of the beam. Photographs of the failed specimens are shown in Figure A-4 and the load vs. displacement curves are shown in Figures A-8 and A-9. For the two cases, the series of events was nearly identical. The failure initiated with fracture of the angle beneath the bottom bolt in a bearing-type failure mode at connection loads of approximately 95% to 100% of the connection ultimate load. Cracks propagated from the bottom bolt hole to the end of the angle on both sides of the bolt (see Figures A-4(a) and (b)). Following this, the top bolt of the connection began to tilt, slightly, about the axis of the beam. The angle then bent out of plane between the bolts, as seen in Figures A-4(c) and (d). Subsequently, the beam failed at the top bolt hole with a crack propagating from that hole to the beam edge (Figures A-4(e) and (f)), and this is indicated in the load vs. deformation plots as a drop in load at approximately 22 mm and 18 mm for Tests IV and V, respectively. Further increases in connection

deflection caused tilting of the middle bolt about the axis of the beam. Although the angles were not completely fractured, the tests were terminated when the connection deflections became large.

None of the five connections failed due to pulling-out of the bolts. Although Tests IV and V exhibited failure mechanisms that have some of the characteristics of pull-out, the failure mechanism was initiated by bearing failure of the bottom bolt and the remaining bolts did not pull through the slotted holes.

The connection twisting response for each test is shown in Figures A-10 through A-14, wherein the sign of the twist is defined in the key diagram. The curves show the twist of the angle and of the beam for the duration of the test. The twist is calculated from the two lateral deflection measurements taken at the top and bottom of the connection and the vertical distance between them. This assumes a rigid body rotation of the connection and does not account for localized deformations that may affect the displacement measurements. This is a reasonable approximation of the connection behaviour until significant localized deformations occurred, usually close to the ultimate connection load. The ultimate deflection of the connection is, therefore, marked on each curve to indicate, approximately, when localized deformations may have affected the results significantly. It can be seen from the figures that the measured connection rotations were small prior to reaching the ultimate connection load, seldom exceeding 1°. It is believed that for a pull-out failure to occur, the connection rotations need to be larger than those exhibited in these tests.

The connection ultimate loads were significantly lower than expected. Table A-3 lists the connection ultimate reaction measured in the laboratory as well as the predicted shear and bearing failure loads as calculated according to CSA–S16–01 (CSA, 2001) and AISC LRFD 1999 (AISC, 1999). The resistance factors in these calculations have been taken as 1.0. For the Canadian standard, the shear failure criterion governs in all cases, but the predicted capacity is up to 55% higher than the test ultimate capacity. The American standard uses the same shear failure criterion as

CSA–S16–01 but uses a different bearing criterion. In the Canadian standard, no provision is made for the effect of end distance of the connection on the bearing capacity, while this is included in the American standard. As well, the American standard reduces the bearing capacity of connections with long slots compared to connections with round holes or short slots. Bearing capacity governs for Test IV when using the American standard but the capacity is still over-predicted, in this case by 21%. It should be noted that these capacities are based on an assumed tensile strength, F_u, of 500 MPa. Although this is a typical value of tensile strength for 350W steel, any increase in material strength would result in even higher predicted capacities. It is concluded, therefore, that single-angle connections with slotted holes and without plate washers may have a reduced capacity when compared to connections with round holes, although pull-out of the bolts appears unlikely to represent the failure mode. Further testing is required to confirm this observation.

A.7 Conclusions and Recommendations

Tests of five single-angle connections with slotted holes and without plate washers were completed. The connections were loaded to failure and load vs. deflection data were gathered. Two failure modes were observed. Three connections failed in pure shear, as predicted by the Canadian standard, and two failed in a combination of bolt bearing and tilting. Pull-out of the bolts was not observed. Regardless of the failure mode, the connection ultimate load was lower than predicted by both the Canadian and American standards. Predicted capacities based on as-built connection geometries and an assumed material strength were approximately 10% to 55% lower than the predicted value. It was therefore concluded that the use of connections with slotted holes and without plate washers may result in a reduction in capacity, but more testing is required to quantify the variables involved. Many parameters that have not been examined here need to be investigated, including the effects of end and edge distances, lateral restraint, and slot dimensions.

The research program described above considered only a small number of connection parameters and consisted of few tests. Therefore, recommendations for changes to the practice of using plate washers for connections with slotted holes

cannot be made with confidence. Although pull-out of the bolts did not occur, a reduction in capacity from that predicted by North American standards was noted.

Table A-1: As-Built Connection Dimensions

Connection Designation	e_{s1} *(mm)*	s_1 *(mm)*	s_2 *(mm)*	s_3 *(mm)*	e_{s2} *(mm)*
I	24.9	75.2	75.1	75.1	25.2
II	25.0	74.4	75.7	74.8	25.4
III	24.3	75.0	74.4	74.7	25.3
IV	24.8	102.3	101.8	—	22.7
V	31.7	103.3	102.2	—	33.0

Connection Designation	e_g† *(mm)*	d_{slot}† *(mm)*	l_{slot}† *(mm)*	t *(mm)*	*Bolt Location in Slot*
I	26.0	20.3	31.4	6.395	middle
II	26.3	20.3	31.4	6.444	end ††
III	24.4	21.7	44.4	6.488	middle
IV	27.4	20.3	31.4	6.477	middle
V	33.8	26.8	42.1	6.342	middle

† Mean values for all bolt holes in connection.
†† Bolt installed at end of slot away from outstanding leg of angle.

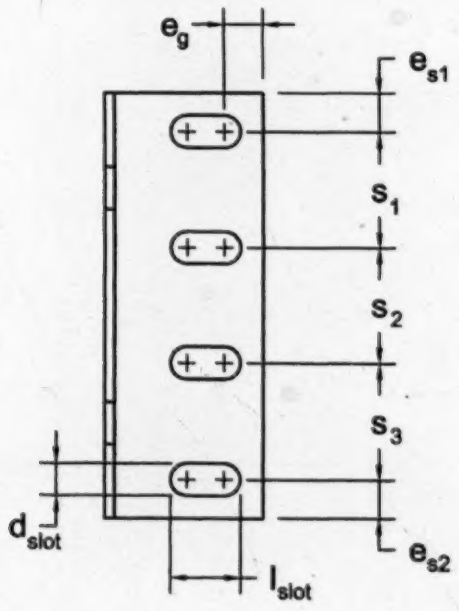

Table A-2: Test Results Summary

Connection Designation	*Ultimate Connection Vertical Reaction (kN)*	*Displacement of Bottom of Connection at Ultimate (mm)*	*Twist of Beam at Ultimate† (°)*	*Twist of Angle at Ultimate† (°)*
I	338.3	32.5	0.46	0.84
II	319.2	28.2	-0.76	0.60
III	316.6	23.5	0.26	0.41
IV	239.6	10.2	-0.54	-0.06
V	268.6	10.1	0.04	-0.09

† Positive values indicate twist in same direction as eccentricity

Table A-3: Predicted Capacity Summary

Connection Designation	*Ultimate Connection Vertical Reaction (kN)*	*CAN/CSA–S16–01*		*AISC LRFD 1999*	
		Shear Capacity (kN)	*Bearing Capacity (kN)*	*Shear Capacity (kN)*	*Bearing Capacity (kN)*
I	338.3	373	733	373	414
II	319.2	375	738	375	419
III	316.6	364	744	364	419
IV	239.6	371	557	371	289
V	268.6	362	725	362	384

Note: Capacities based on measured geometry and assumed tensile strength (F_u) of 500 MPa. All resistance factors taken as 1.0.

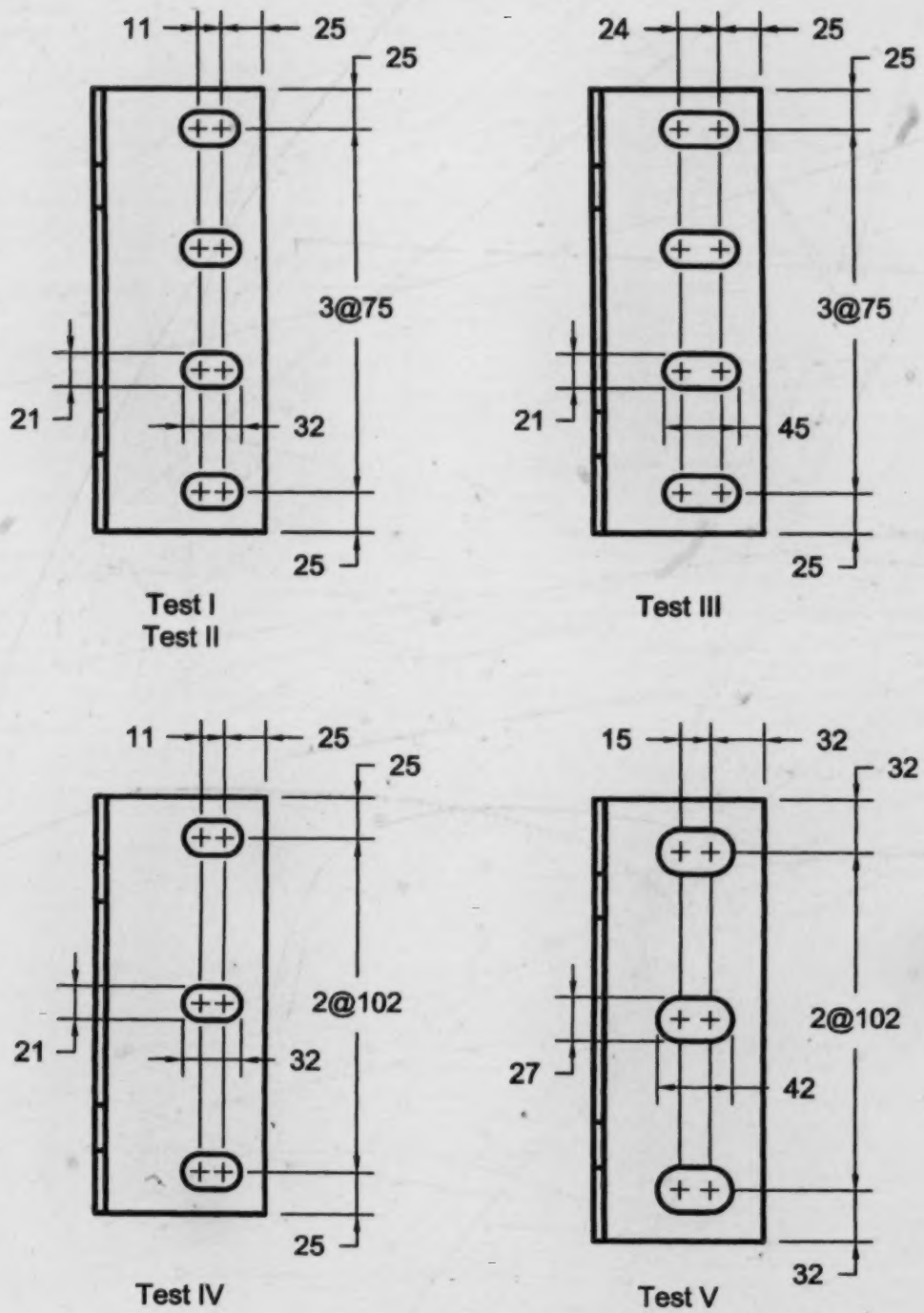

Note: All angles L102x102x6.4

Figure A-1: Nominal Connection Properties

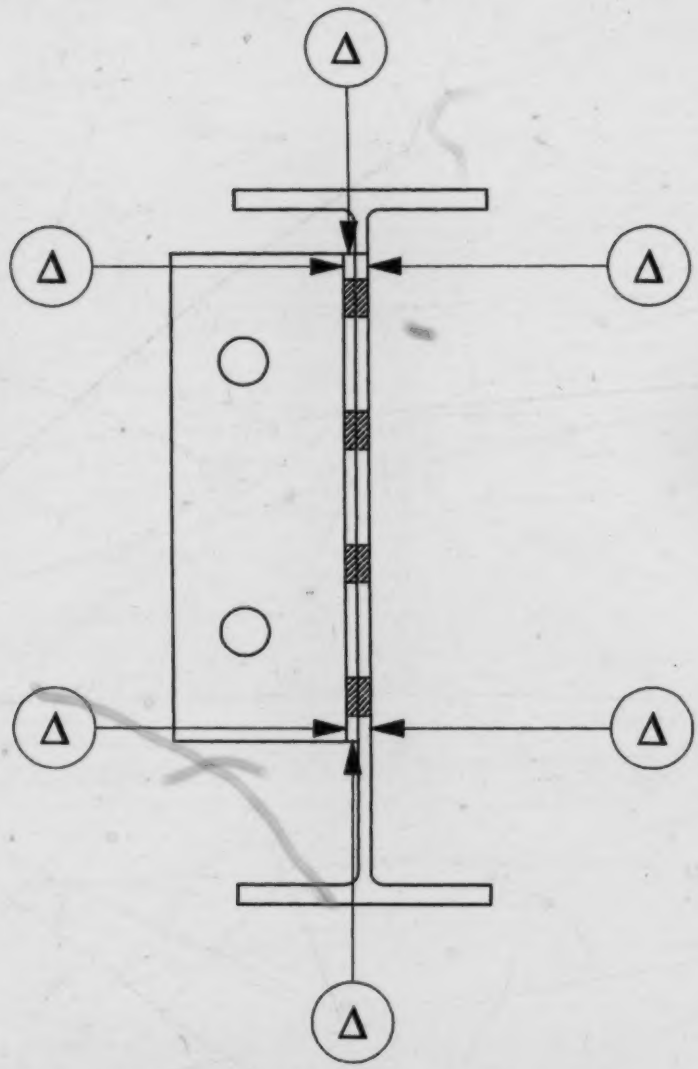

Figure A-2: Additional Connection Instrumentation

(a) Test I

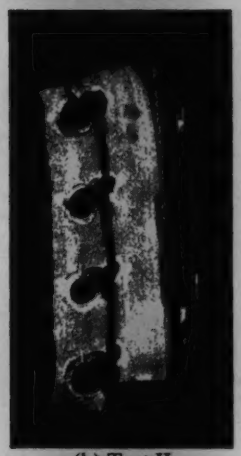

(b) Test II

(c) Test III

Figure A-3: Connections Failed in Pure Shear

(a) Test IV – Angle

(b) Test V – Angle

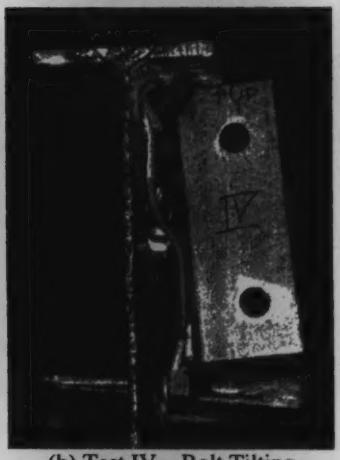

(b) Test IV – Bolt Tilting

(c) Test V – Bolt Tilting

(d) Test IV – Beam

(e) Test V – Beam

Figure A-4: Connections Failed by Bolt Bearing and Tilting

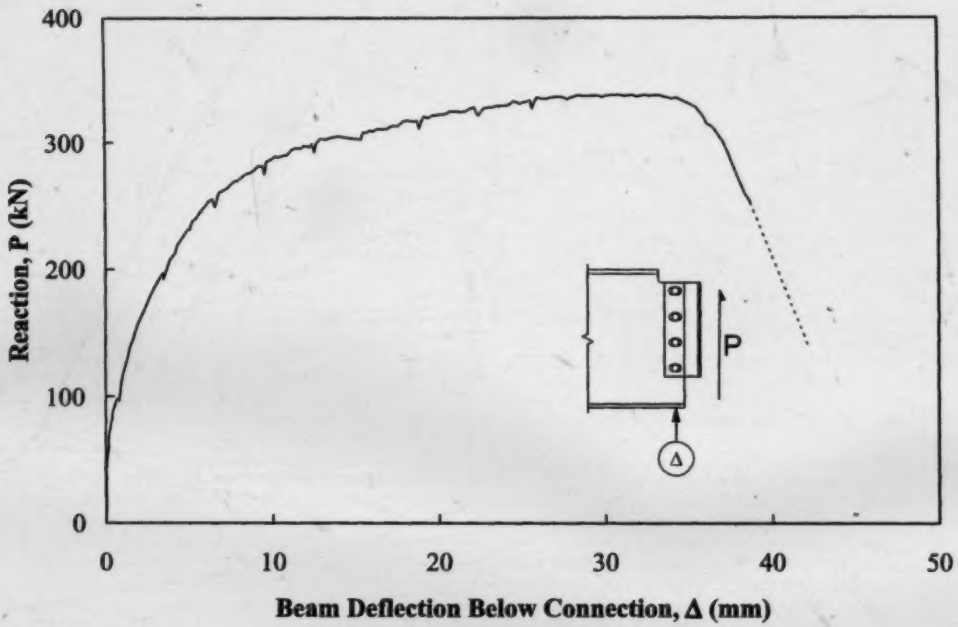

Figure A-5: Load vs. Deflection Curve, Test I

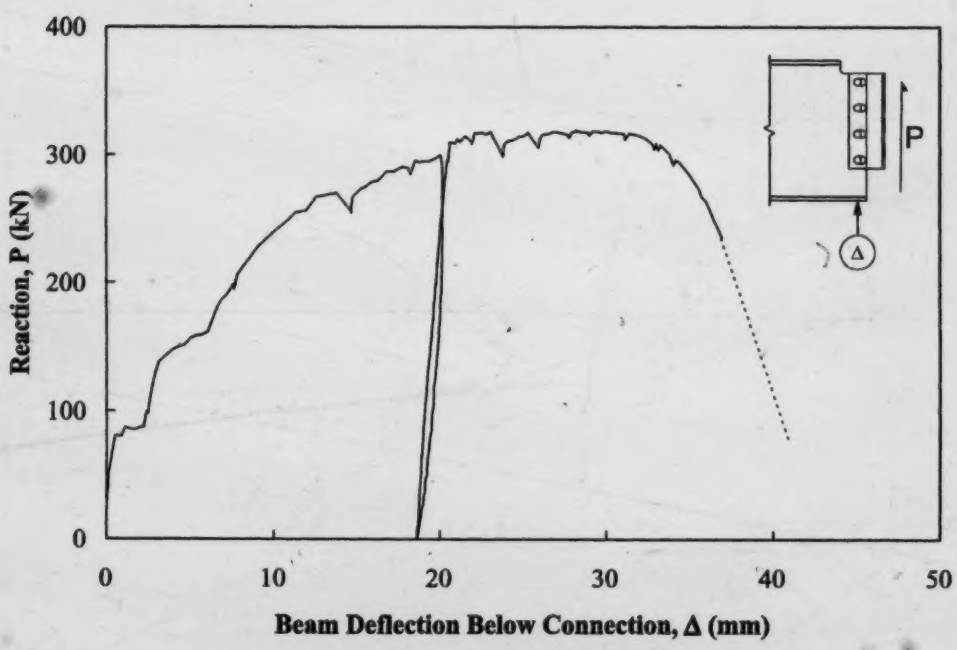

Figure A-6: Load vs. Deflection Curve, Test II

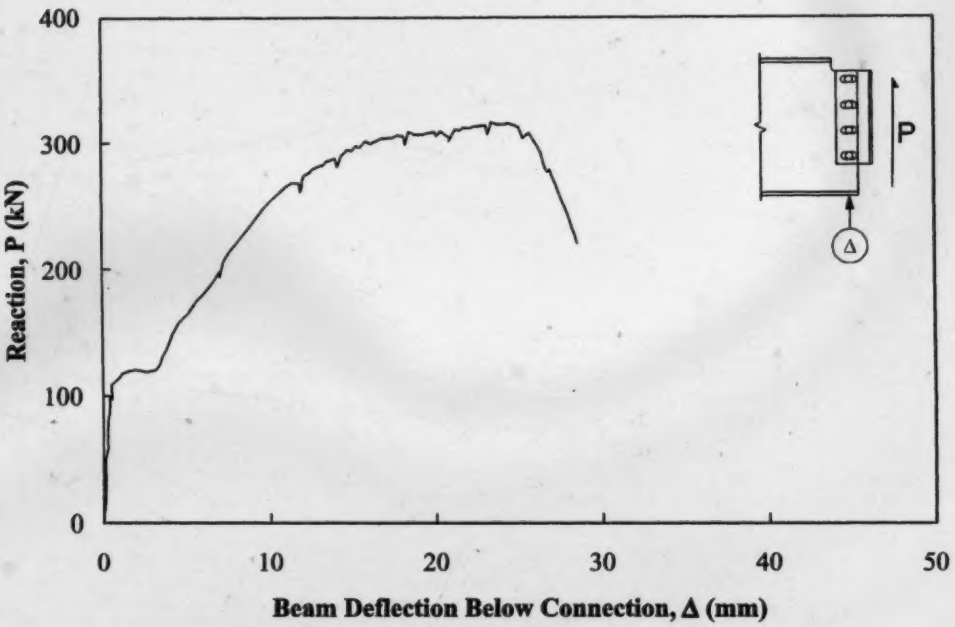

Figure A-7: Load vs. Deflection Curve, Test III

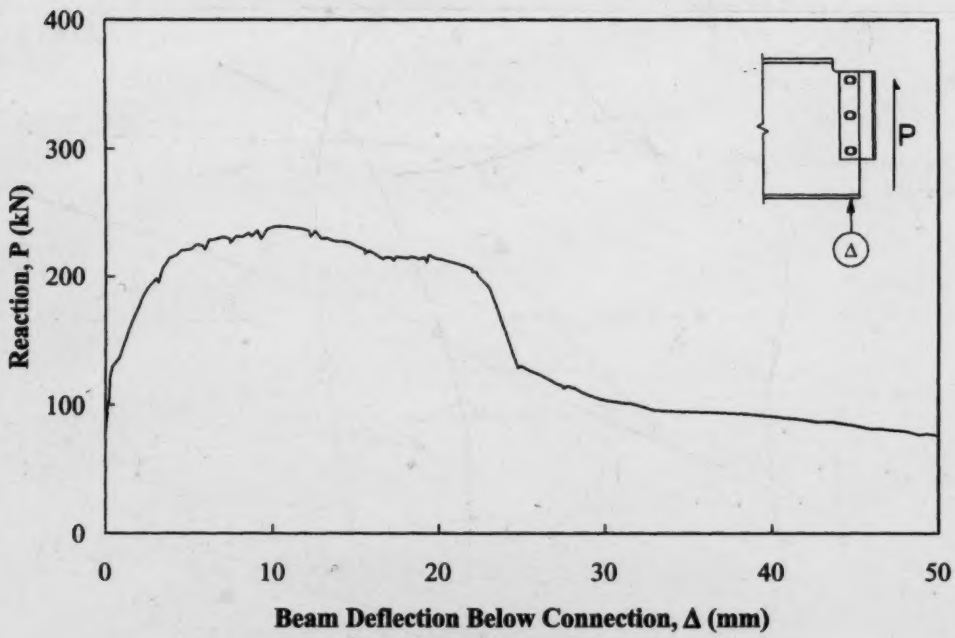

Figure A-8: Load vs. Deflection Curve, Test IV

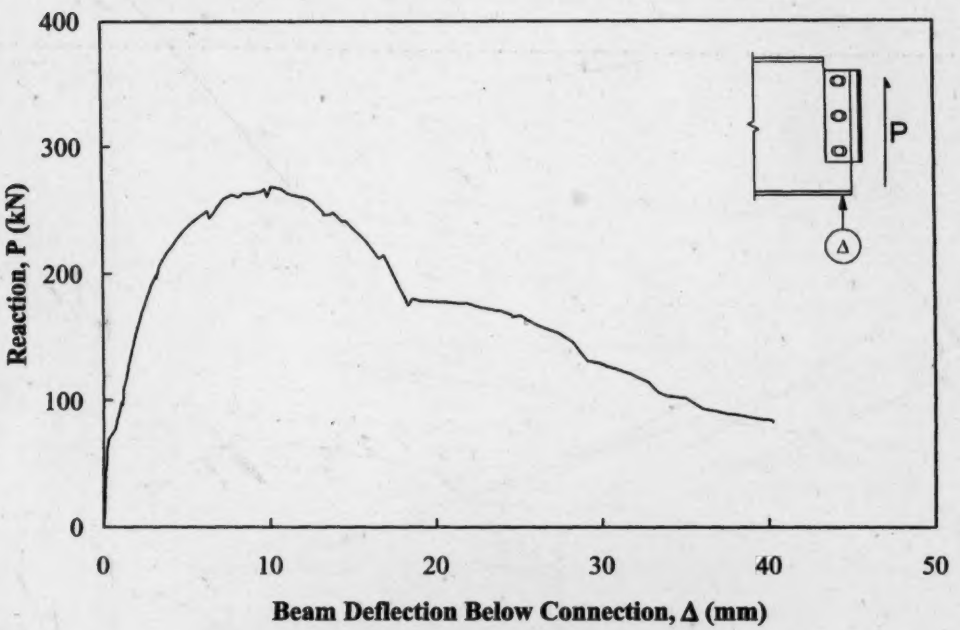

Figure A-9: Load vs. Deflection Curve, Test V

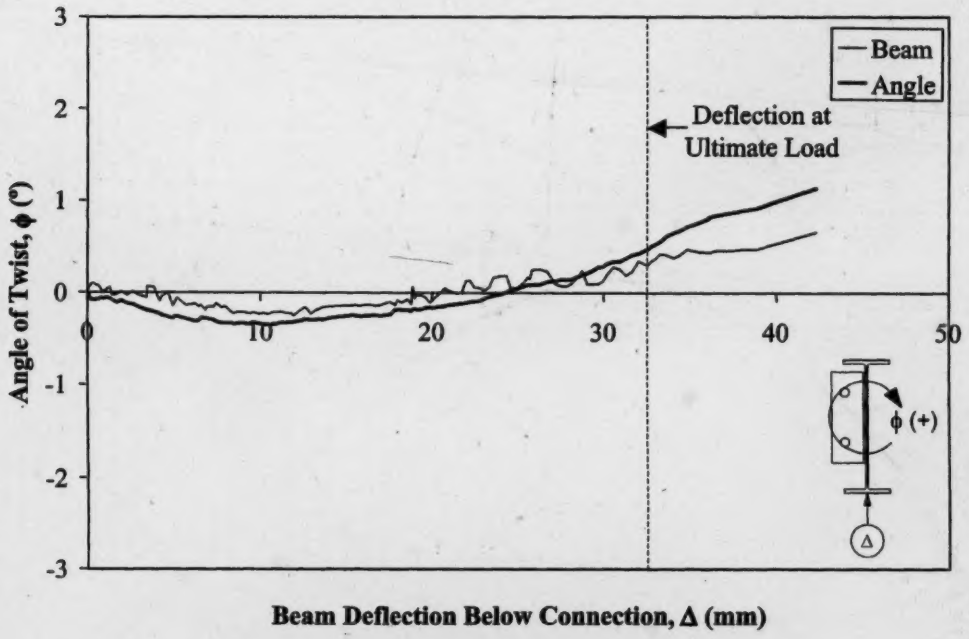

Figure A-10: Twist vs. Deflection Curve, Test I

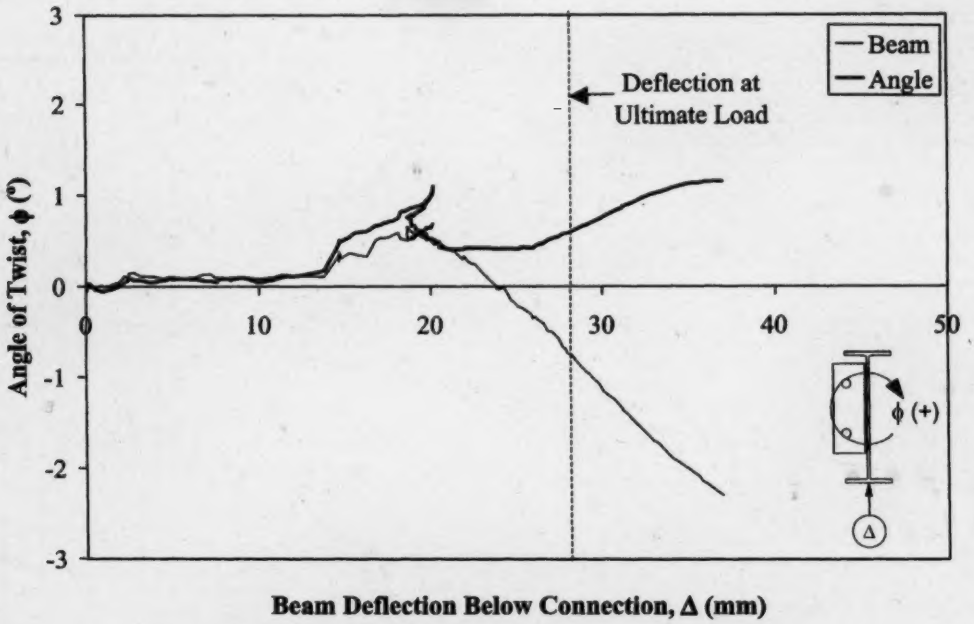

Figure A-11: Twist vs. Deflection Curve, Test II

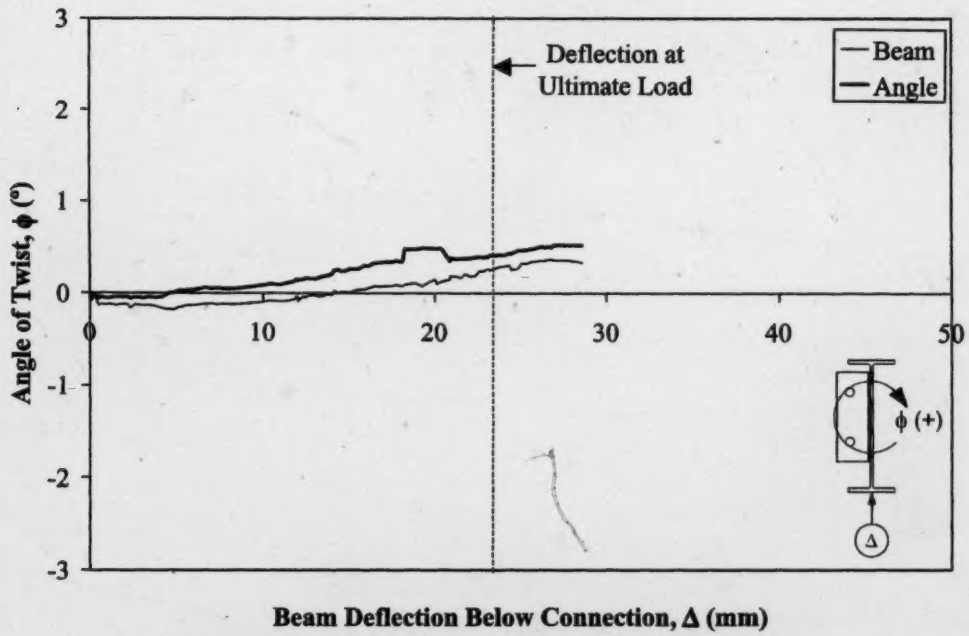

Figure A-12: Twist vs. Deflection Curve, Test III

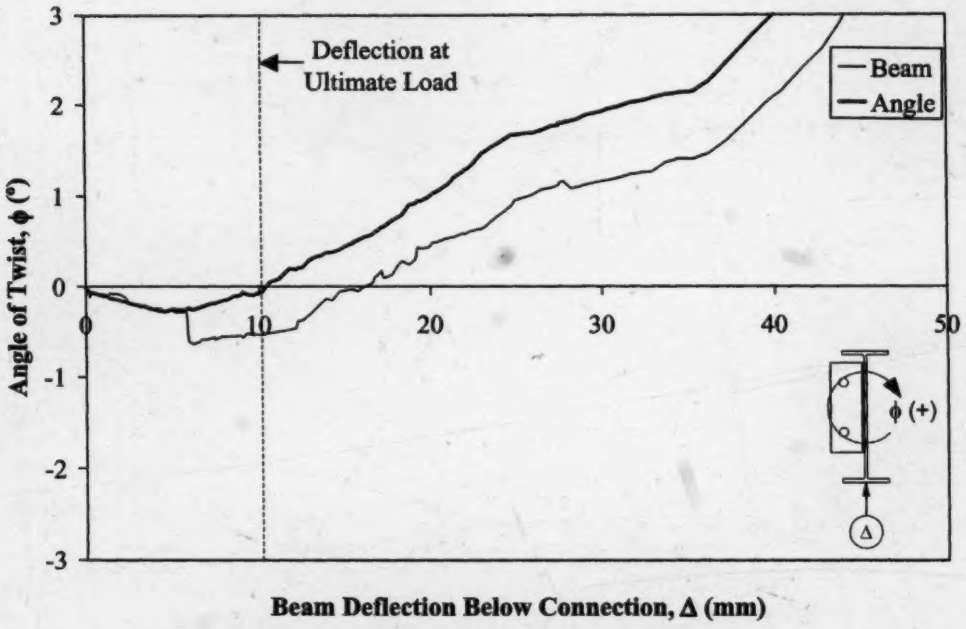

Figure A-13: Twist vs. Deflection Curve, Test IV

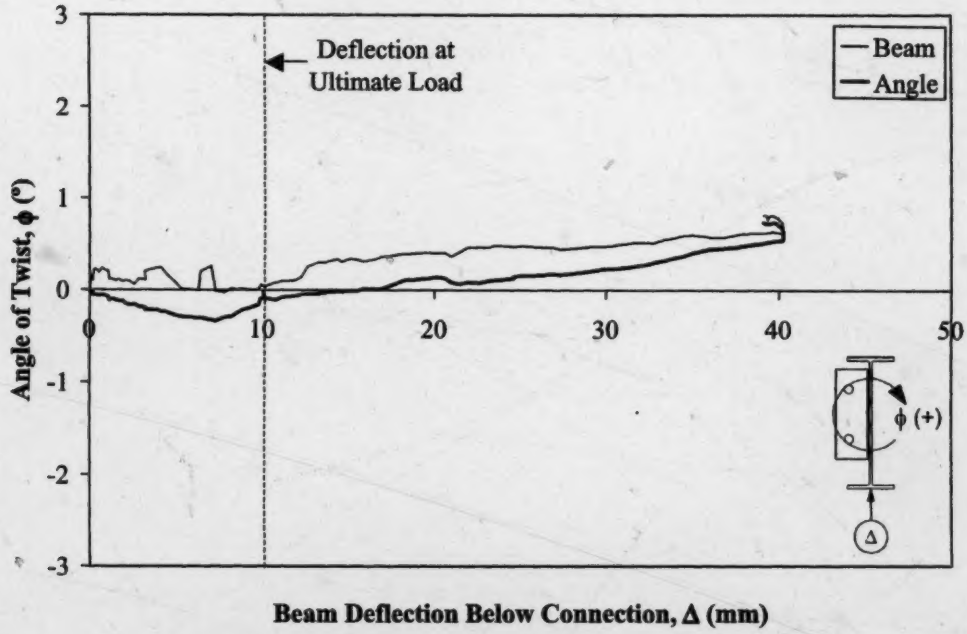

Figure A-14: Twist vs. Deflection Curve, Test V